The intracellular stress response to some disease-causing mutants of the human V2 vasopressin receptor

Inaugural-dissertation to obtain the academic degree
Doctor rerum naturalium (Dr. rer. nat.)

submitted to the Department of Biology, Chemistry and Pharmacy
of the Freie Universität Berlin

by

KATJA LAUTZ
from Münster

Berlin, December 2008

First Reviewer: Prof. Dr. Ricardo Hermosilla

Second Reviewer: Prof. Dr. Stephan Sigrist

Date of defence: 13. August 2009

“You can’t possibly be a scientist if you mind people thinking that you’re a fool.”

(Douglas Adams)

Acknowledgments

Herrn Prof. Dr. Walter Rosenthal möchte ich für die finanzielle Unterstützung und die Möglichkeit danken, diese Arbeit in der Abteilung für Molekulare Pharmakologie und Zellbiologie sowie dem Leibniz-Insitut für Molekulare Pharmakologie (FMP) Berlin anzufertigen.

Mein besonderer Dank gilt meinem Betreuer Herrn Prof. Dr. Ricardo Hermosilla für die Aufnahme in die Gruppe, seine jahrelange, großartige Förderung und Forderung und seinem Rat nicht nur zu wissenschaftlichen Themen.

Meiner Arbeitsgruppe und den Kollegen in Dahlem und in Buch danke ich herzlich für die nette Aufnahme, Unterstützung und Ablenkung. Insbesondere bedanke ich mich bei Dr. Isabel Schwieger und Solveig Großmann für diverse Korrekturen und Aufmunterungen. Ohne Euch wäre die Arbeit im Labor und die Zeit dazwischen nicht das Gleiche gewesen. Insbesondere möchte ich meinen Lieblingspraktikantinnen Angela Mensen und Verena Perneczky danken; Angela für die wundervollen Calnexin-Blots und Verena nicht nur für die geleistete sehr gute Arbeit im Labor, sondern auch für diverse andere produktive Stunden.

Des Weiteren möchte ich Dr. Dorothea Lorenz (FMP) für die Anfertigung der EM-Bilder, Dr. Katinka Jung (GEMATRIA Test Lab) für die Untersuchung der Redoxkapazität und Prof. Dr. Norbert Hübner und seiner Gruppe für die Hilfe bei den Micro Arrays danken.

Meinem Mann Dr. Thomas Lautz danke ich für die unaufhörliche Unterstützung und Ermutigung in der Wissenschaft und im Alltag, für die Geduld, das Zuhören und das für-mich-da-sein, besonders in den letzten Monaten. Wir sind ein Team!

Außerdem danke ich meiner Familie und meinen Freunden für die Unterstützung und Ablenkung in den letzten Jahren.

Content

Summary

Conformational diseases or endoplasmatic reticulum (ER) storage diseases are a class of disorders associated with aberrant protein accumulation in tissues and cellular compartments of the secretory pathway. To date, more and more diseases are discussed to be linked to ER stress and the induction of two specific signaling pathways, the unfolded protein response (UPR) and the ER-overload response (EOR). One of them may be the X-linked nephrogenic diabetes insipidus (NDI), which is characterized by the inability of the kidney to absorb water in response to the hormone arginin vasopressin (AVP). This rare hereditary disorder is induced by different mutations within the sequence of the *AVPR2* gene resulting in misfolded V2 vasopressin receptors (V2R), which are transport-defect and therefore among other effects intracellularly retained. Besides the disturbed water absorption little is known about the additional cellular effects of these retained receptor proteins. Therefore the human V2R and several naturally occurring disease-causing mutants were used as model proteins to study the effects of the intracellular retention of misfolded proteins in different compartments of the secretory pathway, namely the ER, ERGIC and Golgi apparatus. In this study the detection and characterization of ER stress induced upon expression of misfolded proteins was carried out showing for the first time that the UPR but not the EOR was activated after stable and/or transient expression of misfolded V2Rs in HEK293 cells. The induction of the UPR was measured by an upregulation of different chaperones by immunoblot analysis and luciferase assay and verified by an extensive activation study of the three known UPR-specific pathways. Simultaneously, analyses of activation of the transcription factor NF-κB as an indicator of EOR revealed no participation of this ER stress pathway in cells expressing NDI-causing mutants. Furthermore, it could be shown that different mutants of a single receptor protein activated different UPR branches. The ER-retained mutant L62P and the ER/ERGIC-localized mutant InsQ292 induced the PERK and ATF6 pathways while mutant G201D, which reaches the Golgi network, exclusively activated the IRE-1 pathway. In addition, the rescue of the intracellularly retained murine V2R to the plasma membrane by different pharmaco- and chemical chaperones resulted in a reduction of UPR detected by a decreased expression of chaperones GRP78 and GRP94 and a reduced activation of the PERK target eIF2α. Micro array analysis of cells expressing ER-retained mutant L62P revealed new and yet unknown target genes of UPR. Some of them were involved

in redox regulation and the negative regulation of apoptosis and therefore elucidated novel and as yet undescribed possibilities to inhibit cell death after persistent ER stress. Furthermore, the analysis of the three known UPR transducers revealed the chaperone GRP94 as a novel interaction partner of the transcription factor ATF6, possibly connected with ER stress. Until this work, the activation of UPR and induction of ATF6 were assumed to be exclusively regulated by binding and dissociation of GRP78. Finally, the usually ER-resident molecular chaperone GRP94 could be found in the nucleus in cells expressing ER-retained mutant L62P for the first time, which was verified by different methodical approaches and pointed to a possible adaptive function resulting in the survival of the cells upon persistent ER stress.

Zusammenfassung

Bei Proteinfaltungskrankheiten wie zystischer Fibrose oder Retinitis pigmentosa wird heutzutage angenommen, dass die Akkumulation von fehlgefalteten, nicht-nativen Proteinen im Endoplasmatischen Retikulum (ER) für das Auftreten von ER-Stress und für die Aktivierung ER-Stress-vermittelter Signalwege verantwortlich ist. Die Hauptsymptome dieser Erkrankungen werden durch das Fehlen des Proteins an seinem Wirkort verursacht, aber ER-Stress kann die Krankheitssymptome zusätzlich verstärken. Spezifische Signalwege werden daraufhin als Antwort aktiviert. Über die UPR („unfolded protein response“) wird speziell die Expression von Chaperonen verstärkt, während die EOR („ER overload response“) zur Aktivierung des Transkriptionsfaktors NF-κB führt.

Das Modellprotein dieser Arbeit, der humane V2 Vasopressin Rezeptor (V2R) gehört zu der Familie der G-Protein-gekoppelten Rezeptoren und wird überwiegend in den Hauptzellen des Sammelrohres der Niere exprimiert. Mutationen in der Sequenz des *AVPR2*-Genes können zu fehlgefalteten, transportdefekten Rezeptoren führen. Ein Großteil dieser fehlgefalteten Rezeptoren wird vom Qualitätskontrollsystem der Zelle erkannt und intrazellulär zurückgehalten, so dass diese Rezeptoren nicht an die Oberfläche gelangen können, um dort die antidiuretische Wirkung ihres Liganden, des Hormons Vasopressin (AVP) zu vermitteln. Durch die verminderte Rezeptorzahl an der Plasmamembran kommt es bei diesen Patienten zu einer stark erhöhten Wasserausscheidung. Neben der gestörten Wasserrückresorption ist allerdings nur wenig von anderen Auswirkungen bekannt, die auf die Retention der fehlgefalteten Rezeptoren zurückzuführen sind. Aus diesem Grund wurde in der vorliegenden Arbeit bei HEK293 Zelllinien, die stabil und transient den humanen V2R und einige in Patienten gefundene krankheitsauslösende Mutanten exprimieren, die Auswirkungen der intrazellulären Retention von fehlgefalteten Proteinen in unterschiedlichen Kompartimenten des sekretorischen Signalweges (ER, ERGIC und Golgi-Apparat) untersucht.

Das Vorliegen einer UPR konnte durch eine verstärkte Expression von Chaperonen und der Aktivierung der drei beschriebenen UPR spezifischen Signalwegen bestätigt werden. Die Analyse der Aktivitatät von NF-κB verdeutlichte hingegen das Fehlen einer Antwort in Form des EOR. Zusätzlich konnte gezeigt werden, dass nicht jede

Fehlfaltung des V2 Rezeptor eine Aktivierung der gleichen UPR Wege mit sich führt. So waren bei HEK293 Zellen, die stabil die ER-retinierte Mutante L62P und die in ER und ERGIC lokalisierte Mutante InsQ292 exprimieren, die Signalwege über die Stress-Sensoren PERK und ATF6 aktiviert, während die Retention im Golgi-Apparat (G201D) nur zu einer Aktivierung des IRE-1 Signalweges in HEK293 Zellen führt. Außerdem führte die Zurückführung (Rescue) an die Plasmamembran des ebenfalls in HEK293 Zellen intrazellulär zurückgehaltenen murinen V2R (mV2R) durch Behandlung mit Pharmako-Chaperonen und DMSO als chemisches Chaperon zu einer Verringerung des UPR. Dies konnte durch eine reduzierte Expression der Chaperone GRP78 und GRP94 in den behandelten Zellen gezeigt werden. Durch Micro Array Analysen von HEK293 Zellen, die stabil die ER-retinierte Mutante L62P exprimieren, konnten neue Zielgene der UPR gefunden werden, die u. a. Redox Regulation und die negative Regulation der Apoptose beinhalteten. Die genauere Analyse dieser Signalwege konnte neue Mechanismen zur Apoptose-Hemmung trotz chronischer ER-Stress Bedingungen aufdecken und neue Ansätze zur pharmakologischen Behandlung aufzeigen. Zusätzlich wurde das Chaperon GRP94 durch Immunopräzipitations-Analysen als neuer Interaktionspartner des UPR Transkriptionsfaktors ATF6 gefunden, der möglicherweise als zusätzlicher Regulator des Signalübermittlers bei ER-Stress fungiert und unter diesen Bedingungen zum ersten Mal auch im Kern detektiert wurde.

Abbreviations

λ	wavelength
AQP2	aquaporin 2
APS	ammonium persulfate
ASK1	apoptosis-signal-regulating kinase
ATF4	activating transcription factor 4
ATF6	activating transcription factor 6
AVP	8-arginine-vasopressin
Bcl-2	B cell lymphoma
BiP	heavy chain binding protein
bp	base pairs
BSA	bovine serum albumin
cAMP	cyclic adenosine monophosphate
cDNA	complementary DNA
CHOP	C/EBP homologous protein
CLX	calnexin
CRT	calreticulin
Cy3	Carbocyanin 3
dH_2O	didistilled water
DMEM	Dulbecco's modified Eagle's media
DMSO	dimethylsulfoxide
DNA	desoxyribonucleic acid
dNTP	desoxynucleotide
DPPH	2,2-diphenyl-1-picrylhydrazil
DTT	1,4-dithiothreitol
E. coli	*Escherichia coli*

EDTA	ethylenediaminetetraacetic acid
e. g.	for example
eIF2	eukaryotic translation initiation factor subunit 2
EOR	ER-overload response
ER	endoplasmic reticulum
ERGIC	ER/GOLGI intermediate compartment
FCS	fetal calf serum
Fig.	figure
FMP	Leibniz-Institut für Molekulare Pharmakologie, Berlin
G-418	geniticin
GAPDH	glyceraldehydes 3-phosphate dehydrogenase
GCOS	GeneChip® Operating Software
gDNA	genomic DNA
GFP	green fluorescent protein
GPCR	G protein-coupled receptor
G protein	guanine nucleotide binding protein
GRK	G protein-coupled receptor kinase
GRP94	glucose regulated protein 94
GTP	guanosine triphosphate
h	hour
HEPES	4-(2-hydroxyethyl)-1-piperazineethanesulfonic acid
HEK	human embryonic kidney
HRP	horseradish peroxidase
Hsp	heat shock protein

IB	immuno blotting
IF	immuno fluorescence
IgG	immunoglobulin G
IP	immuno precipitation
IRE-1	inositol-requiring enzyme 1
kb	kilobase pairs
kDa	kilodalton
KDEL	lysine-aspartic acid-glutamic acid-leucine
LB	Luria Bertani
LSM	laser scanning microscopy
MG-132	carbobenzoxy-L-leucyl-L-leucyl-L-leucinal, proteasome inhibitor
NDI	nephrogenic diabetes insipidus
NF-κB	nuclear factor κ B
NP-40	nonidet P-40
PAGE	polyacrylamide gel electrophoresis
PBN	N-tert-butyl phenylnitrone
PBS	phosphate buffered saline
PCR	polymerase chain reaction
PDI	protein disulfide isomerase
PERK	PKR-like ER kinase
PMSF	phenylmethylsulfonyl fluoride
PKA	protein kinase A
POD	horseradish peroxidase
PVA	polyvinylalcohol
PVP	polyvinylpyrrolidone
RIPA	radioimmunoprecipitation assay

RNA	ribonucleic acid
ROS	reactive oxygen species
rpm	rounds per minute
RT-PCR	reverse transcription PCR
s	second
SDS	sodiumdodecyl sulfate
SOB	“super optimal broth” medium
SOC	“super optimal broth” medium, glucose added
TAE	tris-Acetate-EDTA
Taq	*Thermophilus aquaticus*
TBS	tris buffered saline
Tg	thapsigargin
TEMED	N, N, N’, N’ – tetramethylethylene diamine
Tm	tunicamycin
TNFα	tumor necrosis factor α
TRAF2	TNF-receptor-associated factor 2
Tris	tris(hydroxymethyl-)aminoethan
Triton-X 100	polyethylene glycol p-(1,1,3,3-tetramethylbutyl)-phenyl ether
TUNEL	terminal uridine deoxynucleotidyl transferase dUTP nick end labeling
Tween 20	polyoxyethylene (20) sorbitan monolaurate
UPR	unfolded protein response
V2R	V2 vasopressin receptor
wt	wild-type
XBP-1	X box–binding protein 1

List of amino acids and their abbreviations

A	Ala	alanine
C	Cys	cysteine
D	Asp	aspartic acid
E	Glu	glutamic acid
F	Phe	phenylalanine
G	Gly	glycine
H	His	histidine
I	Ile	isoleucine
K	Lys	lysine
L	Leu	leucine
M	Met	methionine
N	Asn	asparagine
P	Pro	proline
Q	Gln	glutamine
R	Arg	arginine
S	Ser	serine
T	Thr	threonine
V	Val	valine
W	Trp	tryptophane
Y	Tyr	tyrosine

1 Introduction

1.1 Protein folding and quality control in the ER

Proteins have to fold into their correct three-dimensional conformation in order to achieve their biological function. Studies of protein denaturation and renaturation indicate that the primary structure (amino acid sequence) of a protein determines its three-dimensional structure. Folding pathways for proteins are fast and tend to follow an energetically favorable route, leading to a stable, low energetic state for the complete folded structure (Dobson 2004).

Cytoplasmic ribosomes catalyze the translation of mRNA into nascent polypeptide chains and synthesize most cellular proteins, which remain in the cytoplasm or are targeted to organelles by signals built into the protein structure. N-terminal signal sequences at growing polypeptide chains define targets destined for the secretory pathway. When ribosomes synthesize such a presequence, nascent proteins are directed to the endoplasmic reticulum (ER), where further protein synthesis is coupled to translocation. The ER is the first stop for proteins destined for incorporation into the ER itself, the Golgi apparatus, the plasma membrane or for secretion from the cell (Fig. 1.1). In mammals, these proteins are synthesized and translocated co-translational into the ER during their synthesis by the ribosome and by its interaction with the heterotrimeric integral ER membrane Sec61 channel (Kalies et al. 1994). The maturation of proteins typically involves covalent processing, like proteolytic cleavage, glycosylation or cross-linking by formation of disulphide-bonds.

The ER contains a number of molecular chaperones and folding enzymes, which are physiologically involved in folding and post-translational modification of proteins (Gething and Sambrook 1992). Furthermore, it provides a unique oxidizing environment in order to facilitate oxidation of cysteine residues in growing polypeptide chains to form disulphide bonds. During the folding process proteins are glycosylated with high mannose sugar side chains on asparagine residues. The newly synthesized proteins are transported in coat protein complex (COP) II-vesicles from ER-exit sites to the ER-Golgi intermediate compartment (ERGIC) (Bannykh et al. 1995). Subsequently, secretory proteins are delivered from the ERGIC to the Golgi apparatus, which is the last known station of quality control in the secretory pathway. Enzymes in the Golgi

network process the glycoproteins and replace the high mannose sugar side chains by complex sugar moieties. Some proteins are additionally modified with O-linked oligosaccharides. Subsequently, proteins are sorted for transport to their final destinations, e.g. to the plasma membrane.

Protein folding is stringently monitored by the quality control system (QCS) of the cell in order to maintain homeostasis in the early secretory pathway (Hurtley and Helenius 1989; Ellgaard and Helenius 2001). The un- or misfolded status of a protein is believed to be controlled by detection of hydrophobic patches and reactive thiols or by the presence of immature glycans. After recognition, the quality control system retains unfolded or misfolded proteins via interaction with chaperones to ensure that only correctly folded or assembled proteins may exit the ER and enter the secretory pathway. According to their definition, chaperones are proteins which mediate the correct assembly of other polypeptides, but are not components of the final functional structures by themselves (Ellis and Hemmingsen 1989). Different classes of chaperones are described holding specific properties in the folding process and quality control. Classical chaperones belong to the family of heat shock proteins (Hsps) involved in the response upon exposure to high temperatures (Burdon et al. 1987). Members of this family are not only found in the ER (GRP78, GRP94), but are also localized in the cytoplasm (Hsp70, Hsp90) in order to prevent accumulation and aggregation of cytosolic proteins. However, under certain stress conditions these chaperones are also found in other compartments of the cell, for example in the nucleus or mitochondria (Vincent and Tanguay 1982).

Members of a second class of ER resident molecular chaperones are the Ca^{2+}-binding lectins calnexin (CLX) and calreticulin (CRT). They also belong to the QCS and are involved in preventing aggregation and facilitation of glycoprotein folding. They form complexes together with the thiol oxidoreductase ERp57 in order to mediate proper folding of glycoproteins through a binding and release cycle, the so-called calnexin/calreticulin cycle (Ellgaard et al. 1999)(Fig. 1.1). Calnexin, an integral membrane protein and its luminal, soluble partner calreticulin recognize specifically monoglycosylated, core N-linked glycans and subsequently bind the nascent glycoprotein. Prior to this step the oligosaccharyl transferase complex (OST) transfers co-translational Glc_3-Man_9-$(GlcNAc)_2$ oligosaccharides to asparagine side chains of newly synthesized glycoproteins, directly after nascent chains enter the ER through the

translocon. The nascent proteins undergo cycles of binding and release from CLX/CRT. During this process the glycoproteins are trimmed by glycosidases, mannosidases and glycosyl transferases in order to achieve the right conformation (Hammond et al. 1994). The retention of unfolded glycoproteins permits foldases, enzymes that catalyze isomerization of polypeptide conformations or exchange of disulphide bonds (ERp57, PPI, PDI), to facilitate the correct folding of the protein. If properly folded proteins assume a transport-competent conformation, the ER mannosidase II generates a Man_7 sugar chain and the glycoprotein is able to leave the ER and enter the secretory pathway (Trombetta and Parodi 2003). Improperly or incompletely folded glycoproteins are reglucosylated by UDP-glucose-glycoprotein glucosyltransferase (UGGT) leading to rebinding to the cycle and continuing until a native conformation is achieved. All immature protein conformations are recognized and retained in an attempt to restore their transport-competent folding state.

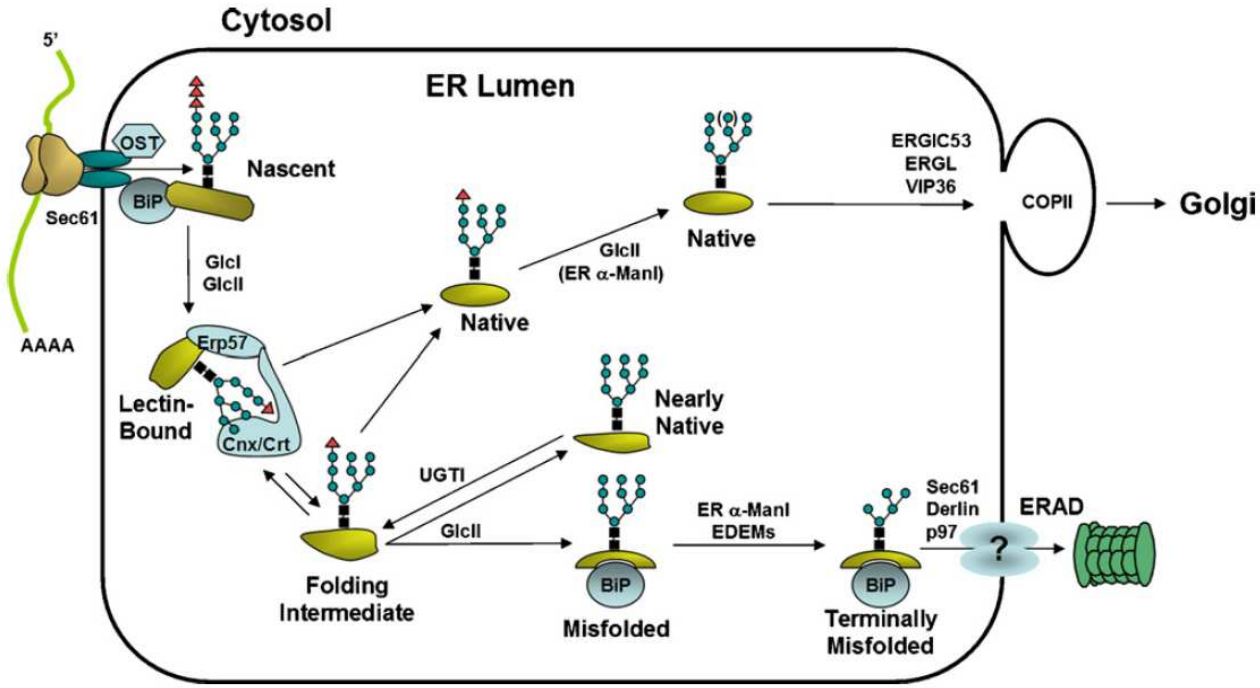

Fig. 1.1: Protein trafficking in the ER. Upon translocation of polypeptides through the integral ER membrane Sec61 channel, N-residues are frequently modified by covalent addition of a preassembled oligosaccharide core (Glc_3-Man_9-$(GlcNAc)_2$). This reaction is catalyzed by the oligosaccharyltransferase (OST), a multisubunit complex associated with the translocon. In order to facilitate unidirectional transport through the translocon, nascent polypeptide chains in the ER lumen interact with BiP (GRP78). Subsequently, rapid deglucosylation of the two outermost glucose residues on the oligosaccharide core

structures, mediated by enzymes glucosidase I and II (GlcI and GlcII), prepares glycoproteins for association with the ER lectins calnexin and calreticulin. The calnexin/calreticulin-associated oxidoreductase ERp57 contributes to protein folding by catalyzing formation of intra- and inter-molecular disulfide bonds. Release from calnexin/calreticulin followed by glucosidase II cleavage of the innermost glucose residue results in preventing further interaction with both lectins. At this point, natively folded polypeptides transit the ER to the Golgi apparatus in a process possibly assisted by mannose-binding lectins ERGIC-53, VIPL (VIP36-Like) and ERGL (ERGIC-53-like). As an essential component of protein-folding quality control, non-native polypeptides are tagged for re-association with calnexin/calreticulin by the UDP-glucose:glycoprotein glucosyltransferase (UGT1) to facilitate their ER retention and to prevent anterograde transport. Polypeptides that remain misfolded are targeted to retrotranslocation and degradation by retrotranslocation, possibly mediated by EDEM or Derlins. Finally, proteins are ubiquitinated and degraded by the 26S proteosome. (Triangles = glucose residues, squares = *N*-acetylglucosamine residues, circles = mannose residues) (figure taken from Kaufman.2007 (Malhotra and Kaufman 2007) with authorization of the journal).

Conformationally defective proteins exit the folding cycle and are targeted for ER-associated degradation (ERAD), which includes retrotranslocation to the cytosol and degradation by the ubiquitin-proteasome system (Werner et al. 1996). This process is an important part of the quality control mechanism to protect cells from damage and assures restoration of normal ER function. Most proteins, which misfold or fail to assemble properly, are degraded by ER-associated degradation. This involves the identification of the misfolded protein by the quality control system, its unfolding and retrotranslocation into the cytosol, deglycosylation, polyubiquitination and finally degradation by the proteasome. Several chaperones seem to be involved in the initial identification and unfolding steps, including calnexin/calreticulin, BiP and PDI (Hammond et al. 1994; Reddy and Corley 1998; McCracken and Brodsky 2003). Misfolded glycoproteins seem to be retained in the ER through repeated rounds of interaction with calnexin/calreticulin. If the QCS machinery is not able to fold proteins correctly even after several rounds of calnexin/calreticulin binding, the sugar chains are trimmed to a Man_8 form by α-1,2-mannosidase I and the substrates cannot be reglycosylated anymore. Man_8 forms are recognized by the lectin EDEM facilitating the release from CLX/CRT and export of the misfolded proteins from the ER by a yet unknown mechanism (Molinari et al. 2003; Oda et al. 2003). Finally proteins are eliminated via the ERAD pathway (Brodsky and McCracken 1999).

Another important function of the ER in mammalian cells is the generation of reactive oxygen species (ROS) in response to toxic agents (H_2O_2). ROS production also occurs as a coproduct in the respiratory chain in mitochondria and of O_2-utilizing enzymes like glucose oxidase NADH/NADPH oxidase or NO synthases. Under physiological conditions, excessive formation of ROS is prevented by an endogenous antioxidant defence system composed of enzymes like superoxide dismutases, glutathione peroxidases, catalases, thioredoxin peroxidases or by redox systems like the NAD^+/NADH, $NADP^+$/NADPH and oxidized glutathione/reduced glutathione (Chaudiere and Ferrari-Iliou 1999).

The ER also serves as an important and dynamic Ca^{2+} store, which can accumulate Ca^{2+} up to levels thousands times greater than in the cytosol (Burdakov et al. 2005). Ca^{2+}, as an intracellular second messenger, is not only essential for the crosstalk between ER and mitochondria; it also leads to the induction of apoptosis (Szanda et al. 2008). Changes in the cytosolic Ca^{2+} levels also regulate numerous cellular processes, such as muscle contraction or glucose mobilization. In addition, the binding of Ca^{2+} to the majority of molecular chaperones and folding enzymes regulates their activity and therefore the amount of luminal Ca^{2+} directly affects post-translational protein modification (Michalak et al. 2002). Depletion of Ca^{2+} in the ER has been shown to inhibit protein folding in several cellular systems (Wetmore and Hardman 1996).

1.2 ER stress, UPR and EOR

In addition to the typical folding load in the ER, an increased burden can emerge from a variety of causes, such as increased synthesis of secretory proteins, expression of misfolded proteins, bacterial and viral infections, disruption of Ca^{2+} homeostasis or nutrient deprivation. In addition to these circumstances, chemical agents, or physical stress, like UV-light or heat shock, also result in the induction of so-called ER stress (Malhotra and Kaufman 2007). Chemical inducers, which are routinely used to induce ER stress, are tunicamycin, which inhibits the N-glycosylation of proteins and leads to accumulation of proteins in the ER, or thapsigargin, an inhibitor of the Sarco/Endoplasmic Reticulum Ca^{2+}-ATPase (SERCA). Thapsigargin raises the cytosolic calcium concentration by blocking the ability of the cell to pump calcium into

the sarcoplasmic and endoplasmic reticulum. This depletion of Ca^{2+} levels also causes ER stress probably due to malfunction of chaperones. The accumulation of misfolded proteins in the ER initiates two pathways, the unfolded protein response (UPR) (Kozutsumi et al. 1988; Kaufman 1999) and the ER overload response (EOR) (Pahl and Baeuerle 1997). Induction of the UPR leads not only to a general decrease in translational initiation in order to reduce the protein load in the ER, but also to an increased translation of genes involved in protein folding and ERAD to alleviate ER stress. If this balance is disturbed, the cell will switch from pro-survival to pro-apoptotic pathways.

In response to ER stress, three ER-localized transmembrane signal transducers are activated and initiate adaptive or lethal responses. These transducers are the two type I transmembrane proteins inositol requiring kinase 1 (IRE-1) (Cox et al. 1993; Mori et al. 1993) and PKR-like ER kinase (PERK) (Harding et al. 1999) and the type II transmembrane transcription factor activating transcription factor 6 (ATF6) (Mori 1999). All three are constitutively expressed in all known metazoan cells. IRE-1, the first identified component of the UPR, was initially found in yeast (Cox et al. 1993; Mori et al. 1993) and is conserved in all eukaryotic cells. The essential and unique properties of IRE-1 signaling have been conserved in all eukaryotic cells, but higher eukaryotes additionally possess the sensors PERK and ATF6 which promote stress adaptation or induction of cell death in a more complex way (Fig. 1.2).

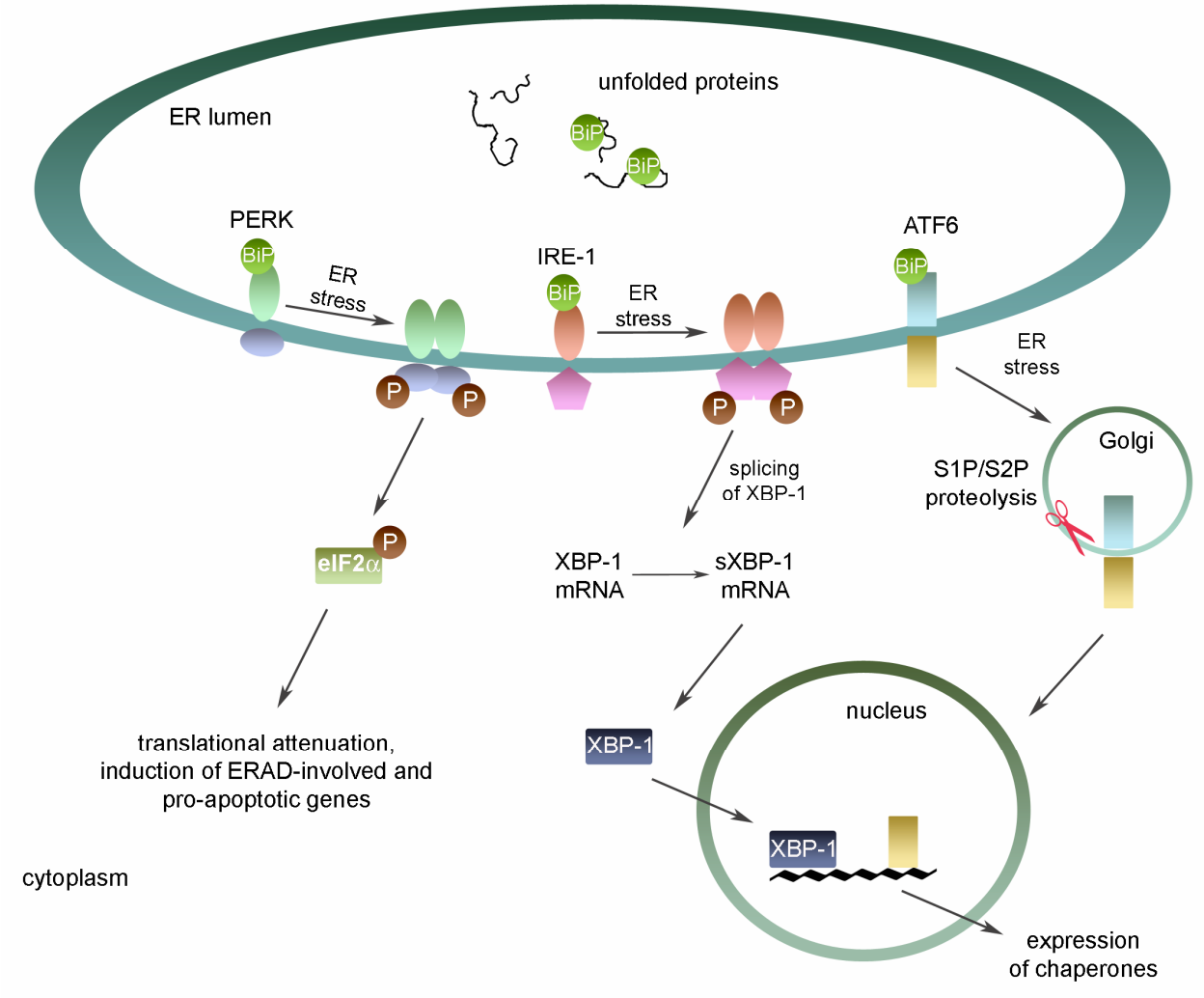

Fig. 1.2: Activation of mammalian UPR. Unfolded proteins in the ER lumen titrate BiP away from three signal transducers of UPR: PERK, IRE-1 and ATF6. Activated PERK phosphorylates translation initiation factor eIF2α resulting in transient attenuation of protein synthesis and an induction of specific mRNAs. Activated IRE-1 splices XBP-1 mRNA in order to generate the active transcription factor XBP-1, which can then mediate the transcriptional upregulation of several pro-survival genes. Upon ER stress ATF6 trafficks to the Golgi, where it is cleaved by S1P/S2P proteases and subsequently migrates into the nucleus to activate expression of chaperones. See text for details.

The early response to ER stress in mammalian cells is the activation of the PERK pathway. The luminal domain of PERK is associated with the chaperone BiP/GRP78 under non-stressed conditions and senses the accumulation of unfolded proteins by dissociation of this negative regulator (Bertolotti et al. 2000) (Fig. 1.2). Upon activation, PERK dimerizes or oligomerizes and its cytoplasmic kinase domain undergoes activation by *trans*-autophosphorylation. Activation of PERK leads to an immediate and transient attenuation of mRNA translation by phosphorylation and thereby to an

inhibition of the α-subunit of eukaryotic translation initiation factor 2 (eIF2α) at S51. The phosphorylation inhibits the guanine nucleotide exchange factor eIF2B, a pentameric complex that recycles eIF2 to its active GTP-bound form. A reduction of active eIF2 leads to a decreased level of translational initiation. As a result, a reduced load of newly synthesized proteins enter the stressed ER (Harding et al. 1999; Iida et al. 2007). In addition to the attenuated protein synthesis, PERK-mediated phosphorylation of eIF2α leads to transcriptional activation of specific mRNAs containing short, inhibitory upstream open reading frames (uORFs) in their 5' untranslated region (Hinnebusch 1997; Novoa et al. 2003). This connection between eIF2α inhibition and activated gene expression is conserved in all eukaryotes (Hinnebusch and Natarajan 2002). In mammalian cells, the mRNA for activating transcription factor 4 (ATF4) is regulated in this manner (Harding et al. 2000a). ATF4 is required for expression of genes involved in amino acid import, glutathione biosynthesis and resistance to oxidative stress (Harding et al. 2003). UPR related target genes are CCAAT/enhancer-binding protein (C/EBP) homologous protein (CHOP), which is involved in the induction of apoptosis and growth arrest and DNA-damage-inducible protein 34 (GADD34) (Jiang et al. 2004), which regulates the phosphatase activity of protein phosphatase 1 (PP1) (Ma and Hendershot 2003). PPI dephosphorylates eIF2α leading to resumption of protein synthesis after restoration of normal ER conditions.

It is also described that high levels of phosphorylated eIF2α result in the activation of nuclear factor κB (NF-κB), but the underlying mechanisms are quite unclear and controversially discussed (Jiang et al. 2003; Deng et al. 2004). It is also known that several other signaling pathways (amino acid starvation, double-stranded RNA accumulation) converge in eIF2α phosphorylation, resulting in the term "integrated stress response" (ISR) for signaling processes downstream of eIF2α (Harding et al. 2003).

ATF6 is an ER membrane bound transcription factor, which is transported upon ER stress from the ER to the Golgi apparatus, where it is cleaved by Golgi-resident proteases S1P (site 1 protease) and S2P (site 2 protease) in order to generate the active ATF6 p50 form (Fig. 1.2). Subsequently, ATF6 p50 moves into the nucleus, binds to the ATF/CRE element (Wang et al. 2000), ER stress response elements I and II (Yoshida et al. 1998; Kokame et al. 2001) and activates gene expression (Mori 1999).

Target genes of ATF6 are ER-resident molecular chaperones (GRP78, GRP94) and foldases, transcription factor XBP-1 or ERAD components, such as the membrane proteins Herp or Derlin-3 (Adachi et al. 2008). Regulation of ATF6 activation most likely occurs by the binding of chaperone BiP, masking two Golgi localization sequences GLS1 and GLS2 (Shen et al. 2002a), but regulatory interactions with calreticulin (Hong et al. 2004) and Nucleobindin 1 (Tsukumo et al. 2007) are also described. Furthermore, structural analyses reveal that several ER-anchored transcription factors are related to ATF6, for example LZIP (also known as luman or CREB4) (DenBoer et al. 2005; Stirling and O'Hare 2006) or OASIS, found in astrocytes (Murakami et al. 2006) leading upon activation to induction of so-called “acute-phase responsive proteins” (Zhao and Ackerman 2006). These observations suggest a connection of UPR transducers with several physiological and pathophysiological systems.

The IRE-1 pathway is evolutionary the oldest pathway and is conserved in all eukaryotic cells. IRE-1 was isolated as a gene required for inositol auxotrophy in budding yeast (Nikawa and Yamashita 1992). The luminal ER stress-sensing domain of IRE-1 shows limited sequence homology to PERK. The chaperone BiP/GRP78 also binds to IRE-1 and dissociates in response to ER stress. However, it remains unclear how the signal transducer IRE-1 senses ER stress and is subsequently activated. Crystallization of the luminal ER stress-sensing region revealed that IRE-1 clusters and actually interacts with unfolded proteins itself (Kimata et al. 2007). Upon activation, IRE-1 oligomerizes resulting in *trans*-autophosphorylation of its kinase domain (Fig. 1.2). However, the kinase domain of IRE-1 is not involved in triggering the UPR pathway, because the only known substrate is IRE-1 itself (Shamu and Walter 1996). Furthermore, its kinase domain activates a site-specific endoribonuclease causing directional splicing of X-box binding protein-1 (XBP-1) mRNA (Yoshida et al. 2001). XBP-1 is a bZIP transcription factor, which binds to ATF/CRE elements. Splicing of XBP-1 introduces a frame shift, which results in an alternative C-terminus with increased transcriptional activation potential. However, in metazoans there are no differences in translation of unspliced and spliced XBP-1 mRNAs (Yoshida et al. 2006). Spliced XBP-1 is more stable and works as a potent activator of UPR target genes (Yoshida et al. 2001), while unspliced XBP-1 is unstable and inhibits expression of target genes. Known XBP-1 target genes are ER-resident molecular chaperones (Lee et al. 2003), several ERAD components and genes involved in lipid biosynthesis (Sriburi et al. 2004).

The exact mechanism how the signal transducers PERK, IRE-1 and ATF6 sense accumulated, misfolded proteins is controversially discussed. The direct recognition model proposes that unfolded proteins bind directly to the luminal domains of the transducers (Ron and Walter 2007), whereas the indirect (chaperone-mediated) model hypothesizes that binding of abundant ER chaperone BiP/GRP78 keeps PERK, IRE-1 and ATF6 inactive. It is shown that BiP/GRP78 interacts with the luminal domains and dissociates upon ER stress conditions (Bertolotti et al. 2000), but this model does not convincingly explain how the high molar ratio of BiP/GRP78 in relation to stress transducers can be synchronized with the sensitivity of the UPR to slight changes in the amount of unfolded proteins (Credle et al. 2005).

Various conditions disturbing the function of the ER were shown to activate NF-κB, a transcription factor previously characterized as a central mediator of immune and inflammatory responses (Schulze-Osthoff et al. 1995). In a great variety of cell types, NF-κB is found in an inactive, cytoplasmic complex bound to IκB, its inhibitory subunit (Baeuerle and Baltimore 1988). Activation occurs via phosphorylation of IκB-α on two serine residues, S32 and S36, and subsequent proteasomal degradation of the inhibitor IκB (Henkel et al. 1993) (Fig. 1.3). Upon exposure of cells to pathological agents, such as pro-inflammatory cytokines, antigen, and UV- or γ-irradiation, or upon bacterial and viral infections, NF-κB activity is rapidly induced (Baeuerle and Henkel 1994). Furthermore, activation of NF-κB is also caused by accumulation of proteins in the ER, a condition called ER-overload (Pahl and Baeuerle 1997) resulting in a specific response of the cell, the ER-overload response (EOR). Both the release of Ca^{2+} from the ER and the subsequent production of reactive oxygen species (ROS) are required for ER-overload-mediated NF-κB activation. Degradation of IκB releases the NF-κB dimer due to exposure of nuclear import sequences and results in a subsequent translocation into the nucleus, where it activates transcription of its target genes. These include important pro-inflammatory proteins such as interferons, cytokines, chemokines, cell-adhesion molecules (ICAM), major histocompatibility (MHC) class I molecules, regulators of apoptosis (Bcl-2, TRAF2) and hematopoetic growth factors (Baeuerle and Henkel 1994).

Some diseases are known to be connected with an activation of NF-κB. The expression of cystic fibrosis (CF) inducing mutant ΔF508-CFTR causes a constitutive activation of

NF-κB by eliciting the ER-overload response. This endogenous NF-κB activation stimulates the transcription of pro-inflammatory cytokines thereby commencing an inflammatory cascade within the CF lung (Knorre et al. 2002). The enhanced expression of urinary prostaglandin E2 (PGE2) in patients suffering from congenital nephrogenic diabetes insipidus has also been described (Fichman et al. 1980) indicating a possible pro-inflammatory response of the cell due to accumulated V2R or AQP2.

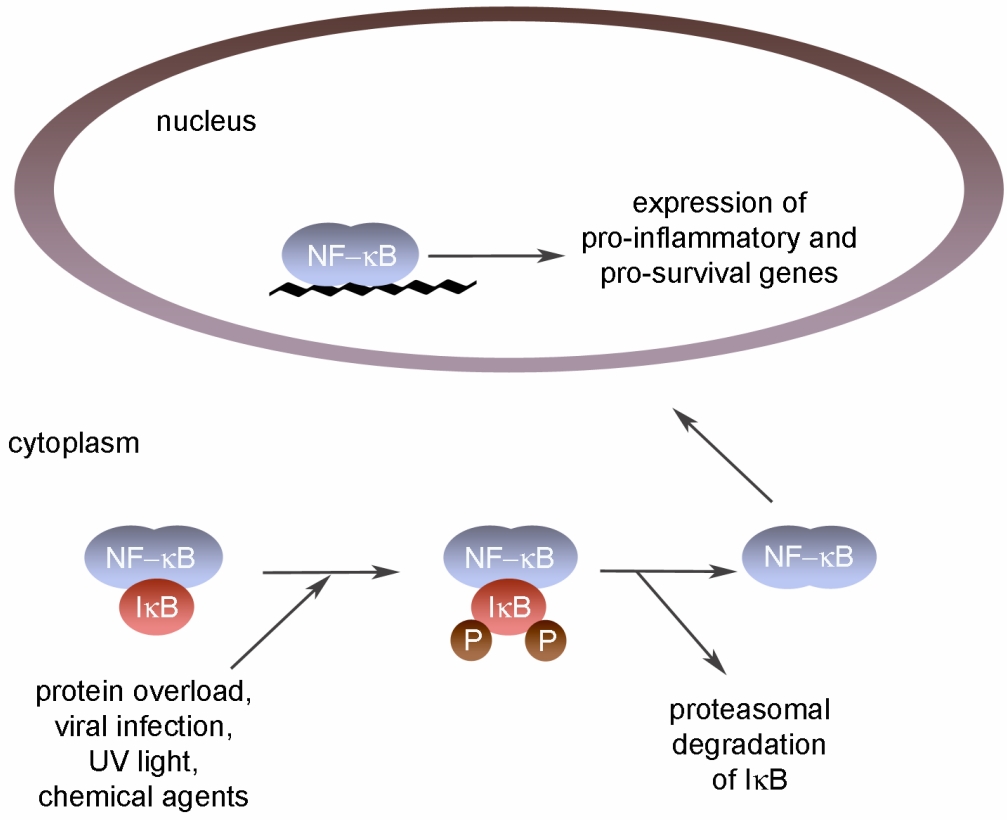

Fig. 1.3: EOR-mediated activation of NF-κB. Inactive NF-κB is found in a cytoplasmic complex bound to IκB, its inhibitory subunit. Upon exposure of cells to pathological agents such as pro-inflammatory cytokines, antigens, UV light, or bacterial and viral infections or accumulation of misfolded proteins, activation occurs via phosphorylation of IκB-α and subsequent proteasomal degradation.

1.2.1 ER stress-mediated apoptosis and adaptation to chronic ER stress

The UPR is a pro-survival response in order to reduce the accumulation of unfolded proteins and restore normal ER functioning (Schroder and Kaufman 2005b). The three transmembrane signal transducers initiate and coordinate several protective responses. These responses include transcriptional induction of chaperones and foldases to increase the folding capacity of the ER (Kozutsumi et al. 1988), transcriptional induction of genes involved in ERAD (Oda et al. 2006) and stimulation of autophagy (Bernales et al. 2006). Transient attenuation of global protein synthesis (Wek and Cavener 2007) is assumed to decrease the amount of unfolded proteins in the ER. Furthermore, stimulation of phospholipid synthesis (Sriburi et al. 2007) to increase the ER size and induction of antioxidant response (Tu and Weissman 2004) to neutralize the generation of ROS are described in ER-stressed cells.

However, if protein accumulation is persistent and ER stress cannot be resolved, signaling switches from pro-survival to pro-apoptotic allowing the regulated destruction of cells that are irreversibly damaged or become a risk to the organism as a whole. But not all UPR signal transducers are involved in inducing programmed cell death. Although ATF6 is known to induce expression of pro-apoptotic transcription factor CHOP (Yoshida et al. 2000), no direct connection of ATF6 to ER stress-mediated apoptosis can be found. In the initial phase of ER stress, activation of PERK aids by inhibiting protein translation (phosphorylation of eIF2α) and therefore reducing the load of nascent proteins in the ER. Furthermore, it was shown that *PERK -/-* cells react to acute ER stress with more sensitivity indicating a link between PERK and survival (Harding et al. 2000b). However, after prolonged stress conditions PERK leads to the induction of CHOP, which is an important element in switching pro-survival to pro-apoptotic signaling. Overexpression of CHOP can cause cell death in the absence of additional apoptotic stimuli. Furthermore, CHOP expression is shown to be present in pathological activation of UPR, whereas CHOP deletion protects cells against ER stress mediated apoptosis, but only to a certain degree (Zinszner et al. 1998). Additionally, CHOP is regulated post-translationally by phosphorylation on S78 and S81 by p38 MAPK resulting in its increased activity (Wang and Ron 1996). This involves the second UPR signal transducer IRE-1, because IRE-1 has been linked to the activation of the pro-apoptotic c-jun N-terminal kinase (JNK) (Urano et al. 2000) and p38 MAPK (Van

Laethem et al. 2006). Furthermore, JNK and MAPK are known to be substrates of ASK1, which is recruited upon ER stress conditions to the IRE-1/TNF receptor activating factor 2 (TRAF2) complex (Fig. 1.4). Activation of JNK is a common response to many forms of cellular stress and is known to influence cell death by regulation of pro- and anti-apoptotic proteins of the Bcl-2 family (Tournier et al. 2000), whereas p38 MAPK, as described before, regulates the activity of CHOP.

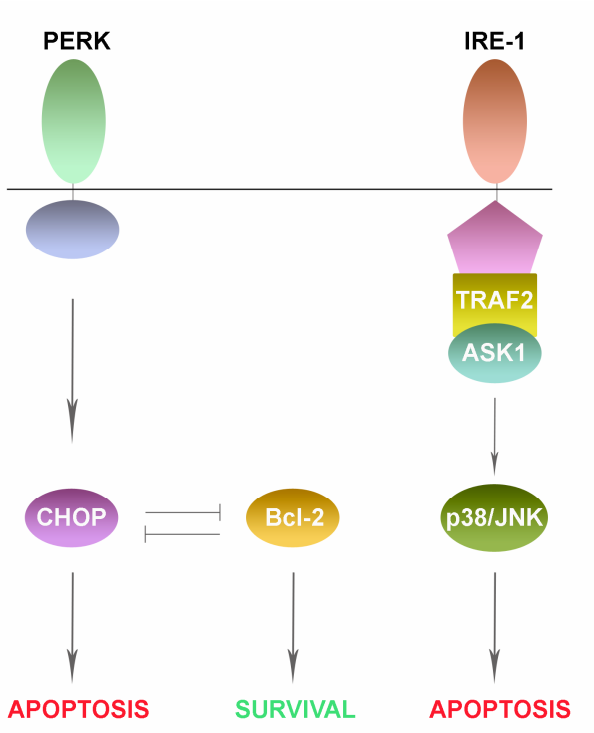

Fig. 1.4: UPR transducers involved in ER stress-mediated apoptosis. Under persistent ER stress the activation of PERK results in induction of pro-apoptotic transcription factor CHOP. Active IRE-1 has been shown to recruit the adaptor molecule TNF-receptor-associated factor 2 (TRAF2). The IRE-1–TRAF2 complex can recruit the apoptosis-signal-regulating kinase (ASK1), which has been shown to transmit various stress signals to the downstream MAPKs JNK and p38. Severe ER stress leads to activation of c-Jun N-terminal kinase (JNK). Both JNK and CHOP eliminate the anti-apoptotic effect of Bcl-2; CHOP blocks expression of Bcl-2, whereas JNK inhibits its activity by phosphorylation. Furthermore, overexpression of Bcl-2 is shown to block CHOP-induced apoptosis resulting in survival of the cell.

Chronic ER stress conditions can not only occur due to persistent expression of misfolded proteins or after viral infection. Even the normal differentiation and maintainance of cells with enhanced production and secretion of proteins, such as

immune cells, endocrine and paracrine cells or hepatocytes (van Anken and Braakman 2005) result in persistent activation of ER stress signaling pathways.

Another described possibility to cope with chronic stress conditions is the so-called heat shock response (HSR) (Liu and Chang 2008). Several genes induced by transcription factor heat shock factor 1 (HSF-1) are activated during both HSR and UPR conditions. In *Saccharomyces cerevisiae* it was shown that the BiP-homolog Kar2/BiP is upregulated under UPR and HSR conditions (Zimmer et al. 1999). Furthermore, stress-induced Hsps can inhibit apoptosis by blocking proteolytic activity of caspases or affecting caspase-independent apoptosis-like processes by interacting with apoptogenic factors such as apoptosis-inducing factor (AIF) or by inhibition of the release of cathepsines from lysosomes (Lanneau et al. 2008). In brief, one can say that HSR allows the survival of the cell by adapting to different stress conditions.

1.3 Conformational diseases

Conformational diseases or ER storage diseases are a class of disorders associated with aberrant protein accumulation in tissues and cellular compartments. To date, more and more diseases are discussed to be linked to ER stress and induction of UPR. Plenty of evidence suggests that ER stress plays a role in the pathogenesis of diabetes mellitus type I by contributing to pancreatic β-cell loss and insulin resistance (Accili et al. 1992). Components of UPR play a dual role in selective destruction of insulin-secreting β-cells by acting as beneficial regulators under physiological conditions or as triggers of β-cell dysfunction and apoptosis under conditions of chronic ER stress caused by large amounts of insulin. Furthermore, it could be shown that exposure to increased glucose levels induce ER stress markers in type II diabetes islet cells, which therefore may be more susceptible to ER stress induced by metabolic perturbations (Marchetti et al. 2007). The best known diseases connected with ER stress due to retention of misfolded proteins are cystic fibrosis (Kerem et al. 1989; Bartoszewski et al. 2008), due to intracellular retained cystic fibrosis conductance regulator (CFTR) and retinitis pigmentosa (Bareil et al. 2000; Ryoo et al. 2007), caused by misfolded rhodopsin leading to ER stress mediated apoptosis. Furthermore, renal ischemia-reperfusion is

described to induce ER stress. It activates UPR via the PERK pathway and causes cellular damage in the renal tubules (Montie et al. 2005). Interestingly, the congenital nephrotic syndrome of the Finnish type (CNF), an autosomal-recessive disorder characterized by massive proteinuria, is caused by intracellular retention of misfolded nephrin in the ER (Liu et al. 2001).

1.4 G protein-coupled receptors

G protein-coupled receptors (GPCRs) represent a large superfamily of heptahelical receptor proteins that regulate a wide variety of biological functions ranging from neurotransmission and hormonal control of physiological responses to sensing of taste, smell, light and pain. Because of their key roles in cellular signal transduction they are the most important class of drug targets in modern pharmacology and target for more than 60% of all currently prescribed drugs (Schoneberg et al. 2004). They can be activated by a variety of ligands such as amines (noradrenalin, dopamine, serotonin and histamine), peptides (angiotensin, vasopressin, opioids), amino acids (glutamate, GABA) or lipids (sphingosine-1-phosphate). After ligand binding the receptors undergo a conformational change that enables them to activate heterotrimeric GTP-binding proteins (G proteins) leading to the activation of different effectors and signaling pathways (Wickman and Clapham 1995). Heterotrimeric G proteins are composed of α-, β- and γ-subunits. Their activation leads to an exchange of GDP to GTP at the α-subunit resulting in conformational changes within the three flexible switch regions of Gα. The β/γ-subunit dissociates from the α-subunit and both, the GTP-bound Gα and the free Gβ/γ, can interact with a diversity of effector molecules including adenylyl cyclase, phospholipase C, ion channels, phosphodiesterase and the small G protein Rho. These effectors modulate the generation of diffusible second messengers altering cell function such as cAMP, diacylglycerol, inositol (1,4,5)-triphosphate or Ca^{2+}.

1.5 The V2 vasopressin receptor and nephrogenic diabetes insipidus

The human V2 vasopressin receptor (V2R) belongs to the family of GPCRs (Birnbaumer et al. 1992; Rosenthal et al. 1992) and is predominantly expressed in the basolateral membrane of principal cells in renal collecting ducts. The receptor consists of 371 amino acids and shares the typical structure of GPCRs, an extracellular N-terminus, seven transmembrane-spanning helices bridged by three intracellular and three extracellular loops and an intracellular C-terminus. After post-translational modification the mature receptor is glycosylated at asparagine 22 (N-glycosylation) and at clusters of serines and/or threonines (O-glycosylation) at the C-terminus (Sadeghi and Birnbaumer 1999), carries a disulfide bond between cysteine 112 in the first extracellular loop and cysteine 192 in the second extracellular loop and a palmitoylation at cysteines 341 and 342 (Schulein et al. 1996; Schulein et al. 2000).

The function of the V2R is the mediation of the antidiuretic action of its ligand, the cyclic nonapeptide 8-arginine-vasopressin (AVP). The neurohypophyseal hormone AVP is the key regulator of water homeostasis in the collecting duct. It is secreted in response to hypovolemia (by ≥ 10%) or increase in plasma osmolarity (by ≥ 2%) and transported by the blood to the kidney. The hormone also increases sodium transport in the collecting duct via the epithelial sodium channel (ENaC) (Bankir et al. 2005) and transfer of urea via the urea (UT-A1) transporter (Fenton et al. 2006). After ligand binding the V2R is subjected to a conformational change and activates a stimulating GTP-binding protein (G_S) (Fig. 1.5). G_S activates specific adenylyl cyclase isoforms in principal cells and GPCR kinases (GRKs). The adenylyl cyclase mediates the synthesis of the second messenger cAMP. The increase of cAMP acitivates the cAMP-dependent protein kinase A (PKA), which subsequently phosphorylates aquaporin 2 (AQP2) water channels. These channels are located in intracellular vesicles and fuse with the apical and basolateral membrane after AQP2 phosphorylation. The translocation and fusion of AQP2 results from the depolymerization of the F-actin cytoskeleton after inactivation of RhoA by PKA (Klussmann et al. 2001). The insertion of AQP2 in the apical membrane increases water influx. Water transport across the basolateral membrane is also facilitated by the constitutively expressed water channels AQP3 and AQP4. The driving force for this hormone-controlled antidiuresis is the osmotic gradient between collecting duct lumen and interstitium of the inner medulla (Klussmann et al. 2000).

In vitro studies have shown that phosphorylation of the receptor by GRK leads to recruitment and subsequent binding of cytosolic β-arrestins. β-arrestin functions as a scaffolding protein and prevents overstimulation by inhibition of further G protein mediated activation despite continued AVP activation. It also targets the receptor to clathrin-coated pits leading to subsequent endocytosis to endosomes (Ferguson 2001). In contrast to β-adrenergic receptors, the activated V2R is stably associated with β-arrestin and ubiquitin, sorted for degradation in lysosomes and does not recycle to the cell surface (Shenoy and Lefkowitz 2005).

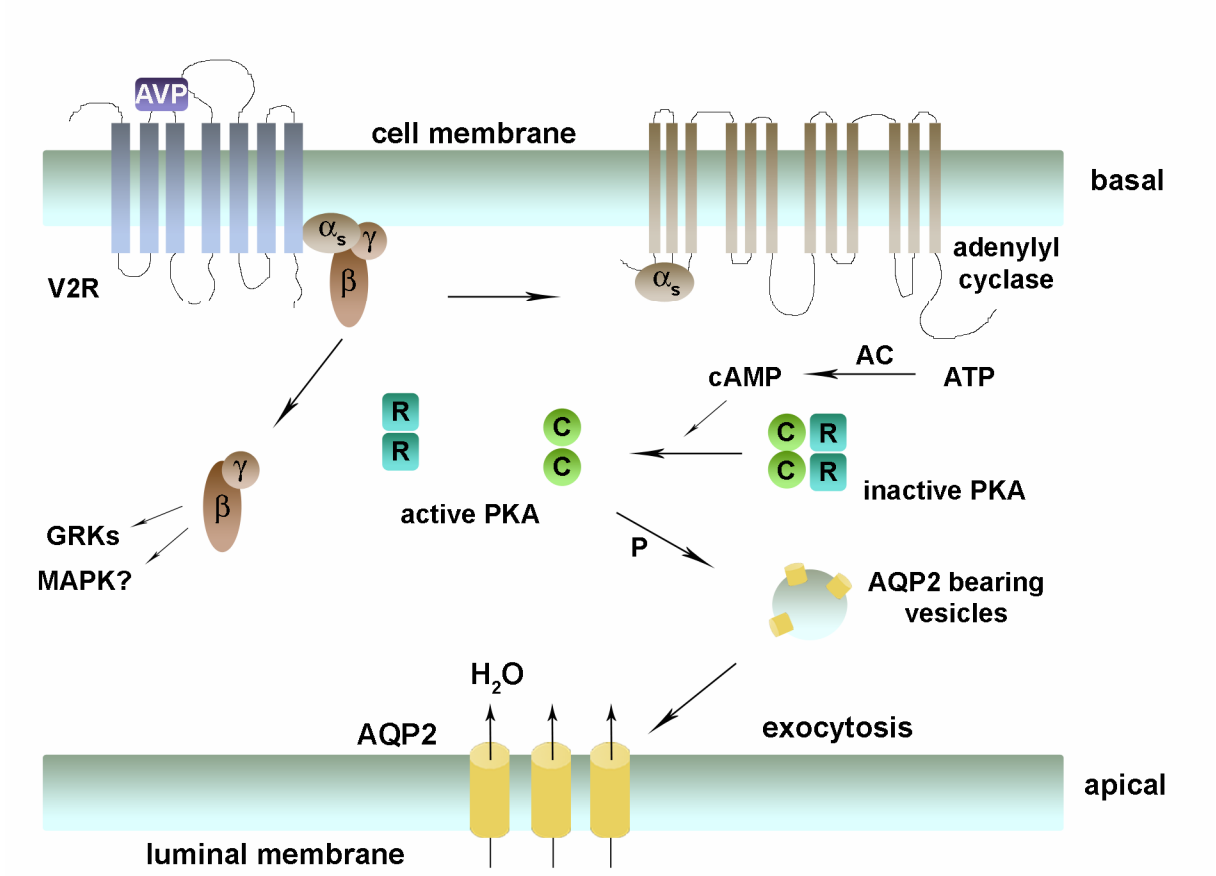

Figure 1.5: Signal transduction of the V2R in principal cells. Binding of the hormone AVP induces a conformational change of the receptor and activates the G protein Gs. The trimeric Gs dissociates in α and βγ subunits, which influence different signaling pathways. Subunit βγ activates GRKs, which contribute to receptor desensitation and most likely to activation of the MAPK pathway. The α subunit mediates activation of membrane associated adenylyl cyclase (AC) leading to production of the second messenger cAMP. In presence of cAMP protein kinase A (PKA) becomes activated by dissociation of its regulatory (R) and catalytic (C) subunits. Active PKA subsequently phosphorylates AQP2 water channels

and facilitates exocytosis and assembly of AQP2 into the apical and basolateral membrane resulting in increased water influx.

Malfunctioning of regulation of water homeostasis can cause a variety of disorders. One example is diabetes insipidus (DI), in which patients are unable to concentrate their urine leading to polyuria (up to 20 l a day) and as a consequence to polydipsia. Central diabetes insipidus (CDI) is characterized by the inability to produce functional AVP, whereas nephrogenic diabetes insipidus (NDI) is referred to the failure of patients to concentrate their urine, despite increased serum AVP levels. NDI can be caused by metabolic disorders, like potassium depletion or hypercalcemia, chronic renal diseases, systemic diseases, like amyloidosis or as side effect of drugs like lithium (Bichet et al. 1997).

Congenital NDI can be divided into X-linked (due to inactivating mutations of the *AVPR2* gene) and autosomal NDI (due to inactivating mutations in the *AQP2* gene). Congenital X-linked NDI is a rare hereditary disorder (estimated prevalence of 1 per 250,000 males) and characterized by the inability of the kidney to absorb water in response to the hormone AVP. More than 211 different mutations within the coding sequences of the *AVPR2* gene are known to cause X-linked NDI (http://www.medicine.mcgill.ca/nephros). These mutations can be classified into three classes according to the state of function and intracellular localization of the mutant proteins (Fujiwara and Bichet 2005). Type 1 receptor mutants reach the cell surface but are incapable of binding the ligand appropriately, type 2 mutant receptors are transport-defective and mutations of the type 3 lead to improperly processed or unstable mRNA and rapid degradation. Some disease-causing and intracellular retained V2R mutants, which are analyzed in this study, are summarized in Tab. 1 and shown in Fig. 2. They are recognized by the cellular quality control system and retained in different compartments within the secretory pathway depending on the folding state of the receptors (Hermosilla et al. 2004). NDI-causing mutant L62P (amino acid exchange localized in the first transmembrane domain) is retained almost completely in the ER, InsQ292 (insertion localized in the transmembrane domain 7) is found in the ER, but also in the ERGIC, while G201D (amino acid exchange localized in the extracellular loop 3) could be found in the ER, ERGIC and in the Golgi apparatus (Tab. 1.1 and Fig. 1.6).

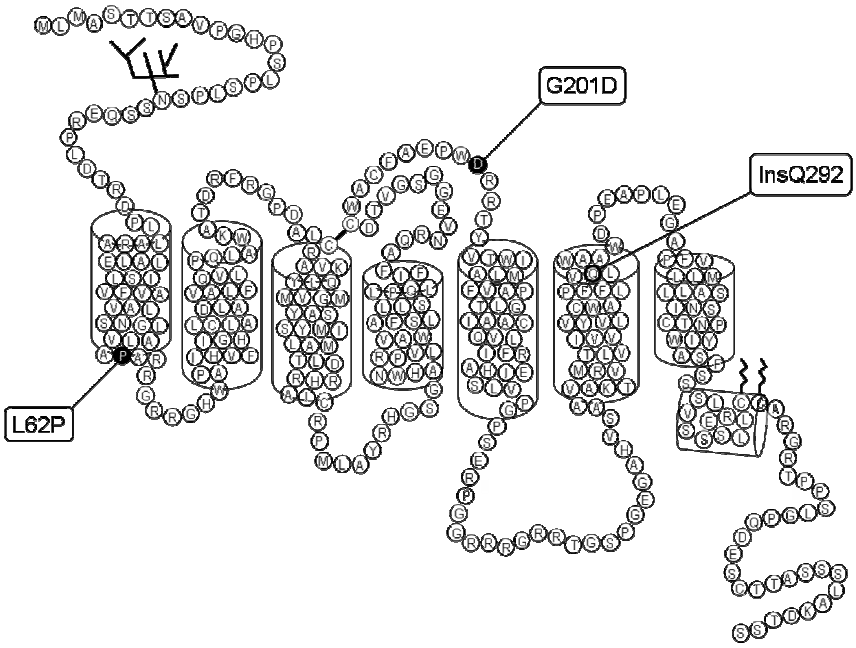

Fig. 1.6: Two-dimensional model of the V2R and three studied NDI-causing mutants. The amino acid sequence of the receptor is shown in one letter code, N-glycosylation at position N22, disulfide bond between C112 and C192 and palmitoylation of residues C341 and C342 are depicted. Substituted (L62P, G201D) and inserted (InsQ292) amino acids of mutants are highlighted. The columns indicate the estimated transmembrane regions of the receptor.

mutation	location	retention site	reference
L62P	TM1	ER	Schülein et al., 1998
G201D	ECL3	ER, ERGIC, Golgi	Schwieger et al., 2008
InsQ292	TM7	ER, ERGIC	Schwieger et al., 2008

Tab. 1.1: Overview of location and retention site of studied NDI-causing mutants.

The most important treatment for NDI is sufficient supply of fluid. As pharmacological therapy, diuretics such as hydrochlorothiazide alone or in combination with inhibitors of prostaglandin synthesis are used, together with a low-salt diet. However, these approaches are not always sufficient, particularly long-term use is often associated with

gastrointestinal and hematopoietic side effects. Some future therapy possibilities are aminoglycoside antibiotics (Schoneberg et al. 2004) or the use of so-called pharmacological chaperones (pharmacochaperones) in order to rescue intracellular V2R mutants to the plasma membrane with the help of cell-permeable V2R antagonists (Wuller et al. 2004) or V1R inverse agonists (Bernier et al. 2004; Bernier et al. 2006)are discussed.

2 Aims of the study

The aim of this thesis was to detect and characterize the ER stress induced upon expression of misfolded proteins, which only differ in the location of one substituted or inserted amino acid. The human vasopressin receptor (V2R) was used as a model to determine if different retention sites of one specific, misfolded protein result in the induction of ER stress and therefore lead to different responses of the cell. Usually, ER stress is examined after induction with chemical agents. Little is known about ER stress responses induced by misfolded and intracellularly retained proteins. In addition, temporal differences in ER stress induction (acute/chronic) were examined to distinguish between acute and chronic UPR activation. Furthermore, another intention of this study was to reduce ER stress by a removal of retained proteins and to elucidate possible signaling pathways which support the survival of the cell under persistent ER stress conditions in order to find new and promising therapy approaches for NDI and other conformational diseases in general.

3 Materials and methods

3.1 Materials

3.1.1 Reagents, chemicals and substances

1 kb DNA ladder	Invitrogen, USA
1,4-dithiothreitol	BioVectra, CAN
2-mercaptoethanol	Carl Roth, GER
2,2-diphenyl-1-picrylhydrazil (DPPH)	Sigma, USA
acetic acid	VWR Prolabo, F
agar	Life Technologies, GER
agarose	Sigma, USA
albumin standard 2.0 mg/ml	Pierce USA
ammonium persulfate	Merck, GER
ampicillin sodium salt	Sigma, USA
aprotinin	Merck, GER
benzamidine	Applichem, USA
bovine serum albumin (BSA)	Sigma, USA
bromphenol blue	Carl Roth, GER
cacodylic acid sodium salt	Carl Roth, GER
chemoluminescence detection kit for horseradish peroxidase (HRP)	Applichem, USA
Coomassie G250 brilliant blue	Serva, GER
D-(+)-sucrose	Carl Roth, GER
dimethylsulfoxide (DMSO)	Applichem, USA

dried milk powder (low fat)	Applichem, USA
Dulbecco's modified Eagle's media (DMEM)	Sigma, USA
ethanol	J. T. Baker, NL
ethidium bromide	Carl Roth, GER
ethylenediaminetetraacetic acid (EDTA)	Sigma, USA
fetal calf serum (FCS)	Biochrom, GER
FuGENE® HD	Roche, CH
Geneticin (G-418)	Calbiochem, USA
GeneChip® Human Genome U133 Plus 2.0 Array	Affymetrix, USA
glucose	Merck, GER
glutaraldehyde	Sigma, USA
glycerine	Applichem, USA
glycine	Applichem, USA
H_2O_2	Roth, CH
HCl	J. T. Baker, NL
HPLC dH_2O	Pierce, USA
Immu-Mount™ mounting medium	Thermo Shandon, USA
isopropanol	Merck, GER
kanamycin	Sigma, USA
L-glutamine	Sigma, USA
Lipofectamine™ 2000 reagent	Invitrogen, USA
magnesium chloride	Merck, GER
magnesium sulfate	Merck, GER
methanol	J. T. Baker, NL

nitrocellulose membrane (Optitran BA-S 85)	Schleicher & Schuell, GER
N, N, N', N' – tetramethylethylene diamine	Sigma, USA
N-tert-butyl phenylnitrone (PBN)	Sigma, USA
orthophosphoric acid	Merck, GER
PageRuler unstained protein ladder	Fermentas, CAN
paraformaldehyde	Merck, GER
penicillin/streptomycin 100 IU/100 µg/ml	Biochrom, GER
phenylmethylsulfonyl fluoride (PMSF)	Carl Roth, GER
PI-103	Calbiochem, USA
poly-L-lysine	Sigma, USA
polyvinylalcohol	Sigma, USA
polyvinylpyrrolidone K25	Fluka, GER
ponceau S	Roche, CH
potassium chloride	Merck, GER
potassium dihydrogenphosphate	Merck, GER
Precision Plus protein Dual Color standards	BioRad, USA
protein A-sepharose	Sigma, USA
PstI restriction enzyme	NEB, USA
Roti®-load 1	Carl Roth, GER
Rotiphorese-gel 30 (37.5:1)	Carl Roth, GER
sodium chloride	Applichem, USA
sodium dihydrogenphosphate	Merck, GER
sodiumdodecyl sulfate (SDS)	Applichem, USA

sodium fluoride	Merck, GER
sodium hydroxide	Carl Roth, GER
sodium pyrophosphate	Sigma, USA
sodium orthovanadate	Sigma, USA
sulfosalicylic acid	Applichem, USA
Taq polymerase	Fermentas, CAN
Taq 10x buffer without $MgCl_2$	Fermentas, CAN
thapsigargin	Sigma, USA
tumor necrose factor α (TNFα)	R&D Systems, USA
tungstosilicic acid hydrate	Fluka, GER
tunicamycin	Sigma, USA
trichloroacetic acid	Merck, GER
tris(hydroxymethyl-)aminomethan	Applichem, USA
triton X-100	Carl Roth, GER
trypan blue	Promega, USA
trypsin/EDTA 10x (0.5 %/0.2 % w/v)	Biochrom, GER
trypsin inhibitor, soybean	Applichem, USA
tryptone	Applichem, USA
Tween® 20	Applichem, USA
wortmannin	Merck, GER
yeast extract	GIBCO, USA

3.1.2 Primary antibodies

monoclonal mouse anti-actin antibody	Sigma, USA
polyclonal rabbit anti-ATF6 antibody	Santa Cruz, USA
polyclonal rabbit anti-Bcl-2 antibody	Cell signalling, USA
polyclonal rabbit anti-GRP78 antibody	Stressgen, USA
polyclonal rabbit anti-calnexin antibody	Stressgen, USA
polyclonal rabbit anti-calreticulin antibody	Stressgen, USA
polyclonal rabbit anti-eIF2α antibody	Santa Cruz, USA
polyclonal rabbit anti-ERp57 antibody	Stressgen, USA
monoclonal mouse anti-Ero1α antibody	abcam, USA
polyclonal rabbit anti-phospho-eIF2α antibody	Biosource, USA
monoclonal mouse anti-GFP antibody	Clontech,USA
polyclonal rabbit anti-GFP antibody	Clontech,USA
monoclonal rat anti-GRP94 antibody	Stressgen, USA
polyclonal rabbit anti-Hsp70 antibody	Stressgen, USA
polyclonal rabbit anti-Hsp90 antibody	Stressgen, USA
monoclonal mouse anti-KDEL antibody	Stressgen, USA
polyclonal rabbit anti-NF-κB p65 antibody	Santa Cruz, USA
polyclonal rabbit anti-PDI antibody	Stressgen, USA
polyclonal rabbit anti-PERK antibody	Santa Cruz, USA
polyclonal rabbit anti-phospho-PERK antibody	Santa Cruz, USA
polyclonal rabbit anti-thioredoxin antibody	abcam, USA

3.1.3 Secondary antibodies

cy-3 conjugated goat anti-mouse IgG	Dianova, USA
cy-3 conjugated goat anti-rabbit IgG	Dianova, USA
gold (15 nm) labeled goat anti-rat IgG	Biotrend, GER
peroxidase-conjugated donkey anti-goat IgG	Dianova, USA
peroxidase-conjugated donkey anti-mouse IgG	Dianova, USA
peroxidase-conjugated donkey anti-rabbit IgG	Dianova, USA
peroxidase-conjugated donkey anti-rat IgG	Dianova, USA

3.1.4 Technical equipment and software

3.1.4.1 Technical equipment

acrylamide-gel cast-stand	BioRad, USA
acrylamide-gel electrophoresis chamber	BioRad, USA
Affymetrix GeneChip® Scanner 3000 7G	Affymetrix, USA
cell counter	Casy®1, Schärfe Sytem, GER
centrifuge	Mikro 20; Hettich, GER
centrifuge, refrigerated	Z 233 MK; Hermle, GER
clean bench	BIOWIZARD, KOJAIR, Heraeus, GER
cryo-ultramicrotome	EM FC6, Leica Microsystems, AT
electron microscope	80kV ZEISS 902 A electron microscope, Carl Zeiss, GER

films	X-OMAT Röntgenfilme; KODAK, GER
incubator	Heraeus, GER
luminometer	Lumat LB 9507, EG&G Berthold, GER
microscope	Laser Scanning Microscope Zeiss 510 META; Carl Zeiss, GER
PCR machine	PTC-200 Peltier Thermal Cycler; MJ Research, USA
pH-meter	MP220 Mettler Toledo, CH
photometer	Gene Quant II; Pharmacia Biotech, GER
pipettes	Eppendorf, GER
power supply	BioRAD, USA
sonicator	Sonopuls UW 2040, Bandelin Electronics, GER
thermomixer	Eppendorf, GER
western blot chamber	BioRad, USA

3.1.4.2 Software

Axio Vision	Zeiss, GER
Corel PHOTO-PAINT 9	Corel Corporation
EndNote 7.0	Thomson ResearchSoft, USA
Excel 2000	Microsoft, USA
GeneChip® Operating Software	Affymetrix, USA
Photoshop 7.0	Adobe, USA
PowerPoint 2000	Microsoft, USA
PRISM 3.1	Graphpad Software, USA

Word 2000	Microsoft, USA

3.1.5 Kits

Dual-Luciferase® Reporter Assay System	Promega, USA
ImProm-II™ Reverse Transcription System	Promega, USA
Invisorb® Spin Cell Mini Kit	Invitek, GER
Qproteome cell compartment Kit	Qiagen, GER
RNeasy® Plus Mini Kit	Qiagen, GER
Eukaryotic Poly-A RNA Control Kit	Affymetrix, USA
One-Cycle cDNA Synthesis-Kit	Affymetrix, USA
Sample Cleanup Module	Affymetrix, USA
GeneChip® IVT Labeling Kit	Affymetrix, USA
GeneChip® Hybridization control Kit	Affymetrix, USA
GeneChip® Hybridization, Wash and Stain Kit	Affymetrix, USA
MycoAlert® Mycoplasma detection assay	Lonza, CH

3.1.6 Oligonucleotides

XBP-1 F 5’ A AAC AGA GTA GCA GCT CAG ACT GC 3'

XBP-1 R 5’ TC CTT CTG GGT AGA CCT CTG GGA G 3'

3.1.7 Vectors

Vector	Kindly provided by
P4xXBP1GL3	L. Glimcher, USA
pEGFP.ATF6 full	R. Prywes, USA
pERdj4GL3	L. Glimcher, USA
pGAD153-luc	S. Howell, USA
pGL3.NFκB	R. Burgos, CL
phRL-TK	D. Carstanjen, GER
pGL3.GRP78	K. Mori, JP
pGL3.GRP78mut	K. Mori, JP
pcDNA3.1	Invitrogen, USA
pEGFP.N1	Invitrogen, USA
pV2R.GFP	R. Schülein, GER
pL62P.GFP	R. Schülein, GER
pInsQ292.GFP	A. Oksche, GER
pG201D.GFP	R. Schülein, GER

3.2 Methods

All buffers and solutions were prepared with deionised water (dH_2O) and stored at 4℃.

3.2.1 Cell cultivation techniques

3.2.1.1 Tissue culture cell lines and storage

Media

complete medium	DMEM	450 ml
	heat-inactivated FCS	10% (v/v)
	glutamine	20 mM

	penicillin	100 IU
	streptomycin	100 µg/ml
complete medium + G418	Complete medium	500 ml
	G-418	80 mg/ml
medium for transfection	DMEM	450 ml
	heat-inactivated FCS	10% (v/v)
	glutamine	20 mM

Cells

HEK293 (Human embryonic kidney cells adenovirus type 5 transformed)	DSMZ, GER

HEK293 cells were grown in DMEM supplemented with 10% (v/v) heat-inactivated FCS, 20 mM glutamine, 100 U/ml of penicillin and 100 µg/ml streptomycin at 37℃ (complete medium) in a humidified atmosphere (95% air / 5% CO_2). The stably expressing HEK293 cell clones were additionally maintained with G-418 (80 mg/ml). For sub culturing the confluent cell monolayers were splitted every 3-4 days using 1 ml trypsin/EDTA solution (0.05% / 0.02%) for 4 min at 37℃ to detach the cells followed by addition of 5 ml complete medium to inactivate trypsin. The seeding densities were 1 x 10^6 cells/25 cm^2 flask or 60 mm dish, 2.5 x 10^6 cells/100 mm dish, 1 x 10^5 cells/35 mm dish and 0.5 x 10^5 cells/well of a 24-well plate. Cells were tested for infection of mycoplasma every four weeks with the MycoAlert® Mycoplasma detection assay (Lonza, Switzerland).

3.2.1.2 Transient and stable transfections

For transfection of HEK293 cells the FuGENE® HD transfection reagent was used according to the manufacturer's instructions. Cells were grown in a 60 mm culture dish to 80% confluence and the growth medium was replaced by 5 ml complete medium without antibiotics. 4 µg of plasmid DNA were diluted in 250 µl of serum-free medium and incubated with 8 µl of FuGENE® HD for 15 min (RT). The transfection mixture was added by dropping to the culture dish containing cells and medium. Cells were incubated for 6 to 48 h in a CO_2 incubator at 37°C.

To generate stably expressing cell lines the stable transfectants have to be selected by a resistance marker located on the inserted plasmid. For selection G-418 was used, an aminoglycoside antibiotic which is toxic for cells without resistance. Cells were grown in 35 mm culture dishes until 90% of confluence. The growth medium was replaced by 2 ml complete medium without antibiotics. Transfection with FuGENE® HD was carried out according to the manufacturer's instructions. After 48 h cells were transferred into a 60 mm culture dish containing 4 ml of complete medium supplemented with G-418. After 24 h cells which did not incorporate the plasmid in their genomic DNA started to die. G-418 supplemented medium was changed every day. After one week the remaining cells were detached with 1 ml trypsin/EDTA solution (0.05%/0.02%) and diluted with complete medium containing G-418 to a volume of 8 ml. 1 ml of this suspension was diluted to a volume of 8 ml with medium (solution A) and the dilution series was continued in an analogous manner until solution G. The different dilutions of cells were transferred to 24-well plates by distributing 1 ml of every dilution in the six wells of the different rows. The complete medium with G-418 was exchanged every second day. After two weeks single colonies of cell clones were visible in some wells. These colonies were isolated and cultivated in 35 mm culture dishes until confluence. Subsequently, the cells were transferred to a 25 cm^2 flask and simultaneously grown on glass cover slips to screen for clones with homogenous expression and clones with different levels of protein expression by life cell imaging.

3.2.1.3 Microscopy

Reagents and solutions

poly–L–lysine stock solution	poly- L–lysine	5 mg
	dH_2O	50 ml
working solution	poly–L–lysine stock solution	10 ml
	dH_2O	ad 40 ml

1 x 10^5 HEK293 cells stably expressing GFP-tagged wild type and mutant V2Rs were grown for 24 to 48 h in a 35 mm culture dish containing a poly-L-lysine coated glass cover slip (Ø 25 mm). For microscopic studies cells were transferred into a heating chamber and covered with 1 ml PBS. The GFP fluorescence was visualized on a Zeiss 510 invert confocal LSM (optical section: < 0.9 µm; single track mode; GFP, λ_{exc}: 488 nm, BP filter: 494 – 548 nm).

3.2.2 DNA techniques

Strains

Escherichia coli (*E.coli*) DH5-α genotype Life Technologies, USA

F-φ80lacZ ΔM15 Δ(lacZYA-argF) U169 endA1 recA1 hsdR17 (rk-,mk+) supE44 thi-1 gyrA96 relA1 phoA

Media and solutions

LB medium	tryptone	1%
	yeast extract	0.5%
	NaCl	1%

	dH_2O, pH 7.5	ad 1 l
$MgCl_2$ / $MgSO_4$ 2 M	$MgCl_2$	20.33 g
	$MgSO_4$	24.65 g
	dH_2O	ad 100 ml
glucose solution 1 M	glucose	18 g
	dH_2O	ad 100 ml
SOC medium	tryptone	10 g
	yeast extract	2.5 g
	NaCl	300 mg
	KCl	250 mg
	dH_2O	485 ml
	pH 7.0	
	autoclave 15 min, 121℃	
add sterile filtered	$MgCl_2$ / $MgSO_4$ 2 M	5 ml
	glucose 1 M	10 ml

Selection

Liquid culture

LB medium supplemented with ampicillin (100 µg/ml) or kanamycin (30 µg/ml)

Agar plates

LB medium supplemented with 1.5% agar and ampicillin (100 µg/ml) or kanamycin (30 µg/ml)

3.2.2.1 Preparation of chemically competent cells

Reagents and solutions

SOB medium	tryptone	20 g
	yeast extract	5 g
	NaCl 5 M	2 ml
	KCl 2 M	1.25 ml
	dH_2O	990 ml
	autoclave 15 min, 121℃	
add before use	Mg Cl_2 2 M	10 ml
TB buffer	PIPES	10 mM
	$CaCl_2$ x 2 H_2O	15 mM
	KCl	250 mM
	$MnCl_2$ x 4 H_2O	55 mM
	dH_2O	990 ml
	pH 6.75	

The *E. coli* DH5-α genotype was selected for the production of competent cells to achieve high cloning efficiency. The method leads to vacancies in the bacterial membranes which enables the competent cells to take up exogenous plasmid DNA.

Day 1

DH5-α bacteria were cultured on an agar plate without antibiotics in an incubator at 37℃ overnight.

Day 2

One single bacteria colony was used to inoculate 5 ml LB medium without antibiotics. The liquid culture was agitated at 220 rpm at 37℃ for 16 h (preparatory culture).

Day 3

20 µl preparatory culture were used to inoculate 400 ml SOB medium at noon, the liquid culture was grown by shaking at 220 rpm at 18℃ for two nights.

Day 5

The growth stadium of the liquid culture was controlled by measurement of the optical density. DH5-α bacteria were grown until an OD_{550} of 0.4 to 0.6 which indicates the log-phase of exponential growing. After harvesting by centrifugation at 2,500 x g for 15 min at 4℃, the pellet was resuspended in 140 ml ice-cold TB buffer and incubated for 10 min on ice. Cells were pelleted by a second centrifugation step (2,500 x *g*, 15 min, 4℃), the supernatant was removed and cells were resuspended in 34.6 ml TB buffer supplemented with 7% DMSO. Cells were incubated for 30 min on ice and aliquots of 200 µl competent cell suspension were directly frozen into a N_2 bath. Competent cells were stored at -80℃.

3.2.2.2 Transformation of *E. coli*

Chemically competent cells were thawn on ice, and 500 ng of plasmid DNA were added and mixed carefully. After 30 min of incubation on ice, the samples were heated for 45 s to 42℃ and placed on ice for additional 2 min for DNA uptake. 400 µl SOC medium (without antibiotics) were added and the bacteria suspensions were incubated for further 30 min with vigorous shaking (600 rpm). For selection, 50 to 75 µl of bacteria culture were spread on agar plates containing the appropriate antibiotic (ampicillin (100 µg/ml) or kanamycin (30 µg/ml)). The agar plates were kept at 37℃ overnight.

3.2.2.3 Plasmid isolation from *E. coli*

One single bacteria colony was used to inoculate 3 ml LB medium supplemented with antibiotics (depending on the plasmid, (ampicillin (100 µg/ml) or kanamycin (30 µg/ml)). The liquid culture was agitated at 220 rpm at 37℃ for 16 h. 2 ml suspension were transferred into 2 ml tubes and bacteria were pelleted by centrifugation (13,000 x *g*, 1

min, RT), the supernatants were discarded. The pellets were stored at -20℃ or directly used for plasmid isolation.

The isolation of plasmid DNA was carried out with the Invisorb® Spin Cell Mini Kit from Invitek according to manufacturer's instructions. Pellets were resuspended by vortexing in 250 µl solution A. Cells were lysed by adding of 250 µl solution B and the tubes were carefully inverted 5 times. After a 4 min incubation, 250 µl solution C was added to the mixtures and the tubes mixed by gently shaking 5 times. For separation of plasmids and debris of bacteria, samples were centrifuged for 5 min at 13,000 x *g* and the clarified supernatant was transferred by decanting to a spin filter placed in a 2 ml tube. After incubation of 1 min the tube was centrifuged for 1 min at 10,000 x *g* at RT to isolate the plasmid DNA absorbed on the spin filter. The filtrate was discarded and bound DNA was washed by addition of 750 µl wash solution and subsequent centrifugation for 1 min at 10,000 x *g*. Another centrifugation step for 3 min at full speed was performed to remove residual ethanol. Spin filters were placed in new tubes and 70 µl HPLC dH_2O were added directly onto the spin filter surface. After incubation for 1 min a final centrifugation step at 10,000 x *g* for 1 min was used to elute the plasmid DNA.

After isolation of plasmid DNA the amount of eluted DNA has to be determined spectrophotometrically by measuring the absorbance of the sample at 260 nm. Therefore 2 µl of DNA was diluted with 78 µl dH_2O and quantified.

The purity of DNA was checked by determination of the ratio between absorptions at 260 and 280 nm, whereas A_{260}/A_{280} ratio should be ≥ 1.7.

3.2.2.4 Restriction analysis for quality control after plasmid isolation

Reaction mix

plasmid DNA	500 ng
NEB buffer 10x	2 µl
NEB 10x BSA	2 µl
restriction endonucleases	0.5 µl each
dH_2O	ad 20 µl

To check the accuracy of the isolated plasmid a restriction analysis of each isolated plasmid was performed. 500 ng of DNA were digested with the appropriate pair of restriction endonucleases and the obtained fragments were subsequently analysed by agarose gel electrophoresis.

3.2.2.5 Agarose gel electrophoresis

Reagents and solutions

TAE buffer	Tris	4.84 g
	acetic acid	1.197 g
	EDTA 0.5 M (pH 8)	2 ml
	dH_2O	ad 1 l
electrophoresis buffer	ethidium bromide 1%	5 µl
	TAE buffer	ad 100 ml

The size and quality of isolated plasmid DNA was controlled by agarose gel electrophoresis on a 1% agarose gel at 80 mV and subsequent staining of the gel with ethidium bromide for 20 min. To visualize the bands the agarose gel was examined under UV light and the size of the fragment was determined by the use of the 1 kb DNA ladder.

3.2.3 RNA techniques

3.2.3.1 Isolation of total RNA

The total RNA was isolated from 1 x 10^6 HEK293 cells and HEK293 cells stably expressing the GFP-tagged and FLAG-tagged V2R and mutant V2R fusion proteins grown on confluent 35 mm culture dishes with the RNeasy plus mini Kit from Qiagen according to the manufacturer's instructions. After aspiration of media und 2 times washing with PBS cells were lysed by addition of 350 µl RLT Plus buffer. The lysate was homogenized by 5 times passing through a syringe with a 20-gauge needle and afterwards transferred to a gDNA Eliminator spin column to remove gDNA. After centrifugation (30 s, 8,000 x *g*, RT) one volume of 70% ethanol was added to the flow-trough and mixed by pipetting. Subsequently the sample was transferred to an RNeasy spin column placed in a 2 ml collection tube and centrifuged for 15 s at 8,000 x *g* at RT. The flow-through was discarded and the bound total RNA was washed by addition of 700 µl buffer RW1 and centrifugation (15 s, 8,000 x *g*, RT). Two additional washing steps were performed each time with 500 µl buffer RPE, supplemented with four volumes of ethanol and centrifugation (15 s, 8,000 x *g*, RT and 2 min, 8000 x *g*, RT). The long centrifugation step dries the spin column membrane, ensuring no ethanol is carried over during RNA elution. Spin filters were placed in new tubes and 50 µl RNase-free dH_2O were added directly onto the spin filter surface. After incubation for 1 min a final centrifugation step at 8,000 x *g* for 1 min was used to elute the RNA.
After elution the amount of total RNA has to be determined spectrophotometrically by measuring the absorbance of the sample at 280 nm. Therefore 2 µl of RNA was diluted with 78 µl RNase-free water and quantified.
The purity of RNA was checked by determination of the ratio between absorptions at 260 and 280 nm, whereas A_{260}/A_{280} ratio should be ≥ 1.9.

3.2.3.2 Reverse transcription and XBP-1 PCR

RNA was reverse transcribed to cDNA by RT-PCR with the ImProm-II™ Reverse Transcription System from Promega according to the manufacturer's instructions.

Hybridization reaction mix

total RNA	1 µg
oligo(dT)$_{15}$ primer 0.5 µg/µl	1 µl
RNase-free water	ad 5 µl

For denaturation and hybridization of RNA and primers the reaction mixture was preheated to 70°C for 5 minutes and immediately pla ced in ice-water for 10 minutes.

ImProm-II™ 5x reaction buffer	4 µl
$MgCl_2$, 25 mM	2 µl
dNTP mix, 10 mM	1 µl
Recombinant RNasin® Ribunuclease Inhibitor	0.5 µl
ImProm-II™ Reverse Transcriptase	1 µl
nuclease-free H_2O	ad 15 µl

cycles	temperature	time
1	94℃	2 min
2-25	94℃	1 min
	60℃	1 min
	72℃	2 min
	72℃	5 min
	4℃	∞

After generation of cDNA, the product was used as a template for the PCR with specific XBP-1 primers.

Reaction:

10x Taq reaction buffer	2 µl
cDNA template	1 µl
Primer XBP-1 F 10 µM	1 µl
Primer XBP-1 R 10 µM	1 µl
dNTPs 2.5 µM	2.5 µl
$MgCl_2$ 25 mM	3 µl
dH_2O	to 50 µl
Taq polymerase	0.5 µl

Cycling parameters:

cycles	temperature	time
1	94℃	4 min
2-35	95℃	10 s
	60℃	30 s
	72℃	30 s
	72℃	10 min
	4℃	∞

Subsequently, PCR was carried out using the specific primer sets for *XBP-1* (XBP-1 F 5’ A AAC AGA GTA GCA GCT CAG ACT GC 3' and XBP-1 R 5’ TC CTT CTG GGT AGA CCT CTG GGA G 3'). PCR products were analyzed on a 3% agarose gel under UV light after staining with ethidium bromide to separate the spliced and unspliced form of XBP-1.

3.2.3.3 Restriction analysis of the XBP-1 PCR product

Reaction mixture

DNA (PCR product)	15 µl
NEB buffer 3 10x	2 µl
NEB 10x BSA	2 µl
PstI	0.5 µl
dH_2O	ad 20 µl

15 µl of the XBP-1 PCR product were used for restriction analysis with PstI. After 1 h incubation at 37℃ the sample was separated and ana lysed on a 3% agarose gel under UV light after staining with ethidium bromide. The size of the PCR fragments was determined by the use of a 1 kb DNA ladder.

3.2.3.4 Micro array

Total RNA was extracted from HEK293 cells using the RNeasy total RNA isolation Kit (Qiagen). The preparation quality was assessed by agarose-formaldehyde gel electrophoresis. 5 µg of RNA isolated from two different clones each of stably transfected HEK293 cells expressing the wild type V2R and mutant L62P tagged with FLAG were labeled with the One-Cycle Target Labeling and Control Reagent Package (Affymetrix), as described in the manufacturer's instructions. Briefly, double-stranded cDNA was synthesized using the One-Cycle cDNA Synthesis Module. Biotinylated cRNA was generated using the IVT labeling kit and cleaned up using the sample cleanup module. After fragmenting of the cRNA for target preparation using the standard Affymetrix protocol, 15 µg fragmented cRNA was hybridized for 16 hours at 45℃ to Affymetrix Human Genome U133 Plus 2.0 arrays, which carry probes representing 47,000 gene sets. Following hybridization, arrays were washed and stained with streptavidin-phycoerythrin in the Affymetrix Fluidics Station 450 and further scanned using the Affymetrix GeneChip Scanner 3000 7G. The image data were analyzed with GCOS 1.4 using Affymetrix default analysis settings. After verification of correlation, a batch analysis was carried out. Subsequently, up- and down regulated genes were analyzed and listed by use of DAVID (http://niaid.abcc.ncifcrf.gov/).

3.2.4 Protein techniques

3.2.4.1 Protein quantification by Bradford

Coomassie reagent (Bradford reagent)	Coomassie brilliant blue G250	100 mg
	ethanol 96%	50 ml
	phosphoric acid 85%	100 ml
	H_2O	ad 1 l
(BSA) 1 mg/ml	albumine standard Pierce 2 mg/ml	500 µl
	H_2O	500 µl
2 N NaOH	NaOH	80 g
	H_2O	ad 1 l

The amount of total protein was measured by the Bradford assay. The colorimetric determination is based on an absorbance shift in the dye Coomassie Brilliant Blue G-250 when bound to arginine and hydrophobic amino acid residues present in proteins under alkaline conditions. The samples were prepared in duplicates and compared with a BSA standard curve. Whole cell lysates (5 µl) were prepared with 45 µl dH_2O and denaturated with 50 µl 2 M NaOH. The BSA standard curve was established by mixing 0, 1, 2, 5, 10, 20, and 40 µg BSA (stock solution 1 mg/ml) with dH_2O, 5 µl RIPA buffer and 50 µl of 2 M NaOH. Both samples and standard mixtures were heated to 60℃ for 10 min, after 2 min at RT they were mixed with 1 ml of the Bradford reagent and the absorption was measured in a 96-well plate at 595 nm. Unknown protein concentrations were interpolated using the 3-parameter polynomial equation of the standard curve. The unknown protein concentration has to be in the range of the BSA standard curve.

3.2.4.2 Total cell lysis

Buffers and solutions

PBS	NaCl	137 mM
	KCl	2.7 mM
	$Na_2HPO_4x\ 2H_2O$	8.1 mM
	KH_2PO_4	1.5 mM
	pH 7.4	
protease inhibitor mix	STI (trypsin inhibitor)	2 µg/ml
	aprotinin	1 µg/ml
	benzamidine	100 mM
PMSF stock solution	PMSF	100 mM
	ethanol	ad 10 ml
RIPA buffer	Tris-HCl ph 7.5	10 mM
	NaCl	100 mM
	triton X-100	1%
	Na-deoxycholate	1%
	SDS	0.1%
	PMSF	1 mM
	protease inhibitor mix	86 µl

Cells were grown in 60 mm culture dishes until confluence. After aspiration of the medium and two washing steps with phosphate buffered saline (PBS), cells were scraped in 300 µl RIPA buffer and transferred into micro centrifuge tubes (pre-cooled at 4℃). Cell membranes were disrupted by sonication (3 times for 1 s). After centrifugation

at 18,620 x *g* for 20 min (4℃), the supernatant was collected in a new tube and directly used for protein quantification or stored at -20℃.

3.2.4.3 Crude membrane preparation

PBSi	PBS	10 ml
	protease inhibitor mix	86 µl

Cells were grown in 60 mm culture dishes until confluence. After aspiration of the medium and washing with PBS, cells were harvested in 1 ml PBSi (10 ml PBS + 86 µl protease inhibitor mix) and transferred into BECKMANN micro centrifuge tubes. The cells were disrupted by sonication (3 times for 1 s). After ultra centrifugation at 60,000 *g* for 45 min (4℃), the supernatant was discarded and the pellet was resuspended with a syringe with a 20-gauge needle in 100 to 200 µl PBSi, depending on the size of the pellet. 20 µl from this suspension were taken for protein quantification and the remaining probe was ultra centrifuged at 60,000 *g* for 45 min (4℃). The supernatant was discarded and the pellet frozen at -20℃. After determination of the total amount of protein the pellet was resuspended in PBS. 40 µg of total protein was applied for SDS PAGE.

3.2.4.4 Analysis of PERK activation

PBS-EDTA	PBS	50 ml
	EDTA	1 mM
lysis buffer PERK	Tris HCl	50 mM
	EDTA	5 mM
	triton X-100	0.2%
	NaF	25 mM
	Na-pyrophosphate	10 mM
	dH_2O	ad 100 ml
added before use	PMSF	1 mM
	Na_2VO_4	0.2 mM
	DTT	1 mM
	protease inhibitor mix	86 µl
	pH 7.4	

Cells were grown in 100 mm culture dishes until confluence. For positive control cells were treated with 2 µM thapsigargin for 2 h before harvesting. After aspiration of the medium and two washing steps with PBS cells were scraped in 2 ml PBS-EDTA and pelleted by centrifugation (5 min at 90 x *g* at 4℃). The supernatant was discarded and cells were homogenised with a syringe with a 20-gauge needle in 100 µl lysis buffer. The suspension was centrifuged for 15 min at full speed (18,620 x *g*, 4℃) and the supernatant was collected in a new tube. After quantification of the total protein amount 20 µg protein were used for SDS PAGE.

3.2.4.5 Analysis of eIF2α activation

1% triton buffer	HEPES	20 mM
	NaCl	150 mM
	triton X-100	1%
	glycerol	10%
	EDTA	1 mM
added before use	Na pyrophosphate	10 mM
	NaF	100 mM
	Na_3VO_4	1 mM
	PMSF	1 mM
	protease inhibitor mix	86 µl

Cells were grown in 100 mm culture dishes until less than 90% confluence. For positive control cells were treated with 2 mM DTT for 1 h before harvesting. After aspiration of the medium and two washing steps with PBS cells were scraped in 2 ml PBS-EDTA and pelleted by centrifugation (5 min at 90 x *g* at 4°C). The supernatant was discarded and the cells were lysed by adding 60 µl lysis buffer (triton buffer) following resuspension and incubation for 5 min on ice. After centrifugation (4°C, 18,620 x *g*, 15 min) the supernatant was collected in a new tube and protein concentration was determined by the Bradford assay. 50 µg of total protein were used for SDS PAGE.

3.2.4.6 Nuclear and cytoplasmic protein extraction

The fractionation of different compartments of the cell was carried out with the Qproteome cell compartment Kit according to the manufacturer's instructions.

Reagents and solutions of the Qproteome cell compartment kit

extraction buffer CE1	1000 µl	cytosolic fraction
extraction buffer CE2	1000 µl	membrane fraction
extraction buffer CE3	500 µl	nuclear fraction
extraction buffer CE4	500 µl	cytoskeletal fraction
Benzonase® nuclease	7 µl	
protease inhibitor solution 100X	10 µl	
PBS		

For the fractionation of cytosolic, membrane and nuclear proteins 4.5 x 10^6 HEK293 cells and HEK293 cells stably expressing GFP-tagged wild type and mutant V2Rs were centrifuged (500 x *g*, 10 min, 4°C) and the supernatant was discarded. The cell pellets were washed two times in 2 ml ice-cold PBS, collected by centrifugation (500 x *g*, 10 min, 4°C) and the cell pellets were resuspended in 1 ml ice-cold buffer CE1. After incubation (10 min, 4°C) and centrifugation (1,000 x *g*, 10 min, 4°C) the supernatants contained the cytosolic proteins. The pellets were resuspended in 1 ml ice-cold buffer CE2 and incubated for 30 min at 4°C. After centrifugation (6,000 x *g*, 10 min, 4°C) the supernatants contained the membrane fraction. The cell pellets were gently resuspended with 13 µl dH_2O and 7 µl Benzonase® nuclease and subsequently incubated for 15 min at RT. Nuclear proteins were extracted by the addition of 500 µl buffer CE3 (10 min, 4°C) and centrifugation (6,800 x *g*, 10 min, 4°C). The supernatant contained the nuclear proteins. The cytoskeletal fraction was obtained by resuspending the pellet in 500 µl buffer CE4.

Equal amounts of proteins were used for SDS-PAGE and the purity of the extracts was verified by determination of the amount of cytosolic localized GAPDH in the nuclear

extract and the nuclear protein lamin in the cytoplasmic fraction. These proteins also served as loading controls.

3.2.4.7 SDS-PAGE and immunoblot

4x Laemmli buffer	glycerol	20%
	Tris HCl pH 6.8	100 mM
	SDS	4%
	β-mercaptoethanol	0.1 M
	bromphenol blue	0.2%
separation gel buffer	Tris HCl pH 8.8	0.75 M
stacking gel buffer	Tris HCl pH 6.8	0.625 M
running buffer	Tris OH	0.025 M
	glycine	0.19 M
	SDS	0.1%
blotting buffer	Tris OH	0.02 M
	glycine	0.15 M
	methanol	20% (v/v)
	SDS	0.015% (w/v)
PBS-T 0.1%	Tween 20	0.1%
	PBS	ad 1.0 l

blocking buffer	low fat milk powder	5% (w/v)
	PBS-T 0.1%	ad 100 ml
ponceau S stock solution	ponceau S	2%
	sulfosalicyllic acid	30%
	trichloroacetic acid	30%
ponceau S staining solution	ponceau S stock solution	5%
	dH_2O	ad 20 ml
antibody buffer	low fat milk powder	2 % (w/v)
	PBS-T 0.1 %	ad 100 ml

for two gels	separation gel 8%	separation gel 10%	separation gel 12%	stacking gel
H_2O	2.5 ml	1.75 ml	1 ml	3.5 ml
Rotiphorese Gel 30	3 ml	3.75 ml	4.5 ml	835 µl
separation gel buffer	5.625 ml	5.625 ml	5.625 ml	
stacking gel buffer				625 µl
20% SDS	56.5 µl	56.5 µl	56.5 µl	25 µl
TEMED	5.65 µl	5.65 µl	5.65 µl	5 µl
ammonium persulfate 10%	79 µl	79 µl	79 µl	25 µl

Tab. 2.1: Reaction mixture for SDS PAGE

Equal amounts of protein were mixed with dH_2O and 4x Laemmli-buffer. After denaturating by heating at 95℃ for 5 min the samples were loaded on SDS-polyacrylamide gels of different concentrations of acrylamide/bisacrylamide, depending on the size of the protein of interest. SDS-PAGE was carried out at 20 mA / gel to separate denatured protein / SDS complexes with the Mini-PROTEAN 3 system from BioRad. Running times were depending on the size of the protein of interest. Molecular weight markers were used to estimate the size of the protein.

After separation, proteins were transferred (4℃, 100 mA / gel, time depended on the size) for immuno detection onto nitrocellulose membranes using the Mini Trans-Blot

Electrophoretic Transfer Cell from BioRad. Transfer was controlled by staining the nitrocellulose membrane with a ponceau S solution for 30 s followed by distaining and washing (three times for 5 min with H_2O). Nitrocellulose membranes were blocked (1 h, RT) with blocking buffer to avoid unspecific binding of antibodies. The first antibody was diluted in PBS-T (0.1% Tween 20, 2% low fat milk powder) and incubated for 1 h (RT) or overnight (4°C). Membranes were washed with PBS-T 0.1% (3 x 10 min) and incubated with a secondary antibody coupled with horseradish peroxidase (HRP) (diluted 1:10.000 in PBS-T; 0.1% Tween 20, 2% low fat milk powder) for 45 min (RT). Blots were washed three times for 15 min with PBS-T 0.1%. Finally, the membranes were incubated for 3 min with 2 ml ECL luminescence solution (Applichem) per membrane and developed using a Kodak X-Omat film.

3.2.4.8 Co-immunoprecipitation

lysis buffer (buffer A):	Tris HCl pH 8.0	50 mM
	NaCl	150 mM
	EDTA pH 8.0	1 mM
	triton X-100	1%
	SDS	0.1%
	dH_2O	ad 100 ml
added before use	PMSF	1 mM
	protease inhibitor mix	86 µl

washing buffer I	Tris HCl pH 8.0	50 mM
	NaCl	500 mM
	EDTA pH 8.0	1 mM
	triton X-100	0.5%
	SDS	0.1%

	dH_2O	ad 100 ml
washing buffer II	Tris HCl pH 8.0	50 mM
	EDTA pH 8.0	1 mM
	triton X-100	0.5%
	SDS	0.1%
	dH_2O	ad 100 ml
	pH 7.4	

Confluent cells in 60 mm culture dishes were placed on ice and washed twice with 1 ml PBS. Cells were lysed in 1 ml ice-cold buffer A by shaking for 10 min at 4°C. Lysates were collected in micro centrifuge tubes, mixed by vortexing and centrifuged at 18,620 x *g* for 20 min at 4°C. Supernatants were transferred to protein-A-sepharose beads (5 mg/60 mm dish of cells) previously loaded with 5 to 8 µl of different precipitating antibodies. The incubation on an end-over-end shaker was carried out from 3 h to overnight. The precipitated proteins were washed two times with 1 ml washing buffer I and one time with 1 ml washing buffer II. After centrifugation (590 x *g*, 5 min, 4°C) the beads were added with 30 µl 2x Roti®-load 1, carefully mixed by vortexing, denaturated for 5 min at 95°C, pelleted by centrifugation (590 x *g*, 5 min, 4°C) and the supernatant was separated by SDS-PAGE.

3.2.4.9 Immunofluorescence

permeabilisation buffer	triton X-100	0.075%
	PBS	ad 50 ml
cacodylic acid solution	cacodylic acid sodium salt	400 mM
	dH_2O	ad 100 ml
sucrose solution	sucrose	1 M
	dH_2O	ad 100 ml
paraformaldehyde solution	paraformaldehyde	10%
	NaOH 5 N	10 µl
	dH_2O	ad 100 ml
fixing solution	cacodylic acid solution 400 mM	12.5 ml
	sucrose solution 1 M	5 ml
	paraformaldehyde solution 10%	12.5 ml
	dH_2O	ad 50 ml
	pH 7.6	

For immunofluorescence studies 2 x 10^5 HEK 293 cells stably expressing the GFP-tagged V2R and NDI-causing mutant V2R fusion proteins were grown on poly-L-lysine-coated glass cover slips (Ø 12 mm) in a 24-well plate. After 24 h, cells were washed twice with PBS (37℃) and fixed for 25 min at RT in fixing buffer. The fixed cells were rinsed three times with PBS for 2 min on ice. Cell membranes were permeabilized with

PBS supplemented with 0.075 % triton X-100 (3 min) on ice and washed three times with ice-cold PBS. For incubation with the first antibody recognizing the protein of interest or a marker protein of an intracellular compartment, the glass cover slips were transferred into a humidity chamber (box with water-soaked filter paper, preheated to 37°C). The antibodies were diluted in PBS to a final concentration from 1:50 to 1:500 and each platelet was covered with 45 µl antibody solution and incubated for 45 min at 37°C in the chamber. Glass cover slips with cells were washed three times with ice-cold PBS for 5 min. Secondary antibodies, which specifically recognize the first antibody and are conjugated with the fluorescent dye Cy3, were diluted in PBS to a concentration of 1:300 –1:500. Again cells were covered with 45 µl of antibody solution and incubated at 37°C for 45 min in the humidity chamber. Glass cover slips were washed for additional three times (5 min each) with ice-cold PBS and embedded in a drop of Immu-Mount™ mounting medium. The fluorescent dye was visualized on a Zeiss 510 invert laser-scanning microscope (optical section: < 0.9 µm; single track mode; Cy3, λ_{exc}: 543 nm, BP filter: 560 – 615 nm).

3.2.4.10 Luciferase assay

The measurement of the activity of the promoter regions of BiP, CHOP, ERdj4 and NF-κB was carried out with the Dual-Luciferase® Reporter Assay System (Promega) according to the manufacturer's instructions. The assay determines the luminescence from two luciferases, the *Renilla* luciferase provides an internal control to quantify the amount of cells in each well and firefly luciferase served for quantification of promoter activity. For co-transfection a ratio of 20:1 (NF-κB, pGL3.NF-κB; CHOP, pGAD153-luc), 25:1 (ERdj4, pERdj4GL3) or 30:1 (BiP, pGL3.GRP78; XBP-1, p4xXBP1GL3) for experimental vector (firefly):co-reporter vector (*Renilla*, phRL-TK) was used. 24 h after transfection cells were serum-starved for 16 h for measurement of NF-κB activity. As positive controls transfected HEK293 cells were stressed with either tunicamycin for 16 h for BiP, CHOP and ERdj4 or for 1 h with 30 ng TNFα for NF-κB activation. After aspiration of media and two times washing with PBS (37°C) cell were passively lysed with100 µl PLB lysis buffer for 15 min at RT. Meanwhile, 100 µl LARII was predispensed into luminometer tubes. The assay was performed with a manual luminometer and for

measurements, a 1 to 2 s delay and 5 to 10 s read time was used. 50 µl PLB lysate were transferred into the luminometer tubes, mixed and the firefly luciferase activity was measured. Subsequently, 100 µl Stop & Glow® Reagent were dispensed and activity of the *Renilla* luciferase was measured. Afterwards the activity of the experimental reporter was normalized by dividing it with the activity of the internal control, thereby minimizing the experimental variability caused by differences in viability of the cells and transfection efficiencies.

3.2.4.11 Measurement of the antioxidative status

Determination of the antioxidative status of living cells was carried out using the Antioxidative Power (AP) test method, described elsewhere (Jung et al. 2006). Three different cell concentrations of each cell line where added to 0.2 mM DPPH used as the test radical and the signal intensity decay of DPPH was measured over 40 minutes by Electron Spin Resonance Spectroscopy using a Magnettech (Germany) MS 300 spectrometer with the following operating parameters: central field: 3359 G, 60 G sweep, 1 G modulation amplitude, 7 dB microwave attenuation, 0.14 s time constant. The data for each cell concentration were fitted with first order kinetics, the reaction time (tr) and the characteristic weight (wc) were calculated and the AP was determined by using the following equation:

$$\mathbf{AP = RA * N\ DPPH / tr * wc}$$

RA is the fixed reduction amplitude and N the number of DPPH free radicals. The AP method is standardized to vitamin C and the AP values can be expressed in number of free radicals neutralized by 1 single cell in one minute or in Antioxidative Units (AU), representing the AP value of 1 ppm vitamin C.

3.2.4.12 Determination of the antiradical potential (ARP)

Different dilutions of each cell line were prepared using PBS and to each dilution H_2O_2 at 0.03% was added. The spin trap PBN was added to the cell lines at a final concentration of 200 mM and the cell suspensions were immediately exposed to UV

radiation for 2 min using a SOL F2 sun simulator (Dr. Hönle AG, Germany) to generate hydroxyl free radicals. The intensity of the PBN spin adduct was measured by Electron Spin Resonance Spectroscopy 1 minute after the irradiation using a Magnettech MS 300 spectrometer. The radical scavenging activity of the cells is inverse proportional to the signal intensity of the PBN adduct.

3.2.4.13 Immunoelectron microscopy

HEK293 cells stably expressing mutant L62P, or as a control, untransfected HEK293 cells, were fixed with 3% formaldehyde/0.5% glutaraldehyde in 0.1 M phosphate buffer for 1.5 h. The fixatives were removed, the cells were washed several times with 0.1 M phosphate buffer and free aldehydes were quenched at room temperature with 100 mM gylcine in 0.1 M phosphate buffer. The cells were scraped in 0.1 M phosphate buffer, centrifuged (3,500 x *g*, 5 min) and the cell pellet was cryoprotected overnight in a mixture of 1.8 M sucrose and 20% PVP in 0.1 M phosphate buffer. Aliquots of 5 µl were mounted on specimen holder pins and plunge frozen in liquid propane. Ultrathin cryosections (80 nm) were obtained according to Tokuyasu (Tokuyasu 1997) using an cryo-ultramicrotome The sections were immunolabeled with a monoclonal rat anti-GRP94 antibody overnight and subsequently with a gold (15 nm) labeled goat anti-rat antibody for 2 h according to standard procedures (Tokuyasu 1997). Finally, cryosections were contrasted using a mixture of 3% tungstosilicic acid hydrate and 2.5% PVA according to Kärgel (Kargel et al. 1996). After blotting of the mixture the sections were dried in the thin film which remains over them. The sections were viewed in a 80kV ZEISS 902 A electron microscope.

4 Results

4.1 Analysis of chronic UPR

The effects and pathways of ER stress are usually examined after induction with chemical agents, such as tunicamycin or thapsigargin. Tunicamycin inhibits the N-glycosylation of proteins and leads to the accumulation of non-glycosylated proteins in the ER. Thapsigargin is an inhibitor of the Sarco/Endoplasmic Reticulum Ca^{2+}-ATPase (SERCA) and leads to an increase in cytosolic calcium concentrations by blocking the ability of the cell to pump calcium into the sarcoplasmic (SR) and endoplasmic reticulum (ER). This depletion of SR/ER Ca^{2+} levels also results in ER stress (Hamamura et al. 2008).

The aim of this study was to investigate the activation of ER stress caused by intracellular retention of misfolded vasopressin receptors (V2R). Patients suffering from X-linked NDI exhibit several mutations of the *AVPR2* gene, which lead to the accumulation of receptors within various compartments of the cell (Oksche and Rosenthal 1998). We used the human V2R as a model to determine if different localization sites (ER, ERGIC and Golgi apparatus) of one specific, misfolded protein result in the induction of the unfolded protein response (UPR).

Until now, no cell line has been described to endogenously express the human V2R. Therefore, HEK293 (human embryonic kidney, clone 293) cell lines stably expressing the wild-type receptor and different NDI-causing V2R mutants were generated. Each receptor variant was tagged with the green fluorescent protein (GFP) at its C-terminus in order to obtain a useful tool to study ER stress. From previous studies it is known that this tag has no influence on localization, trafficking and pharmacological properties of the receptor (Hermosilla et al. 2004). The localization of the mutations within the amino acid sequence of the V2R is shown in figure 1.7.

4.1.1 Expression of wild-type and NDI-causing mutants of the V2R

The expression and cellular localization of wild-type V2R and the different studied mutants in HEK293 cells were determined by laser scanning microscopy of living cells (Fig. 4.1 A). As expected, wild-type receptor and mutant V2Rs were localized as described before (Hermosilla et al. 2004). L62P (amino acid exchange at the

interface of the first transmembrane domain and cytoplasm) was retained almost completely in the ER, InsQ292 (amino acid insertion in the transmembrane domain 7) was localized in the ER, but also in the ERGIC, while G201D (amino acid exchange in the extracellular loop 3) could be found in the ER, ERGIC and in the Golgi apparatus (Tab. 1.1)

Moreover, laser scanning microscopy allowed to analyze a potential expression variability between HEK293 cells stably expressing wild-type and mutant V2Rs (Fig 4.1 A). All cell lines showed equal expression intensities. Overall expression of the wild-type V2R and the three different mutants was further examined by immunoprecipitation with untransfected HEK293 cells serving as a control (HEK; Fig. 4.1 B). The control showed two slight unspecific bands of 40 and 70 kDa. The wild-type V2R was expressed as two specific forms the core-glycosylated immature receptor, (#) represented by the band running at 60-65 kDa and the complex-glycosylated form of the mature receptor (∗) at 75-88 kDa. These two forms could also be detected for the Golgi-retained mutant G201D. In contrast, L62P and InsQ292 were only expressed as the core-glycosylated receptor (#) but not as the complex-glycosylated receptor form.

These results show that the GFP-tagged wild-type V2R and the mutants studied localize to different compartments of the secretory pathway, which is in good agreement with the data described before (Hermosilla et al. 2004). Moreover, similar expression levels of the various V2R constructs allow a direct comparison of the cell lines and therefore can be used for the detection of the UPR.

A

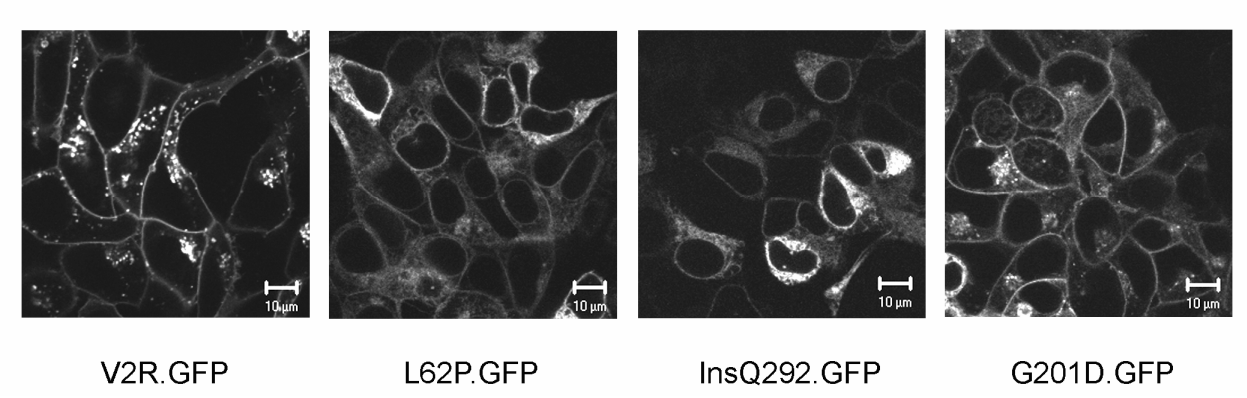

B

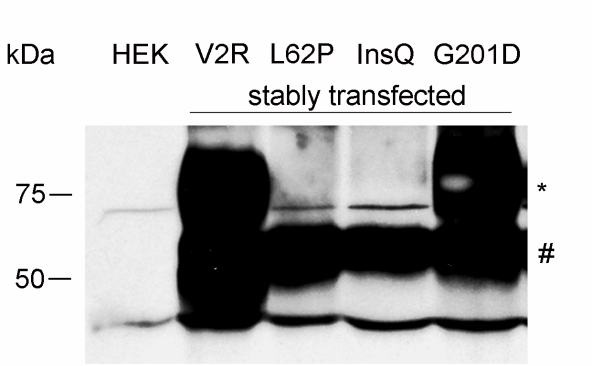

Fig. 4.1: Expression of GFP-tagged V2R constructs. A Laser scanning microscopy of living HEK293 cells stably expressing wild-type and mutant V2Rs. Scale bar, 10 µm. Scans show representative cells. **B** Western Blot analysis of immunoprecipitated GFP-tagged V2R receptor constructs. HEK293 cells stably expressing wild-type and mutant V2Rs were lysed and receptors were immunoprecipitated with a rabbit anti-GFP antibody. Expression of receptors was detected with a monoclonal mouse anti-GFP antibody. As a negative control untransfected HEK293 cells were used (HEK). The mutant InsQ292 is labeled as InsQ. The asterisk (*) indicates complex-glycosylated receptor form, (#) indicates the core-glycosylated receptor form. Data are representative of three independent experiments.

4.1.2 Induction of the unfolded protein response

The activation of the UPR results in an upregulation of UPR target genes, such as genes encoding for chaperones, pro-apoptotic genes or genes involved in amino acid metabolism, lipid synthesis or oxidative stress. An early response to different kinds of cell stress is the upregulation of chaperones. The best described chaperone for the induction of the UPR is the glucose regulated protein 78 (GRP78 / BiP) (Malhotra and Kaufman 2007). Other important chaperones include GRP94 (Lee 2001), the lectins calnexin and calreticulin (Hammond et al. 1994), foldases such as PDI (Sitia and Molteni 2004) and redox-regulating proteins Ero1α, ERp57 or thioredoxin (Reddy and Corley 1998; Tu and Weissman 2004). In order to verify an induction of UPR due to intracellular accumulation of misfolded V2R mutants the expression of these chaperones was analyzed in HEK293 cells stably expressing the various V2R constructs. Untransfected HEK293 cells and the wild-type V2R served as a negative control whereas HEK293 cells treated with tunicamycin were used as a positive control.

Immunoblot analysis of whole cell lysates of HEK293 cells stably expressing the V2R constructs revealed a strong upregulation of GRP78 and GRP94 in tunicamycin-treated cells but not in untreated cells, indicating an activation of the UPR (Fig. 4.2 A). Expression of GRP78 was enhanced not only in HEK293 cells expressing V2R mutants but also in those cells expressing the wild-type V2R. In contrast, GRP94 showed a specific upregulation only in HEK293 cells expressing the mutant receptors. The increased expression of GRP78 was verified by performing a luciferase assay, in which the enzyme activity was correlated with the activation of the promoter region of GRP78 (Fig. 4.2 B). The ratio of the measured Firefly -(indicating the GRP78 promoter activity) and the Renilla-luciferase activity (as a control, showing the total amount of transfected cells) was analyzed with Prism 3.0. ANOVA Dunnett's Multiple Comparison Test was used to determine statistical differences. Consistent with the results in figure 4.2 A, the promoter activity of GRP78 was increased in tunicamycin-treated cells (positive control) and in cells expressing wild-type receptor or each of the studied mutants. The upregulation of GRP78 was highly significant ($p < 0.001$) in tunicamycin-treated cells and HEK293 cells stably expressing the V2R mutants L62P, InsQ292 and G201D. The activation of the

GRP78 promoter region was less strong but still significant ($p < 0.05$) in HEK293 cells expressing the wild-type V2R.

A

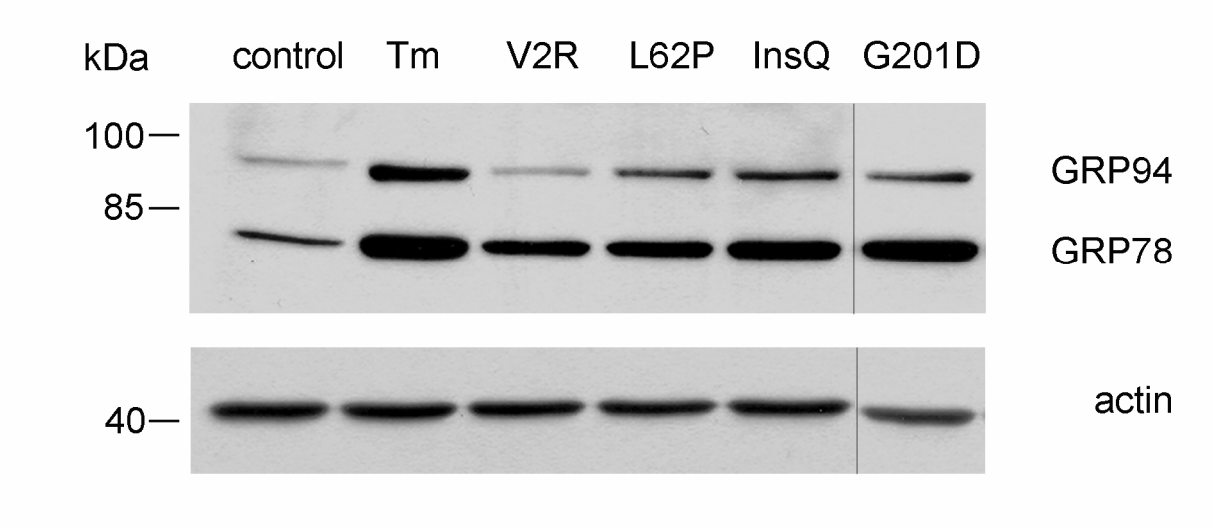

B

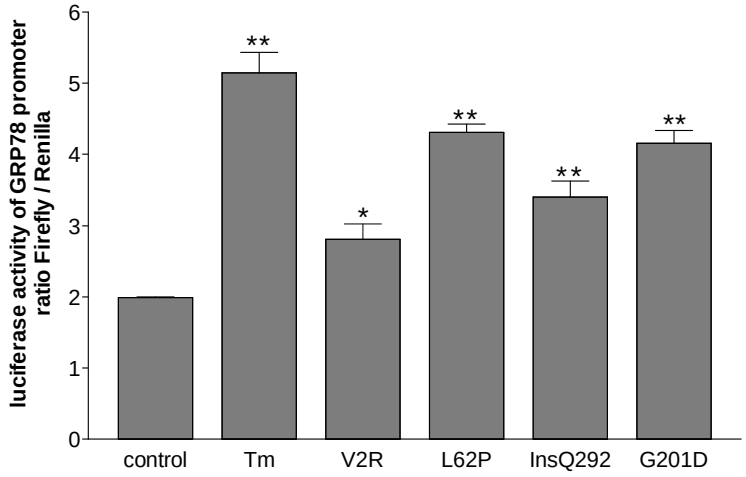

Fig. 4.2: Expression levels of chaperones. A Whole cell lysates of HEK293 cells stably expressing the V2R constructs as indicated, were subjected to immunoblot analysis detecting GRP94 and GRP78 by using an anti-KDEL antibody. The mutant InsQ292 is labeled as InsQ. Vertical lines indicate positional markings where lanes were extracted. Actin served as a loading control. Similar data were obtained in six independent experiments. **B** GRP78 promoter activity of untreated cells (control), cells treated with tunicamycin (Tm; 2.5 µg/ml for 16 h) and cells expressing the V2R constructs was analyzed by luciferase assay. Statistical analysis was performed with the software Prism 3.0. ANOVA Dunnett's Multiple Comparison Test was used to analyze statistical differences (* = $p < 0.05$, ** = $p < 0.001$).

Semi-quantitative expression analyses of the lectin calnexin performed with various methods are shown in figure 3. Immunoblot analysis of whole cell lysates of HEK293 cells stably expressing the V2R constructs revealed a slight upregulation of calnexin in tunicamycin-treated cells and mutant L62P expressing cells (Fig. 4.3 A). Cells expressing wild-type V2R and mutants InsQ292 and G201D displayed no change in calnexin expression level. The expression of calnexin was densiometrically evaluated, normalized to the expression of the loading control actin (normalized expression) and subjected to ANOVA Dunnett's Multiple Comparison Test (Prism 3.0; Fig. 4.3 B). Compared to the control, tunicamycin-treated cells showed a significant upregulation ($p < 0.05$). In cells expressing mutant L62P an even higher significant increase of calnexin expression was detected ($p < 0.001$). In order to confirm these data, immunofluorescence assays of wild-type V2R and mutant L62P expressing cells were performed. A higher fluorescence intensity was visible in mutant L62P expressing cells indicating a higher intracellular expression level of calnexin (Fig. 4.3 C). The fluorescence intensity in HEK293 cells was analyzed quantitatively (Fig. 4.3 D). Consistent with the pictures (Fig. 4.3 C), a right shift of the graph was detectable in mutant L62P expressing cells (red), indicating a higher frequency of pixels with high fluorescence intensity.

A

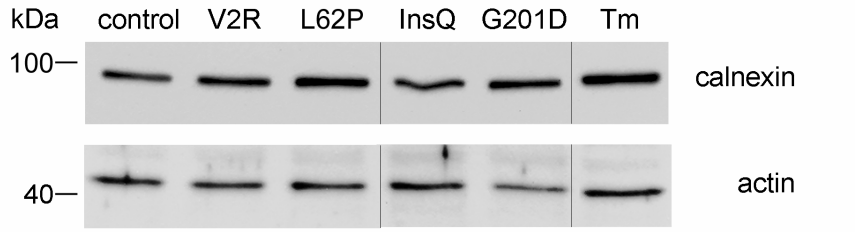

B

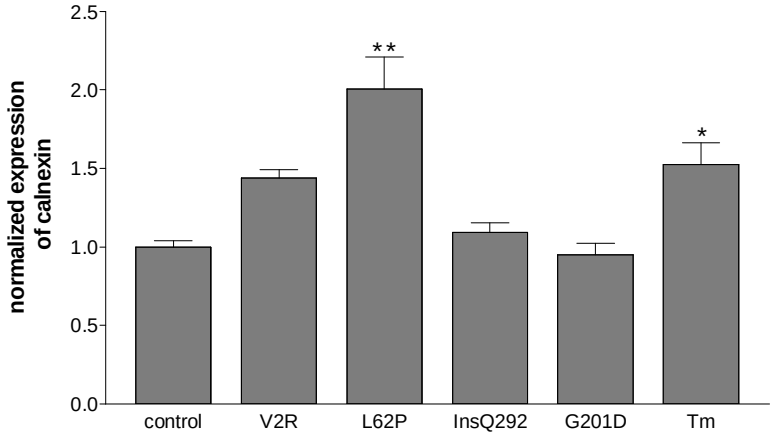
normalized expression of calnexin
2.5
2.0
1.5
1.0
0.5
0.0
**
*
control
V2R
L62P
InsQ292
G201D
Tm

C

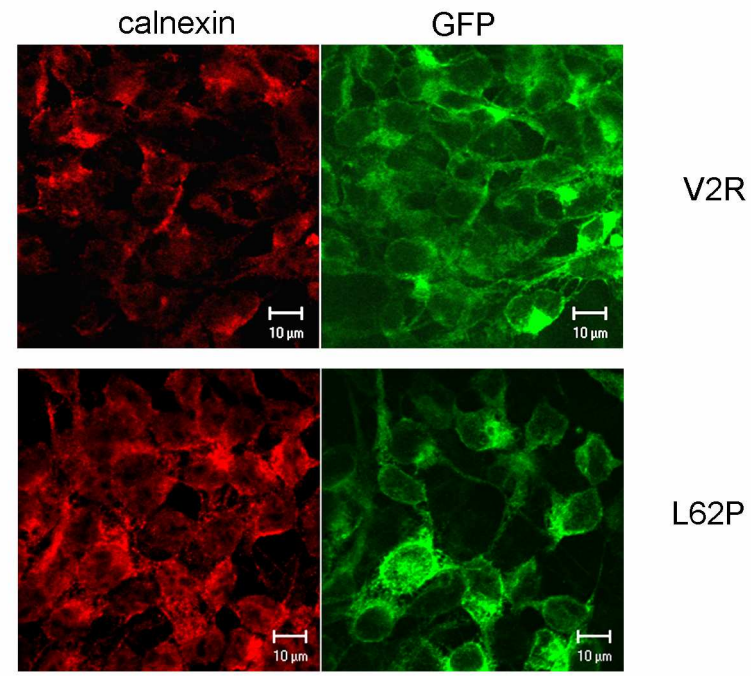
calnexin
GFP
V2R
L62P
10 µm
10 µm
10 µm
10 µm

D

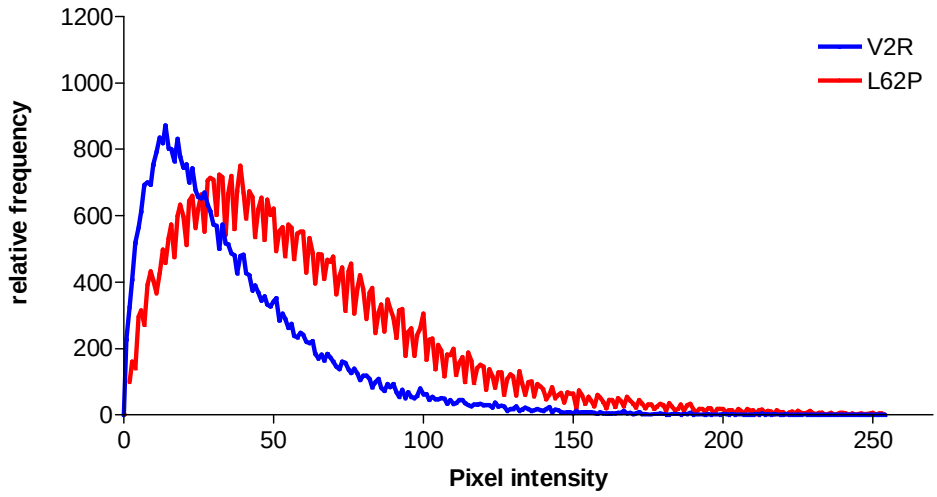

Fig. 4.3: Detection of chronic UPR. A Analysis of whole cell lysates of HEK293 cells stably expressing wild-type and mutant V2Rs by Western blotting with an anti-calnexin antibody (rabbit). As a negative control non-transfected HEK293 cells (control) were used. Tunicamycin-treated cells (Tm; 2.5 µg/ml, 16 h) served as a positive control. The mutant InsQ292 is labeled as InsQ. Vertical lines indicate positional markings where lanes were extracted. Data are representative of five independent experiments. **B** Statistical analysis of the calnexin expression normalized to the expression of actin was performed with the software Prism 3.0. ANOVA Dunnett's Multiple Comparison Test was used to analyze statistical differences (∗ = $p < 0.05$, ∗∗ = $p < 0.001$). **C** Immunofluorescence assay of cells expressing wild-type V2R and L62P mutant. After permeabilization cells were incubated with an anti-calnexin antibody (rabbit) and a second goat anti-rabbit antibody conjugated with Cy3 (left). The scans show representative cells. Scale bar, 10 µm. Similar data were obtained in three independent experiments. **D** Quantitative analysis of fluorescence intensity in HEK293 cells expressing V2R or L62P, performed with the software Prism 3.0.

The functions of a chaperone are predominantly assisted by so-called co-chaperones. One of this type of proteins is ERdj4, supporting the functions of GRP78 (Shen et al. 2002b). The fact that GRP78 is upregulated in cells expressing the studied mutants and V2R (shown in Fig. 4.2) leads to the hypothesis that the corresponding co-chaperone ERdj4 is similarly involved. In order to test this, luciferase assays of HEK293 cells stably expressing V2R constructs were performed (Fig. 4.4). A significantly enhanced expression of ERdj4 was only detectable in the positive control and in samples from mutant G201D ($p < 0.05$) suggesting that ERdj4 expression was not associated to an increased expression of GRP78.

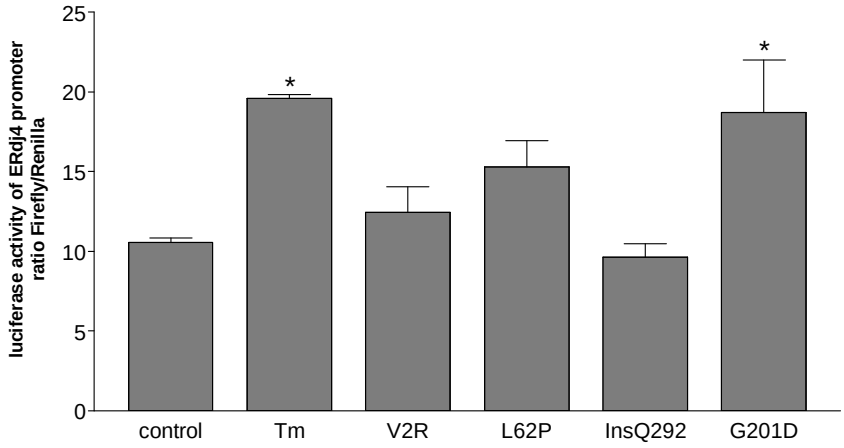

Fig. 4.4: Activation of ERdj4. Induction of co-chaperone ERdj4 was analyzed by luciferase assay. Untreated cells (control) were used as a negative control and tunicamycin-treated cells served as a positive control (Tm; 2.5 µg/ml for 16 h). Statistical analysis was performed with the software Prism 3.0. ANOVA Dunnett's Multiple Comparison Test was used to analyze statistical differences (∗ = $p < 0.05$).

Taken together these results indicate that in HEK293 cells stably expressing wild-type and mutant V2Rs an upregulation of several ER resident molecular chaperones, which are known to be involved in the UPR is induced. However, it is not clear if the overexpression of chaperones is due to an activation of UPR in the studied cell lines. Furthermore, HEK293 cells stably expressing wild-type and mutant V2Rs induce different chaperone overexpression patterns despite comparable expression levels of the receptor protein.

4.1.3 Activation of UPR sensors by disease-causing V2R mutants

The findings that chaperones are upregulated in cells expressing mutant V2Rs are not sufficient to prove the initiation of the UPR. Since an enhanced expression of chaperones could be due to the activation of several stress pathways (Liu and Chang 2008), the next step in confirming UPR activation was to detect the induction of the three different UPR pathways described in mammalian cells (Kaufman 1999), namely the activation of PERK, IRE-1 and ATF6.

Activation of the PERK pathway

One of the three signal transducers of the UPR, which senses misfolded proteins, is the PKR-like ER kinase (PERK) (Yan et al. 2002). Upon activation, PERK dimerizes, becomes autophosphorylated and its active kinase domain phosphorylates the translation initiation factor 2, subunit α (eIF2α) (Fels and Koumenis 2006) (Fig. 1.2). In order to study activation of PERK, its phosphorylation status was examined by immunoblot analysis (Fig. 4.5 A). Untransfected HEK293 cells served as a negative control whereas treatment of cells with 2 µM thapsigargin for 2 h was included as a positive control. The amount of total PERK protein served as a loading control.
Thapsigargin-treated cells and cells expressing mutants L62P and InsQ292 showed an increased amount of phosphorylated PERK as compared to the negative control. Moreover, the phosphorylation status of eIF2α, the target protein of PERK, was determined (Fig. 4.5 B) by immunoblot analysis in the same way as performed for PERK. The activation of eIF2α, detected by its enhanced phosphorylation status, could be observed in all whole cell lysates apart from the negative control. These results are in disagreement with the activation profile of PERK, where only cells expressing mutants L62P and InsQ292 show an increased activation of the stress sensors.
These findings demonstrate that the PERK pathway alone does not account for the induced UPR pathway in the different cell lines. It is likely that in addition to PERK another kinase is responsible for the activation of eIF2α in the cell lines studied.

A

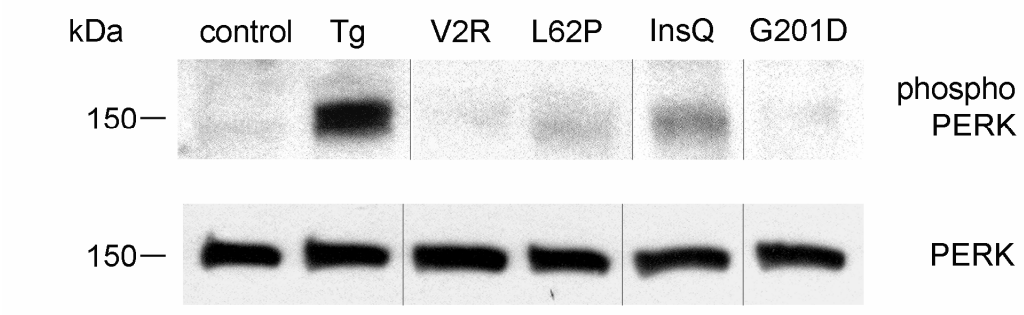

B

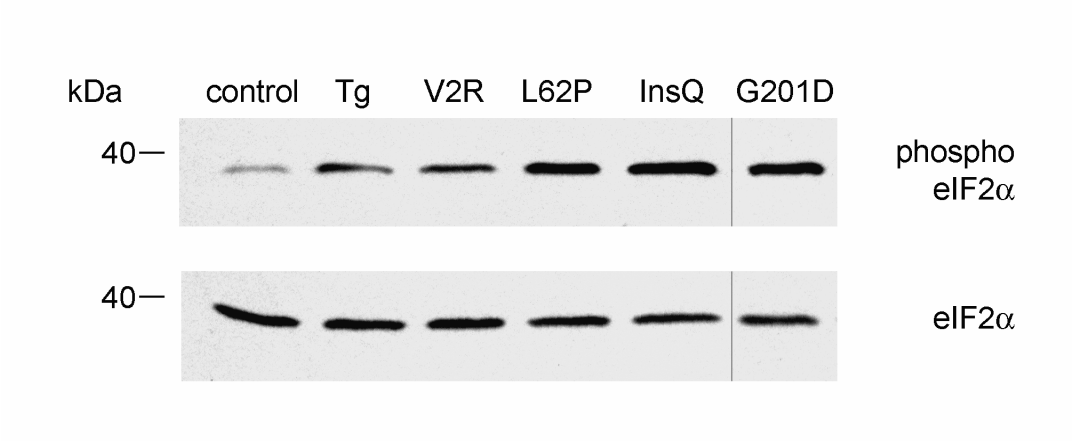

Fig. 4.5: A Activation of the PERK pathway. Whole cell lysates of HEK293 cells stably expressing the V2R constructs as indicated, were subjected to immunoblot analysis using an anti-phospho-PERK antibody (top). Untransfected HEK293 cells (control) and thapsigargin treated cells (Tg) (2 µM, 2 h) were included as negative and positive controls, respectively. Total protein levels of PERK served as a loading control. The mutant InsQ292 is labeled as InsQ. Vertical lines indicate positional markings where lanes were extracted. **B** Whole cell lysates of HEK293 cells stably expressing the V2R constructs as indicated, were subjected to immunoblot analysis using an anti-phospho-eIF2α antibody (top). Total amount of eIF2α protein served as a loading control. Vertical lines indicate positional markings where lanes were extracted. Data were collected from three individual experiments.

Activation of the IRE-1 pathway

Another UPR signal transducer analyzed in this study was IRE-1. First found in yeast, IRE-1 is the best-studied UPR transducer (Cox et al. 1993). Upon activation IRE-1 oligomerizes and undergoes autophosphorylation. Under UPR conditions, IRE-1 activity initiates the removal of a 26 nucleotide intron from the *XBP-1* mRNA. This splicing reaction creates a translational frame shift to produce a larger form of XBP-1 that contains a novel transcriptional activation domain in its C-terminus. The spliced XBP-1 variant is a transcriptional activator that plays a fundamental role in activating a variety of UPR target genes. To determine the activation of IRE-1, the splicing of XBP-1 was analyzed. Total RNA was isolated from HEK293 cells stably expressing the V2R constructs and reverse-transcribed. After PCR-amplification with a specific XBP-1 primer pair, the products were separated on a 3% agarose gel. Untransfected and thapsigargin-treated HEK293 cells served as negative or positive controls, respectively. Both the spliced and unspliced XBP-1 PCR fragments could be

detected in the positive control, whereas only the unspliced fragment was detectable in the negative control (Fig. 4.6 A). A distinct appearance of a double band (indicating spliced and unspliced XBP-1) was visible in samples of cells expressing the mutants InsQ292 and G201D. These results were confirmed by luciferase assays measuring the activity of the transcription factor XBP-1 (Fig. 4.6 B). Statistical analysis of the results was performed with the software Prism 3.0. ANOVA Dunnett's Multiple Comparison Test was used to analyze statistical differences. A significant activation of XBP-1 was detectable in the positive control ($p < 0.001$) and in mutant G201D expressing cells ($p < 0.05$).

Taken together these results indicate an activation of the IRE-1 pathway as determined by the activation of XBP-1 in HEK293 cells stably expressing mutant G201D.

A

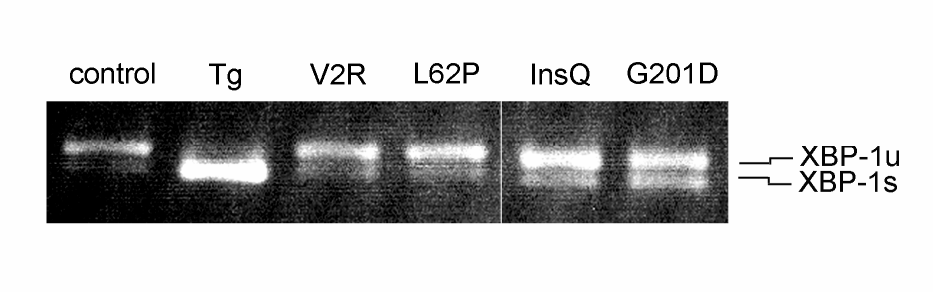

B

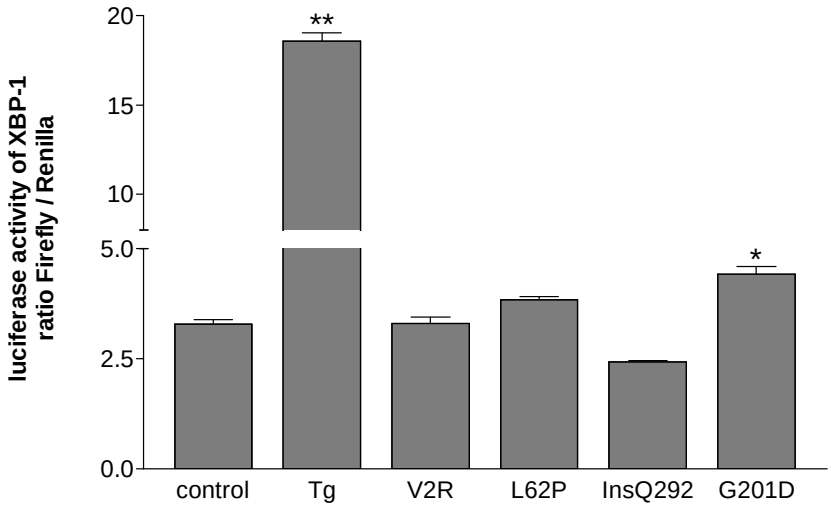

Fig. 4.6: Activation of XBP-1. A Total RNA was isolated from HEK293 cells stably expressing the V2R constructs as indicated. RNA was reverse-transcribed and subsequently amplified with a specific XBP-1 primer pair. Products were separated on a 3% agarose gel. The spliced and unspliced XBP-1 PCR fragments were detected by ethidium bromide staining. Untransfected HEK293 cells served as a negative (control) and thapsigargin-treated cells (Tg; 2 µM, 2 h) as a positive control. The mutant InsQ292 is labeled as InsQ. Vertical lines indicate positional markings where lanes were extracted. Similar data were obtained in four independent experiments. **B** Detection of XBP-1 activity by luciferase assay. Untreated cells (control) or thapsigargin-treated cells (Tg; 2 µM, 16 h) were used as negative and positive control, respectively. Statistical analysis was performed with the software Prism 3.0; ANOVA Dunnett's Multiple Comparison Test was used to analyze statistical differences (∗ = $p < 0.05$, ∗∗ = $p < 0.001$).

Activation of the ATF6 pathway

The ER membrane bound transcription factor ATF6 is transported from the ER to the Golgi apparatus upon ER stress. In the Golgi apparatus it is cleaved by Golgi-resident proteases S1P (site 1 protease) and S2P (site 2 protease) to generate the active ATF6 p50 form (Fig. 2). Subsequently, ATF6 p50 moves to the nucleus to regulate the expression of chaperones (Mori 1999).

Whole cell lysates of HEK293 cells stably expressing the wild-type receptor or mutant V2Rs were subjected to immunoblot analysis 48 h after transient transfection of the pGFP.ATF6 plasmid (Fig. 4.7). This transient transfection of pGFP.ATF6 was performed to increase the signal intensity as the amount of endogenous ATF6 was too small to be detected. The band of the inactive form of ATF6 (p90) appeared at 130 kDa, while the active form (p50) appeared at 80 kDa, due to its fusion to GFP. Actin served as a loading control. A stress induced cleavage of ATF6 as indicated by the appearance of the ATF6 p50 form was detectable in the positive control and in lysates of cells expressing mutants L62P and InsQ292.

Taken together, these results demonstrate that pGFP.ATF6 is a useful tool to analyze and detect the activation of ATF6. However, the ATF6 pathway was only activated in cells expressing mutants L62P and InsQ292 but not in samples from mutant G201D expressing cells.

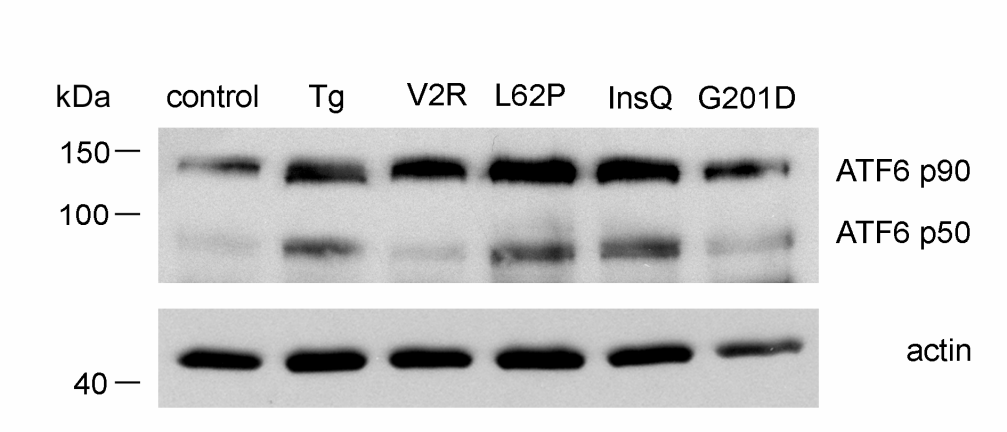

Fig. 4.7: Activation of ATF6. Detection of ATF6 expression by immunoblot analysis of whole cell lysates of HEK293 cells stably expressing the wild-type V2R or different mutants 48 h after transient transfection of the pGFP.ATF6 plasmid. ATF6 was detected with an anti-ATF6 antibody (top). The upper band represents the inactive ATF6 form (p90) and the lower the active form (p50). Actin served as a loading control. As controls non-transfected HEK293 cells (control) and thapsigargin-treated cells (Tg; 2 µM, 16 h) were used. The mutant InsQ292 is labeled as InsQ. Similar data were obtained in three independent experiments.

The results of the present work demonstrate that the different UPR pathways known are activated in all studied cell lines expressing different mutant V2Rs. However, not all three pathways were simultaneously activated indicating different activation patterns of the UPR. The ER-retained mutant L62P and the ER/ERGIC-localized mutant InsQ292 induced the PERK and ATF6 pathways while mutant G201D, which reaches the Golgi network, activated the IRE-1 pathway.

In addition to the precise characterization of UPR pathways activated by intracellular retained V2R mutants, it was also analyzed whether a reduced UPR induction leads to a receptor rescue to the plasma membrane as described before (Wuller et al. 2004). The next part of this study examined the effects of the reduction of intracellularly retained receptor proteins on the UPR.

4.1.4 Rescue of V2Rs and reduction of UPR

It has been shown before that some intracellularly retained V2R mutants can be rescued to the plasma membrane by treating cells with so-called “pharmacochaperones” (Wuller et al. 2004). SR121463B or satavaptan, a non-peptidic antagonist of V2R, stabilizes the receptor conformation leading to increased transport ability to the plasma membrane. SR49059 known as an antagonist of the V1R mediates the same effect resulting in a rescue of intracellularly retained receptors to the cell surface (Bernier et al. 2004). The use of chemical chaperones like DMSO, glycerol or 4-phenyl butyric acid can also increase the stability of native proteins and assists the refolding of unfolded polypeptides (Brown et al. 1996). In this study, the effects of pharmacochaperones and chemical chaperones on ER stress were tested as a proof of principle, measured by the amount of GRP78 as a marker of UPR. As a model, the murine V2R (mV2R) was used which is located in ER, ERGIC and Golgi when stably expressed in HEK293 cells. To a minor amount the mV2R is also located at the plasma membrane.

The expression and localization of the mV2R in HEK293 cells was analyzed by laser scanning microscopy of living cells in presence or absence of the pharmacochaperones SR121463B or SR49059 for 24 h (Fig. 4.8 A). Stably expressed in HEK293 cells, the mV2R.GFP was localized to the ER, ERGIC, Golgi apparatus and to some extent at the plasma membrane. Treatment with SR121463B resulted in a receptor localization at the plasma membrane and only a small amount of mV2R was intracellularly retained. The same effect was detectable after incubation with the V1R antagonist SR49059, the mV2R.GFP was rescued to the plasma membrane. In order to study the effect of the reduced intracellular retention of the receptor on UPR, immunoblot analysis was performed with HEK293 cells stably expressing mV2R and with an anti-KDEL antibody to determine the degree of induced UPR (Fig. 4.8 B). As negative and positive controls untransfected HEK293 cells and tunicamycin-treated cells were used, respectively. Stable transfection of mV2R.GFP in HEK293 cells resulted in an upregulation of GRP78 and GRP94 expression. After treatment with SR121463B for 16 h as well as for 24 h, a reduced expression of both proteins was detectable. The effects of the pharmacochaperones SR49059 and OPC-31260 (V2R antagonist) were analyzed by immunoblot analysis of whole cell lysates of HEK293 cells stably expressing mV2R (Fig. 4.8 C). Compared to untreated cells (control), the incubation with SR49059 in different

concentrations (1 µM or 100 nM) or treatment with OPC-31260 led to a reduction of GRP94 and GRP78 expression.

Taken together, these findings indicate that treatment with different pharmacochaperones (SR121463B, SR49059) lead to a rescue of the intracellularly retained mV2R to the plasma membrane. Furthermore, the reduction of retained receptor proteins results in a diminished induction of UPR, measured by the expression level of the UPR-specific markers GRP78 and GRP94.

A

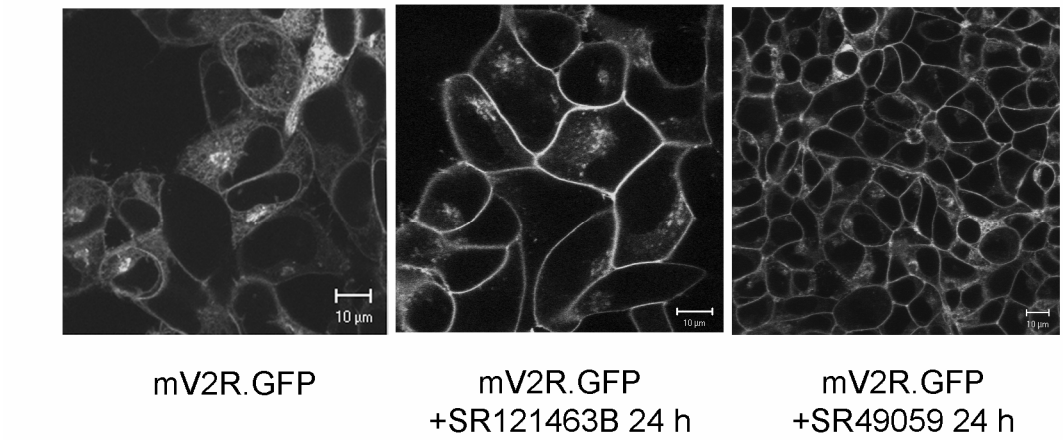

B

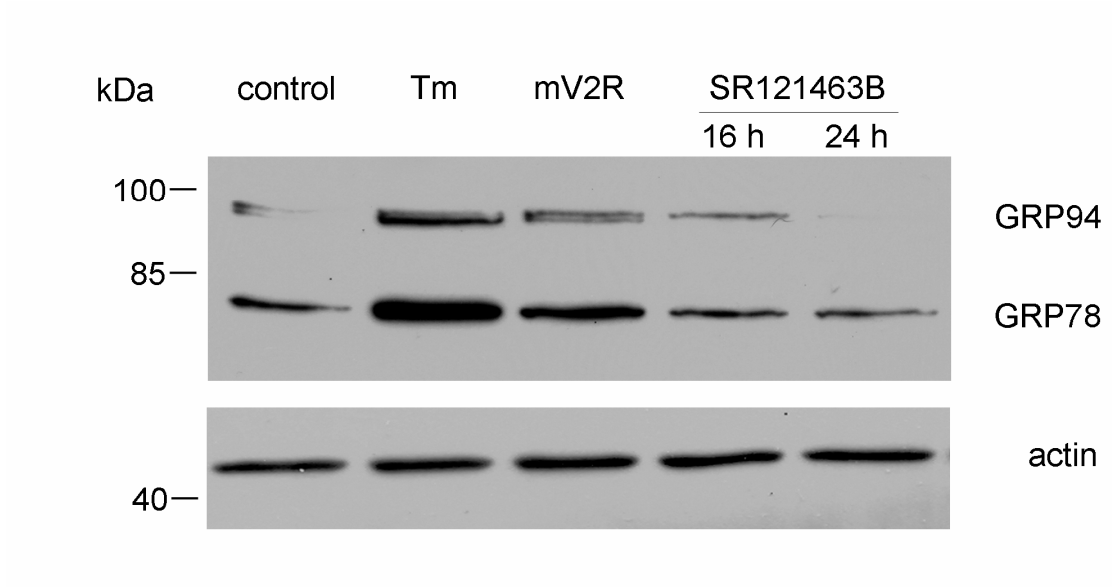

C

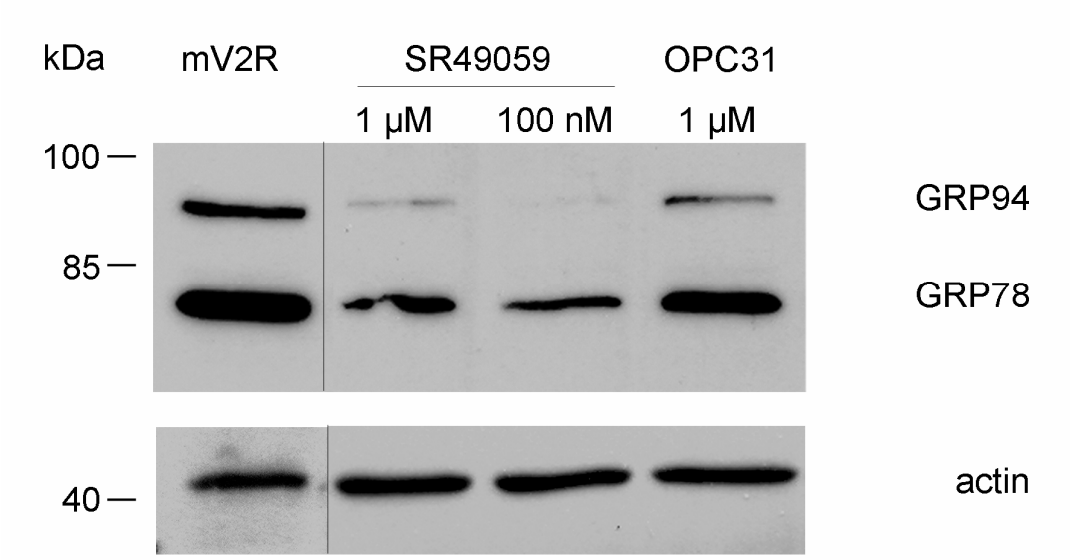

Fig. 4.8: Rescue of the mV2R and reduction of UPR. A Laser scanning microscopy of living HEK293 cells stably expressing mV2R.GFP. Untreated cells served as a control (mV2R.GFP, left) or were treated with 1µM SR121463B for 24 h (middle) or treated with 1µM SR49059 for 24 h (right). Scale bar, 10 µm. Similar data were obtained in three independent experiments. **B** Immunoblot analysis of whole cell lysates of HEK293 cells stably expressing murine V2R detecting GRP94 and GRP78 with an anti-KDEL antibody. As controls, non-transfected HEK293 cells (control) and HEK293 cells treated with 2.5 µg/ml tunicamycin for 16 h (Tm, positive control) were used. Actin served as a loading control. Cells were either left untreated (mV2R) or treated with 1µM SR121463B for 16 h and 24 h. **C** Immunoblot analysis of whole cell lysates of HEK293 cells stably expressing mV2R detecting GRP94 and GRP78 with an anti-KDEL antibody. Actin served as a loading control. Cells were left untreated (mV2R), treated with 1 µM SR49059 and 100 nM SR49059 for 24 h or with 1 µM OPC-31260 for 24 h (OPC31). Vertical lines indicate positional markings where lanes were extracted. Similar data were obtained in three independent experiments.

Further investigations of the UPR induction by measurement of the PERK pathway activation were performed to support the obtained results. Immunoblot analysis of whole cell lysates of HEK293 cells stably expressing the murine V2R with an anti-phospho-eIF2α antibody was carried out. As negative control untransfected HEK293 cells were used. In mV2R expressing cells the amount of phosphorylated eIF2α was much higher as compared to the negative control. After treatment of the cells with the pharmacochaperone SR121463B for 24 h, the activation of eIF2α appeared to be more reduced than in untreated cells (Fig. 4.9).

These findings demonstrate that the reduction of the amount of intracellularly retained receptor proteins results not only in a lower expression of UPR-involved

chaperones (GRP78 and GRP94) but also leads to a diminished activation of the PERK pathway.

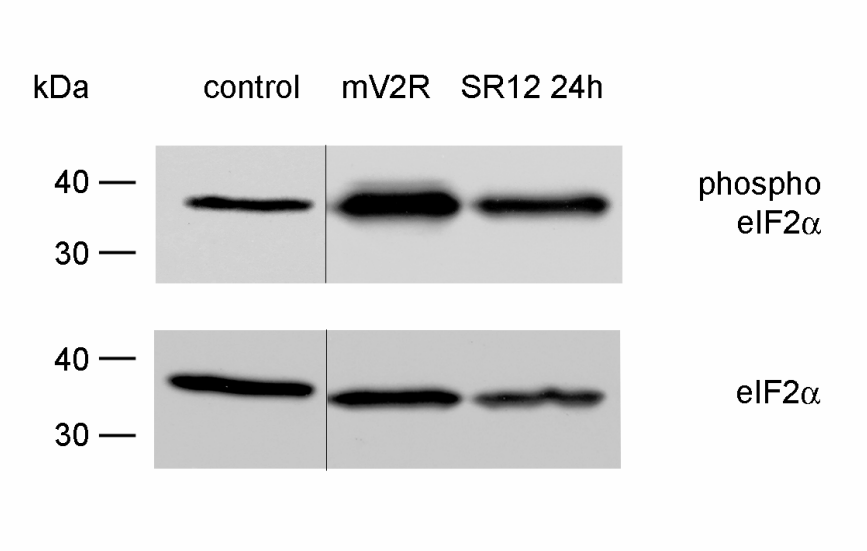

Fig. 4.9: Rescue of the mV2R and reduced activation of eIF2α. Immunoblot analysis of whole cell lysates of HEK293 cells stably expressing mV2R performed with an anti-phospho-eIF2α antibody. As a control non-transfected HEK293 cells (control) were used. Total eIF2α served as a loading control. Vertical lines indicate positional markings where lanes were extracted. Cells were either left untreated (mV2R) or treated with 1µM SR121463B for 24 h (SR12 24 h).

Laser scanning microscopy of living HEK293 cells stably expressing mV2R.GFP was performed to study the effects of DMSO as a chemical chaperone (Fig. 4.10 A). After incubation with 0.01% DMSO for 72 h, the receptor localized predominantly to the plasma membrane of the cells. The effects of receptor rescue to the plasma membrane on the activation of UPR is shown in Fig. 4.10 B. Immunoblot analyses of whole cell lysates of HEK293 cells stably expressing mV2R were performed detecting GRP94 and GRP78 with an anti-KDEL antibody. Untreated HEK293 cells stably expressing mV2R.GFP were used as a control for UPR induction. After incubation with DMSO in different concentrations (0.01 - 0.0001%) the expression of GRP78 and GRP94 was reduced as compared to the control. This effect was more pronounced for GRP78.

A

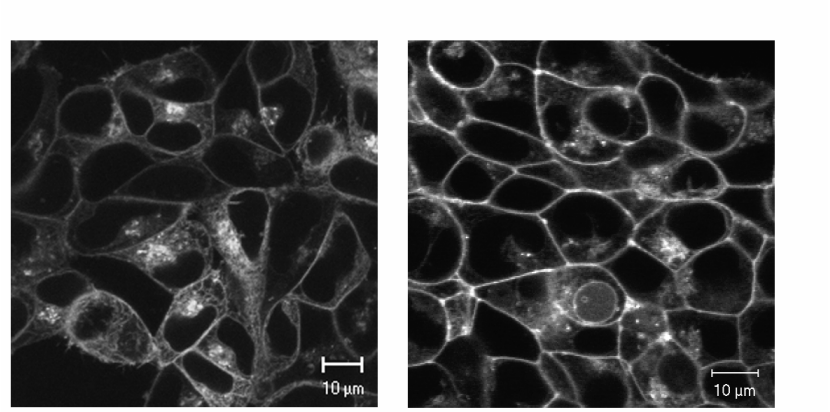

B

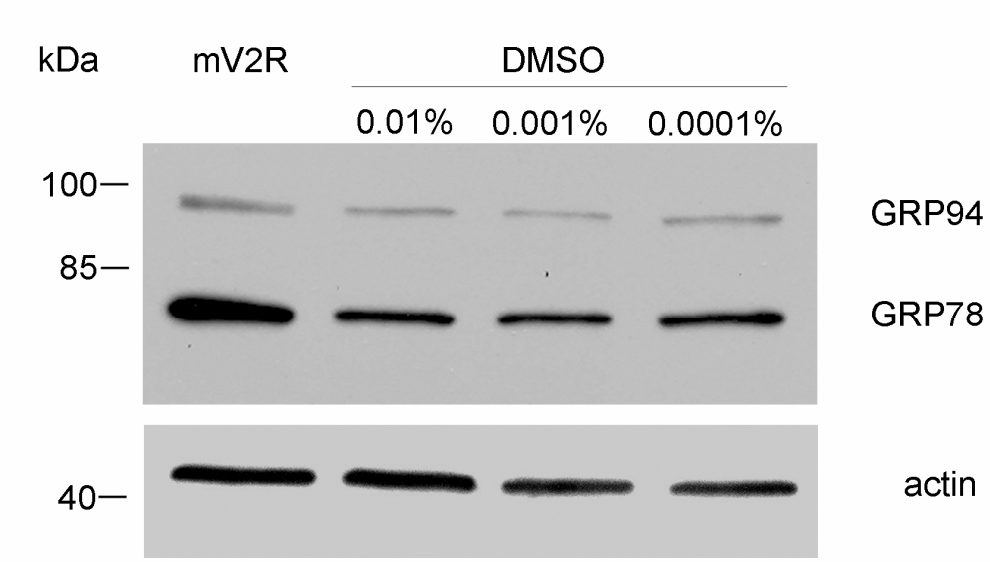

Fig. 4.10: Rescue of the mV2R and reduction of UPR. A Laser scanning microscopy of living HEK293 cells stably expressing mV2R.GFP. Cells were either left untreated (left) or treated with 0.01% DMSO for 72 h (right). **B** Immunoblot analysis of whole cell lysates of HEK293 cells stably expressing mV2R performed with an anti-KDEL antibody detecting GRP94 and GRP78. Actin served as a loading control. Cells were either left untreated (mV2R), treated with DMSO in different concentrations (0.01%, 0.001%, 0.0001%) for 72 h. Similar data were obtained in three independent experiments.

Taken together, these findings indicate that both pharmacochaperones (SR121463B, SR49059) and chemical chaperones (DMSO) are able to rescue the intracellularly retained murine V2R to the plasma membrane. Furthermore, both treatments result not only in a reduced expression of UPR-specific chaperones but also lead to a diminished activation of at least one UPR pathway, the PERK pathway. These results indicate that it is possible to reduce the UPR by lowering the amount of intracellularly retained proteins after treatment with pharmacochaperones and the chemical chaperone DMSO.

4.1.5 Micro array analysis

Upon induction of UPR, genes involved in protein folding are known to be upregulated. In order to find novel up- or downregulated genes in HEK293 cells stably expressing mutant flag.L62P under chronic UPR conditions, micro array analysis of 47,000 genes was carried out using Affymetrix Human Genome U133 Plus 2.0 arrays. A detailed table of genes can be found in the appendix. As expected, several genes of the categories ER, protein folding and unfolded proteins were found to be upregulated in HEK293 cells stably expressing mutant L62P as compared to the wild-type V2R. Furthermore, negative regulators of apoptosis, like the suppressor of cytokine signaling or BAX inhibitor 1 were upregulated, while inducers of apoptosis (apoptosis-inducing factor 3, apoptotic protease-activating factor 1) were downregulated. Several genes implicated in redox regulation, like thioredoxin or glutaredoxin were also upregulated (Tab. 4.1)

functional category	fold induction
unfolded protein binding	
calnexin	2.7
heat shock protein 90 kDa alpha (cytosolic), class B member 1	1.9
heat shock 70 kDa protein 1A	1.9
protein folding	
heat shock transcription factor 2	2.1
nuclear transcription factor Y, gamma	2.6
heat shock 105kDa/110kDa protein 1	2.2
negative regulation of apoptosis	
tumor necrosis factor receptor superfamily, member 10d	3.6
suppressor of cytokine signaling	4.2
myeloid cell leukaemia sequence 1 (Bcl-2 related)	3.2
testis enhanced gene transcript (BAX inhibitor 1)	1.4
apoptosis inhibitor 5	1.8
fas (TNF receptor superfamily, member 6)	1.5
bcl-2-antagonist of cell death	1.6
oxidoreductases	
thioredoxin	1.4
thioredoxin domain containing	2.2
glutaredoxin	2.3
peroxiredoxin 6	1.7
protein disulfide isomerase family a, member 6	1.5
nad(p)h dehydrogenase, quinine 2	1.8
glutathione-reductase	1.7

Tab. 4.1: Micro array analysis of cells expressing mutant L62P. Total RNA from two different clones of stably transfected HEK293 cells expressing the wild-type V2R or mutant L62P tagged with FLAG was isolated and subjected to Affymetrix analysis. After verification of correlation, batch analysis was carried out. Upregulated genes were analyzed and listed by the use of the DAVID database (http://niaid.abcc.ncifcrf.gov/).

As expected, the obtained data indicate an important role of genes involved in folding and unfolding processes in chronic ER stress. In addition, micro array analysis reveals a great amount of novel UPR target genes and involved pathways yet unknown to be linked to ER stress and UPR. Due to the considerable quantity of up- and downregulated genes obtained in this study, a focus was set on genes associated with both regulation of apoptosis and redox regulation revealing a connection with outliving ER stress.

In summary, it can be demonstrated that chronic ER stress obtained by stable expression of misfolded receptor proteins leads to an induction of UPR as measured by overexpression of ER chaperones calnexin, GRP94 and GRP78. Furthermore, an activation of each of the three UPR signaling pathways of PERK, IRE-1 and ATF6 was detectable. However, no activation of all three pathways in every analyzed mutant could be measured. In addition, a reduction of UPR in HEK293 cells stably expressing the murine V2R was obtained after treatment with pharmacochaperones and the chemical chaperone DMSO, resulting in a rescue of the intracellularly retained receptor protein to the plasma membrane. New and yet unknown target genes of the UPR were detected by micro array analysis of stably transfected HEK293 cells pointing out an importance of both regulation of apoptosis and redox regulation.

4.2 Analysis of acute UPR

ER stress can be induced after acute and chronic conditions. So far the analysis of UPR induced by misfolded proteins was studied 24 h after transient transfection or in cell clones stably expressing the misfolded protein. The aim of the present work was to analyze UPR not only in HEK293 cells 6 h after transient transfection of mutant receptors but also in HEK293 cells stably expressing the V2R constructs to distinguish UPR induction under acute and chronic conditions to obtain a complete and precise analysis of ER stress.

4.2.1 Transient expression of the wild-type V2R and NDI-causing mutants

The expression levels of the wild-type V2R receptor and the three different mutants L62P, InsQ292 and G201D were examined after transient transfection to find out wether the expression of the receptor is comparable in each of the cell lines. For expression analysis, cells were lysed and subjected to immunoprecipitation analysis (Fig. 4.11). The V2R was expressed in two specific forms, the core-glycosylated immature receptor form (#), represented by the band running at 60-65 kDa, and the complex-glycosylated form of the mature receptor (*) at 75-88 kDa. These two forms could be detected in the wild-type and the Golgi-retained mutant G201D containing samples. In the other two mutants, L62P and InsQ292, only the core-glycosylated receptor form (#) was present indicating that transiently transfected mutant receptors were equally glycosylated. This is in good agreement to the data obtained from HEK293 cells stably expressing these receptor constructs (Fig. 4.1 B). Moreover, the expression analysis of the transiently transfected cell lines revealed equal expression intensities of the receptor. Despite equal quantities of transfected plasmid DNA, the wild-type V2R showed the highest amount of expressed receptor, whereas expression intensities of mutants L62P and G201D were comparable and InsQ292 was expressed half as much as the wild-type V2R. These data are consistent with similar observations obtained before (Hermosilla et al. 2004).

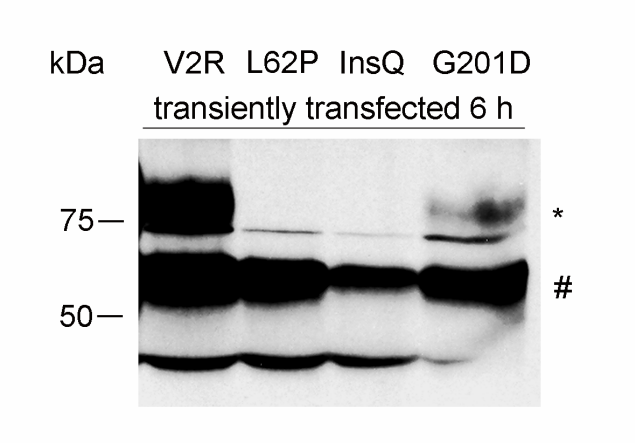

Fig. 4.11: Immunoprecipitation of GFP-tagged V2R receptor constructs. HEK293 cells were lysed 6 h after transient transfection with receptor plasmids and receptors were immunoprecipitated with a rabbit anti-GFP antibody. Expression of receptors was detected with a monoclonal mouse anti-GFP antibody. The mutant InsQ292 is labeled as InsQ. The asterisk (*) indicates the complex glycosylated receptor form, the (#) indicates the core-glycosylated form. Data are representative of three independent experiments.

4.2.2 Detection of acute UPR

To analyze the acute UPR the induction of chaperones was examined 6 h after transient transfection of V2R wild-type and mutant plasmids. Immunoblot analysis revealed that GRP94 and GRP78 were upregulated in cells expressing the V2R mutants InsQ292 and G201D, whereas PDI appeared to be slightly upregulated in each studied mutant and cells expressing the wild-type receptor (Fig. 4.12). HEK293 cells transfected with pEGFP-plasmid served as a negative control. Equal protein loading was controlled by immunoblot analysis with an anti-actin antibody.

The results indicate differences between the expression levels of chaperones under chronic and acute ER stress in the studied mutants. In HEK293 cells stably expressing V2R wild-type and mutants chaperone GRP78 was upregulated in every examined cell line, whereas under acute stress conditions expression of GRP78 appeared to be increased only in cells expressing mutants InsQ292 and G201D. Furthermore, no changes in the expression level of the foldase PDI could be observed upon chronic stress (Fig. 4.4), while PDI was slighty upregulated after transient transfection of wild-type V2R and mutants in HEK293 cells.

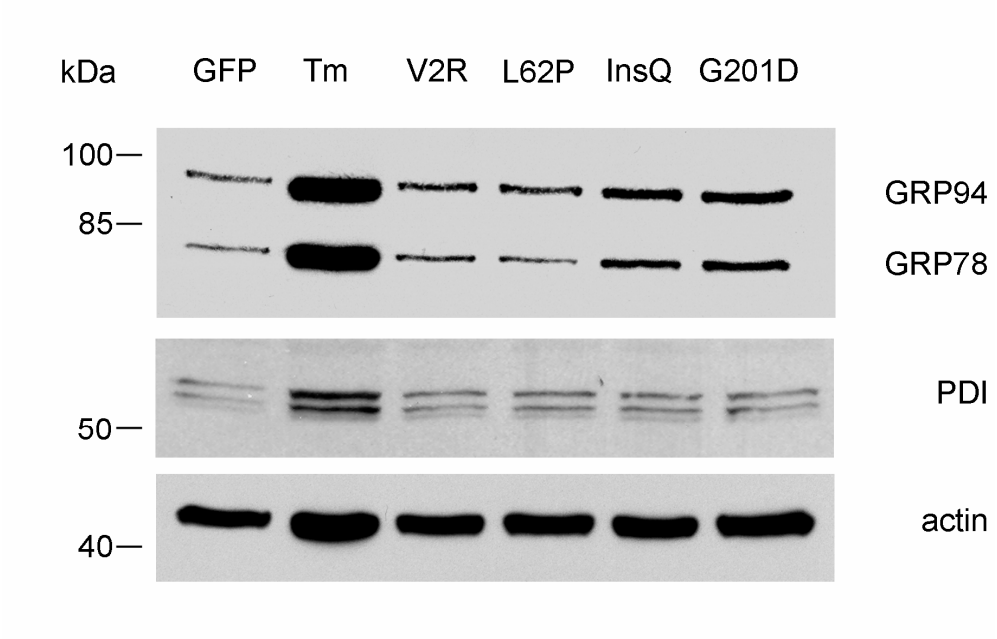

Fig. 4.12: Detection of acute UPR. Immunoblot analysis of whole cell lysates of HEK293 cells 6 h after transient transfection of wild-type or mutant V2Rs detecting GRP94 and GRP78 with an anti-KDEL antibody and PDI with an appropriate antibody. HEK293 cells transfected with pEGFP plasmid were used as a negative control (GFP) and HEK293 cells treated with 2.5 µg/ml tunicamycin for 16 h as a positive control (Tm). The mutant InsQ292 is labeled as InsQ. Actin served as a loading control. Similar data were obtained in six independent experiments.

The activation status of the UPR pathways was also analyzed under acute stress conditions. Immunoblot analysis of whole cell lysates of transient transfected HEK293 cells showed an enhanced phosphorylation state of eIF2α in mutants L62P and InsQ292, compared to pEGFP-transfected cells (Fig. 4.13).The further analyses of acute ER stress are restricted of these two mutants due to their different activation patterns under chronic ER stress. The obtained results indicate that eIF2α was already activated 6 h after transient transfection of misfolded receptor proteins. These data are consistent with the ones obtained under chronic ER stress, where eIF2α is also indicated to be involved in ER stress.

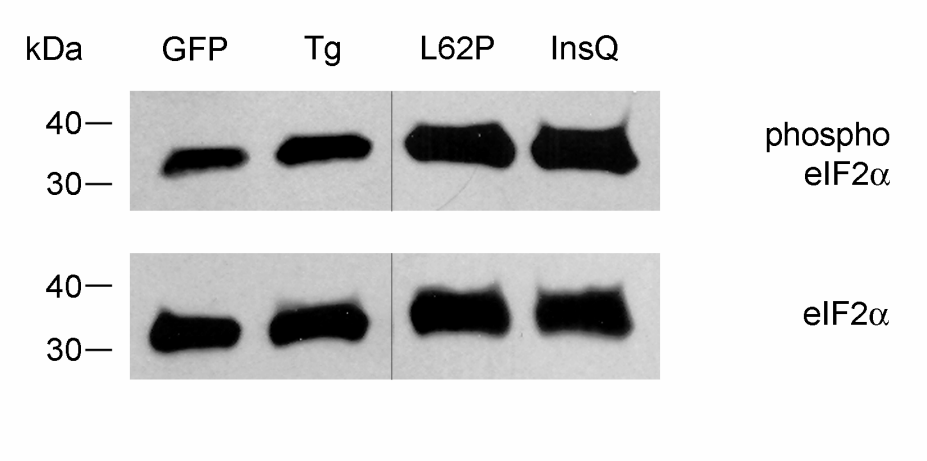

Fig. 4.13: Activation of eIF2α. Immunoblot analysis of whole cell lysates of HEK293 cells 6 h after transient transfection of mutant V2Rs detected with an anti-phospho-eIF2α antibody (top). Total eIF2α served as a loading control. The mutant InsQ292 is labeled as InsQ. Vertical lines indicate positional markings where lanes were extracted. Similar data were obtained in three independent experiments.

In addition, the splicing of XBP-1 by the signal transducer IRE-1 was examined. Total RNA was isolated from HEK293 cells 6 h after transient transfection of the mutant V2Rs L62P and InsQ292 and reverse-transcribed. After amplification by PCR with specific XBP-1 primers, no activation of XBP-1 was detectable under acute UPR conditions (Fig. 4.14). These results are consistent with the data obtained from chronic ER stress regarding the activation of XBP-1.

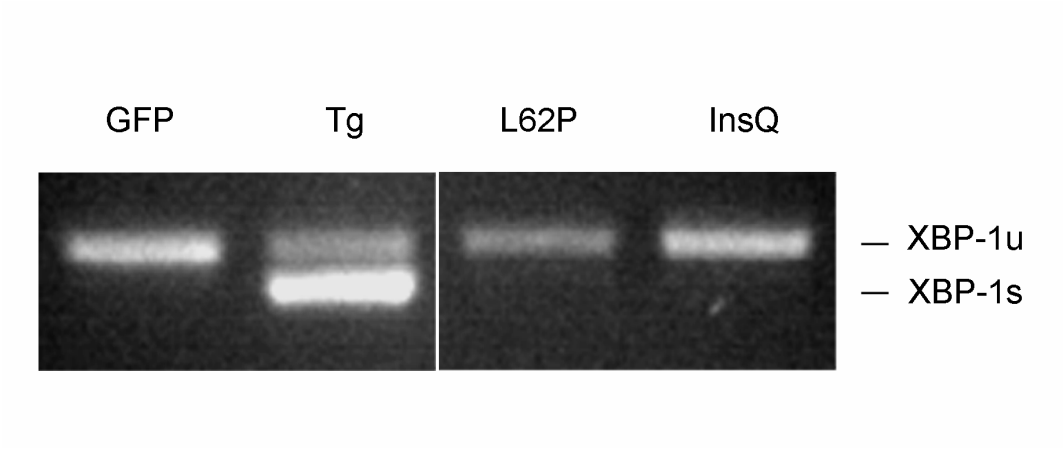

Fig. 4.14: Activation of XBP-1. Total RNA was isolated from HEK293 cells 6 h after transient transfection of mutant V2Rs and reverse-transcribed. After amplification by PCR with specific XBP-1 primers, the products were separated on a 3% agarose gel. The spliced and unspliced XBP-1 PCR fragments could be detected. As a negative control HEK293 cells transfected with pEGFP plasmid were used, HEK293 cells treated with 2 µM thapsigargin for 2 h served as positive control (Tg). The mutant InsQ292 is labeled as InsQ. Vertical lines indicate positional markings where lanes were extracted. Similar data were obtained in three individual experiments.

In summary, upon acute UPR induced by the transient transfection of misfolded receptor proteins, an upregulation of UPR-specific chaperones GRP78 and GRP94 and an activation of eIF2α (PERK pathway) could be detected. However, no activation of the other two pathways could be shown. Furthermore, the expression patterns of the chaperones under acute ER stress conditions differed from those obtained in stably transfected cell lines.

4.3 Detection of the ER-overload response (EOR)

Besides the characterization of the UPR and involved pathways, the ER-overload resonse (EOR) is described being another ER stress pathway (Pahl and Baeuerle 1997). The EOR is characterized by an activation of the transcription factor nuclear factor κB (NF-κB) (Pahl 1999). For EOR-mediated activation of NF-κB, a release of Ca^{2+} from the ER and the generation of reactive oxygen species is required. The activation of transcription factor NF-κB is triggered by the phosphorylation of the inhibitory subunit IκBα by the kinase IKKβ. This leads to ubiquitination and proteasomal degradation of the inhibitory subunit, so that NF-κB (p65 and p50) can be phosphorylated and translocates into the nucleus in order to regulate the transcription of anti-apoptotic, inflammatory or proliferative genes (Pahl 1999). To date it has been shown that overexpression of viral proteins or the μ-heavy chain induce both UPR and EOR. It remains to be elucidated if in addition to UPR the EOR stress response pathway is activated upon chronic or acute ER stress.

4.3.1 Analysis of chronic EOR

In order to analyze the activation of EOR, the activation of the NF-κB p65 subunit was determined by luciferase assays measuring the activity of the NF-κB p65 promoter region. Only the positive control, namely HEK293 cells treated with the EOR-inducing substance TNFα, show highly significant changes ($p < 0.001$) as compared to untreated HEK293 cells (Fig. 4.15). However, in all studied cell lines

stably expressing V2R wild-type and mutants L62P, InsQ292 and G201D no induction of NF-κB p65 was existent and detectable.

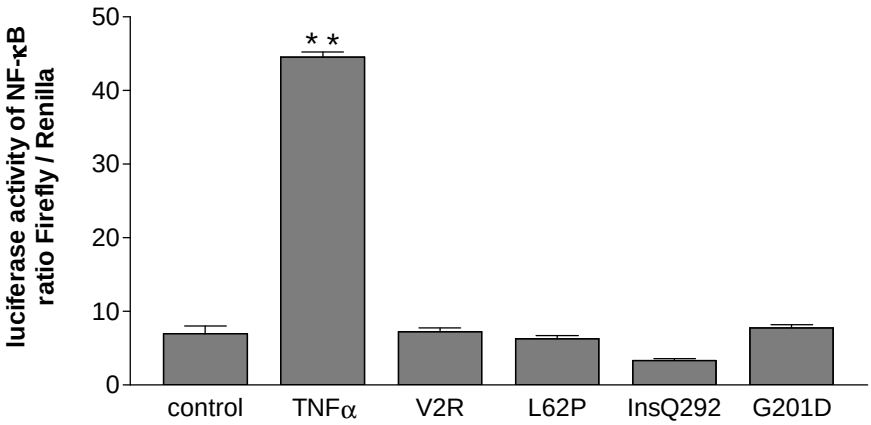

Fig. 4.15: Analysis of NF-κB activity by luciferase assay. Whole cell lysates of HEK293 cells stably expressing the V2R constructs as indicated, were subjected to luciferase assay. HEK293 ells were either left untreated (control) or treated with TNFα (TNFα) 30 ng for 1 h. Statistical analysis was performed with the software Prism 3.0; ANOVA Dunnett's Multiple Comparison Test was used to analyze statistical differences (** = $p < 0.001$). Similar data were obtained in three independent experiments.

Another possibility to measure the activation of NF-κB p65 under chronic stress conditions is to detect the amount of translocated transcription factor into the nucleus. For this reason fractionation of untransfected HEK293 cells and cells stably expressing wild-type and mutant V2Rs was performed and the nuclear fraction was used for immunoblot analysis with an anti-NF-κB p65 antibody. Consistent with the results obtained before, only in TNFα treated cells (positive control) NF-κB translocated into the nucleus, while the studied cell lines expressing mutants and wild-type receptor showed no increased nuclear expression (Fig. 4.16).

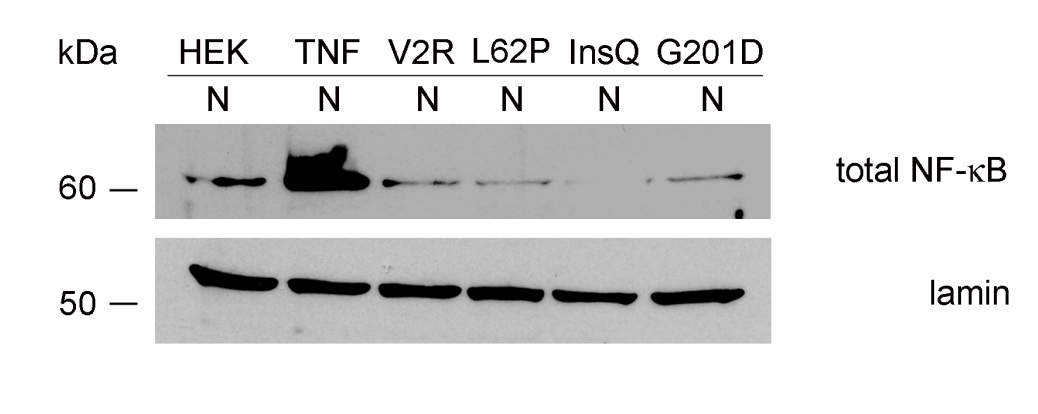

Fig. 4.16: Nuclear expression of NF-κB. Immunoblot analysis of nuclear fractions of HEK293 cells stably expressing V2R wild-type and mutants detected with an anti-NF-κB p65 antibody (top). As controls untransfected HEK293 cells (HEK) were used as negative and HEK293 cells treated with 30 ng TNFα for 1 h (TNF) as positive control. The mutant InsQ292 is labeled as InsQ. Lamin served as a loading control. Similar data were obtained in three independent experiments.

These results indicate that no induction of EOR could be measured though chronic ER stress conditions are present. It remains to be elucidated if acute ER stress results in an induction of EOR.

4.3.2 Analysis of acute EOR

The induction of EOR under acute stress conditions was analyzed 6 h after transient transfection of mutant receptor contructs L62P and G201D. Therefore, fractionation of transiently transfected HEK293 cells was done and the nuclear and cytoplasmic fractions were used for immunoblot analysis with an anti-NF-κB p65 antibody. Consistent with the results obtained for chronic EOR, only in TNFα treated cells (positive control) NF-κB translocates into the nucleus, while cells expressing the studied mutants and wild-type receptor show no nuclear expression of NF-κB (Fig. 4.17, indicated with *****).

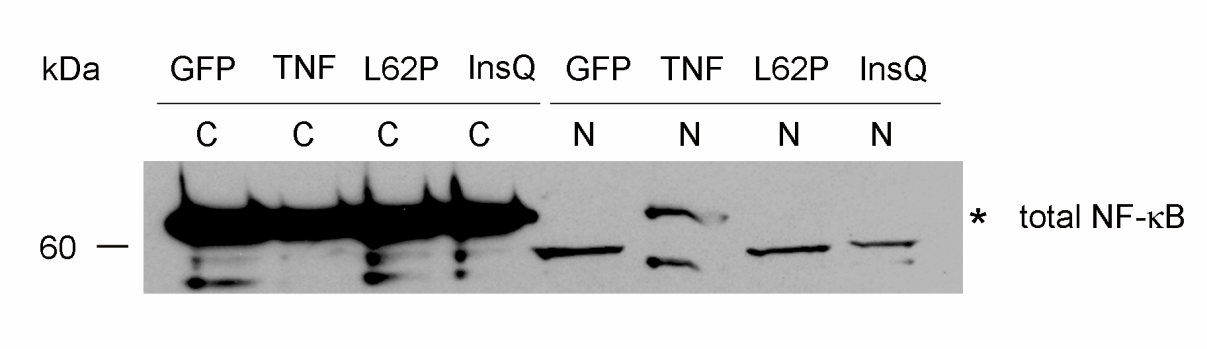

Fig. 4.17: Translocation of NF-κB. Immunoblot analysis of cytoplasmic (C) and nuclear (N) fractions of HEK293 cells 6 h after transient transfection of mutant V2R plasmids with an anti-NF-κB p65 antibody. HEK293 cells transfected with pEGFP plasmid were used as a negative control, HEK293 cells treated with 30 ng TNFα for 1 h as positive control (TNF). The mutant InsQ292 is labeled as InsQ. Similar data were obtained in three independent experiments.

In summary, these findings demonstrate that the second ER stress pathway, the EOR, was not activated under chronic and acute ER stress conditions as obtained by both HEK293 cells stably and transiently expressing misfolded proteins.

4.4 Pro-apoptotic and anti-apoptotic signaling

It is known that conditions of chronic UPR can result in the induction of so-called ER stress-mediated apoptosis (Szegezdi et al. 2006). The cell is not capable of reducing the amount of retained proteins in the ER and thus pro-apoptotic pathways are activated. Since several genes involved in regulation of apoptosis were upregulated as a result from chronic ER stress, as shown in the data table of the micro array analysis (Tab. 4.2), the next step was to verify these findings on protein level. Whole cell lysates of stably transfected HEK293 cells were analyzed with an anti-Bcl-2 antibody (Fig. 4.18 A). While the cytoprotective effects of Bcl-2 have been demonstrated in a variety of apoptotic models, the exact mechanism is not entirely clear. The anti-apoptotic protein Bcl-2 was slightly upregulated in cells stably expressing mutants InsQ292, G201D and wild-type receptor, whereas cells expressing mutant L62P and cells treated with TNFα (positive control) showed a decreased expression as compared to the control. Actin served as a loading control.

Furthermore, ER stress-mediated apoptosis was analyzed after 6 h of transient transfection (Fig. 4.18 B). Immunoblot analysis of lysates of HEK293 cells transiently transfected with wild-type receptor and V2R mutants was carried out using an anti-Bcl-2 antibody (rabbit). Under these acute ER stress conditions anti-apoptotic Bcl-2 was slightly upregulated in cells expressing mutants InsQ292 and G201D, while L62P expressing cells and TNFα-treated cells showed a decreased expression of Bcl-2. Actin was used as a loading control.

A

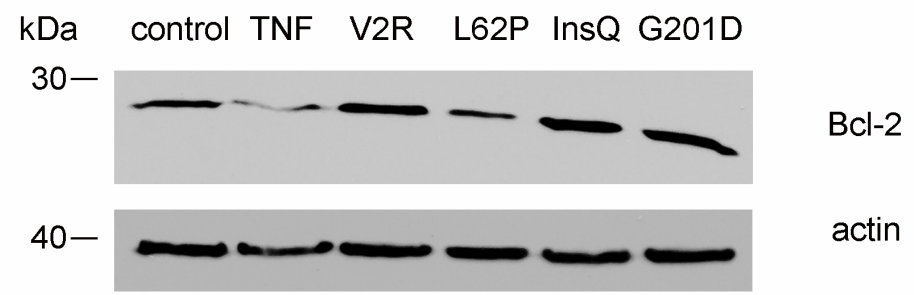

B

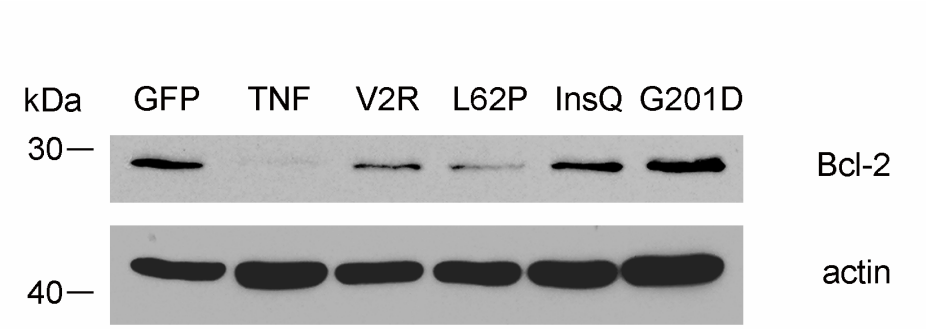

C

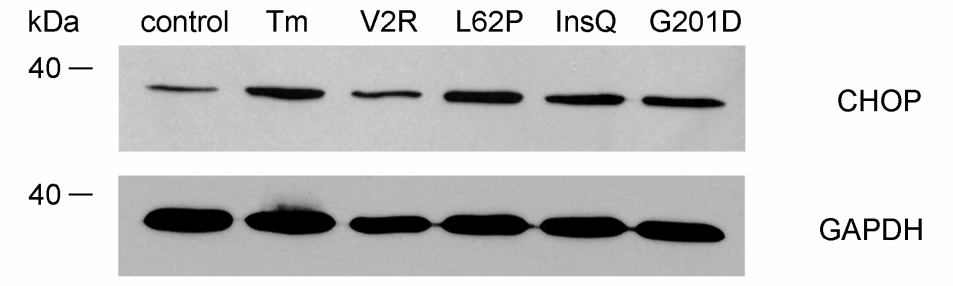

D

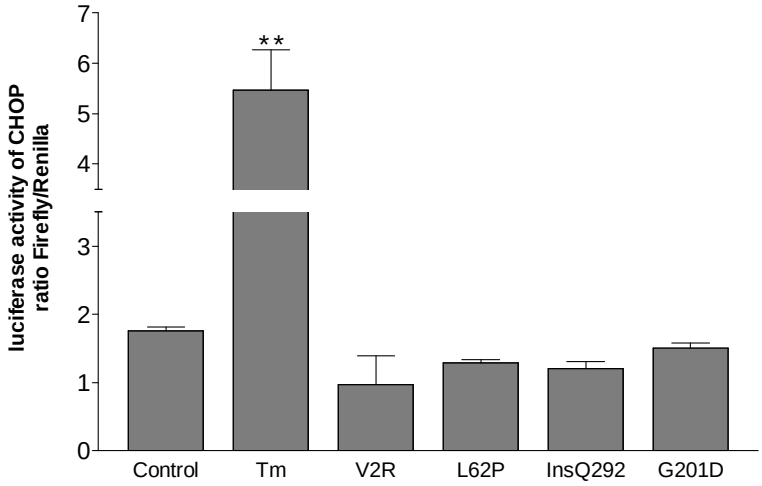

Fig. 4.18: Apoptotic and anti-apoptotic signaling. A Immunoblot analysis of whole cell lysates of HEK293 cells stably expressing V2R wild-type and mutants detecting Bcl-2 with an anti-Bcl-2 antibody. As a negative control non-transfected HEK293 cells and as a positive control HEK293 cells treated with 30 ng TNFα for 1 h (TNF) were used. The mutant InsQ292 is labeled as InsQ. Actin served as a loading control. **B** Immunoblot analysis of lysates of HEK293 cells transiently transfected with V2R.GFP and mutants for 6 h with an anti-Bcl-2 antibody. As a negative control non-transfected HEK293 cells and as a positive control HEK293 cells treated with 30 ng TNFα for 1 h (TNF) were used. Actin served as a loading control. **C** Immunoblot analysis of whole cell lysates of stably expressing HEK293 cells detecting CHOP with an anti-CHOP antibody. As controls the same conditions as in **A** were used. GAPDH served as a loading control. **D** Analysis of the pro-apoptotic transcription factor CHOP by luciferase assay. Cells were either left untreated (control) or were treated with 2.5 µg/ml tunicamycin (Tm) for 16 h. Statistical analysis was performed with the software Prism 3.0; ANOVA Dunnett's Multiple Comparison Test was used to analyze statistical differences (** = $p < 0.001$).

Another important transcription factor regarding apoptosis is the C/EBP homologous protein (CHOP). This pro-apoptotic protein is one of the target proteins of the PERK signaling pathway and seems to be activated during ER stress-mediated apoptosis (Szegezdi et al. 2006). Immunoblot analysis of whole cell lysates of HEK293 cells stably expressing wild-type and mutant V2Rs was performed with an anti-CHOP antibody (rabbit). An upregulation of CHOP in the positive control and in cells expressing mutant L62P could be observed (Fig. 4.18 C). GAPDH served as a loading control. In order to confirm these results, luciferase assays of CHOP activation were performed (Fig. 4.18 D). However, a statistically significant

upregulation was only visible in the positive control, in tunicamycin-treated HEK293 cells.

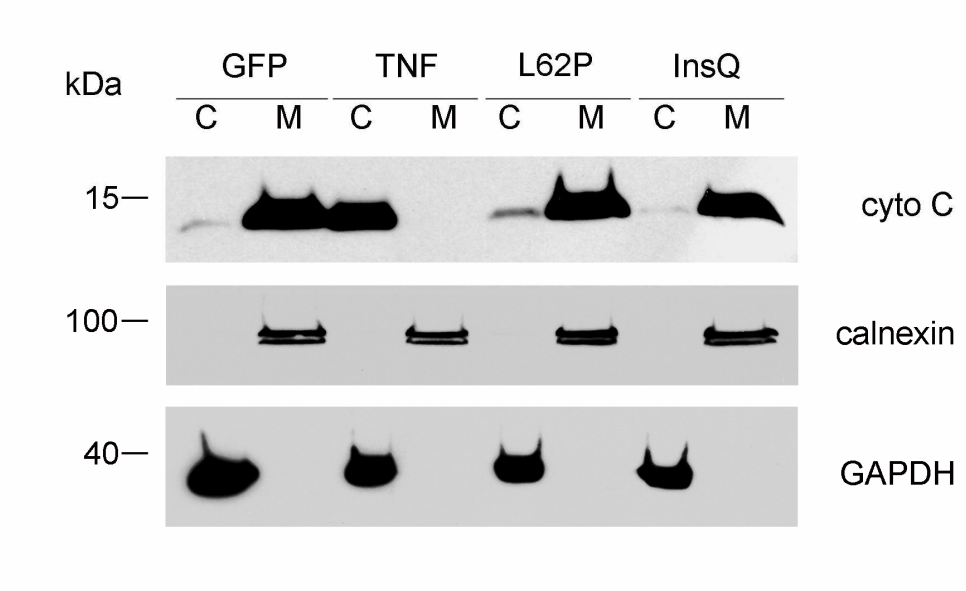

Fig. 4.19: Detection of translocation of cytochrome c. Isolated cytosolic (C) and membrane (M) fractions of HEK293 cells transiently transfected with V2R mutants for 6 h were analyzed by SDS-PAGE and immunoblotting with an anti-cytochrome c antibody. Controls were HEK293 cells transfected with GFP plasmid (control) and HEK293 cells treated with 30 ng TNFα for 1 h (TNF). The mutant InsQ292 is labeled as InsQ. Purity of cell fractions was confirmed by the detection of calnexin and GAPDH in all isolated fractions. Data are representative of three independent experiments.

The pivotal question is, if the different expression patterns of pro- and anti-apoptotic proteins lead to the induction of apoptosis. One possibility to measure apoptosis is the activation of cytochrome *c*. Cytochrome *c* is released from the mitochondria in response to pro-apoptotic stimuli (Jiang and Wang 2004). Therefore, isolated cytosolic (C) and membrane (M) fractions containing plasma membrane, ER and mitochondria of HEK293 cells transiently transfected with V2R mutants L62P and InsQ292 were subjected to immunoblotting with an anti-cytochrome *c* antibody (Fig. 4.19, top). Positive control, TNFα-treated HEK293 cells, and cells expressing mutant L62P both showed a release of cytochrome *c* by detecting the protein in the cytosolic fractions. Immunoblot analysis with anti-calnexin and anti-GAPDH antibodies was carried out to determine the purity of the different fractions. The ER-resident chaperone calnexin could only be detected in the membrane fractions, while the

cytosolic protein GAPDH appeared as expected only in the cytosolic fractions indicating pure fractions.

In summary, these results demonstrate that anti-apoptotic protein Bcl-2 is upregulated in cells expressing mutants InsQ292 and G201D under conditions of both chronic and acute ER stress. L62P expressing cells show a downregulation, whereas the pro-apoptotic protein CHOP is upregulated. Furthermore, the induction of apoptosis in this cell line can be detected by measuring the release of cytochrome c from the mitochondria. Therefore, the survival of the cells expressing this specific mutant has to be regulated by other anti-apoptotic pathways.

4.5 Nuclear expression of chaperones

Beside their function as folding assistants, some chaperones are known to additionally stabilize cellular proteins under stress conditions and protect nascent protein chains during normal growth. Chaperones Hsp90 and Hsp70 specifically interact with a mitochondrial protein import receptor at the outer mitochondrial membrane and are also required for the translocation of precursor proteins (Young et al. 2003). A specific role for molecular chaperones in the regulation of the nuclear import of steroid receptor and therefore regulation of its function within the nucleus is also described (Elbi et al. 2004). In addition, Hsp70 can also inhibit its own transcription by interacting with the heat shock transcription factor HSF-1 in the nucleus (Shi et al. 1998). Until now, chaperone GRP94 as member of the Hsp90 family could only be found in the cytoplasm. It could be an interesting hypothesis if GRP94 is detectable in the nucleus resulting in equal effects.

Therefore the translocation of the chaperone GRP94 into the nucleus was analyzed. The results of immunofluorescence analysis of HEK293 cells (control) and cells stably expressing L62P as an example are shown in Fig. 4.20 A. GRP94 could be detected in the nucleus of HEK293 cells stably expressing L62P, whereas untransfected cells showed no or only few nuclear signals of GRP94. Consistent with the data obtained from immunofluorescence analysis, immunoblot analysis of nuclear fractions of stably expressing HEK293 cells revealed that the highest amount of nuclear GRP94 could be found in cells expressing mutant L62P, whereas in untransfected HEK293 cells GRP94 was only present to a small degree and in

InsQ292 to an even lesser extent (Fig. 4.20 B). The test of purity of the obtained and analyzed fractions was performed by detecting the nuclear protein lamin and the cytosolic protein GAPDH in the different extracts and revealed no contaminations. Furthermore, nuclear translocation of GRP94 was determined by electron microscopy. Untransfected HEK293 cells as a control and mutant L62P were used and immunoelectron microscopy was performed as described. However, only in cells expressing mutant L62P, GRP94 could be detected in the ER compartment and, most importantly, within the nucleus (Fig. 4.20 C). In untransfected HEK293 cells (control) no GRP94 signals could be visualised, most probably due to the reduced expression of this chaperon in HEK293 cells under physiological conditions as shown before in the immunoblot analysis (Fig. 4.2 A).

A

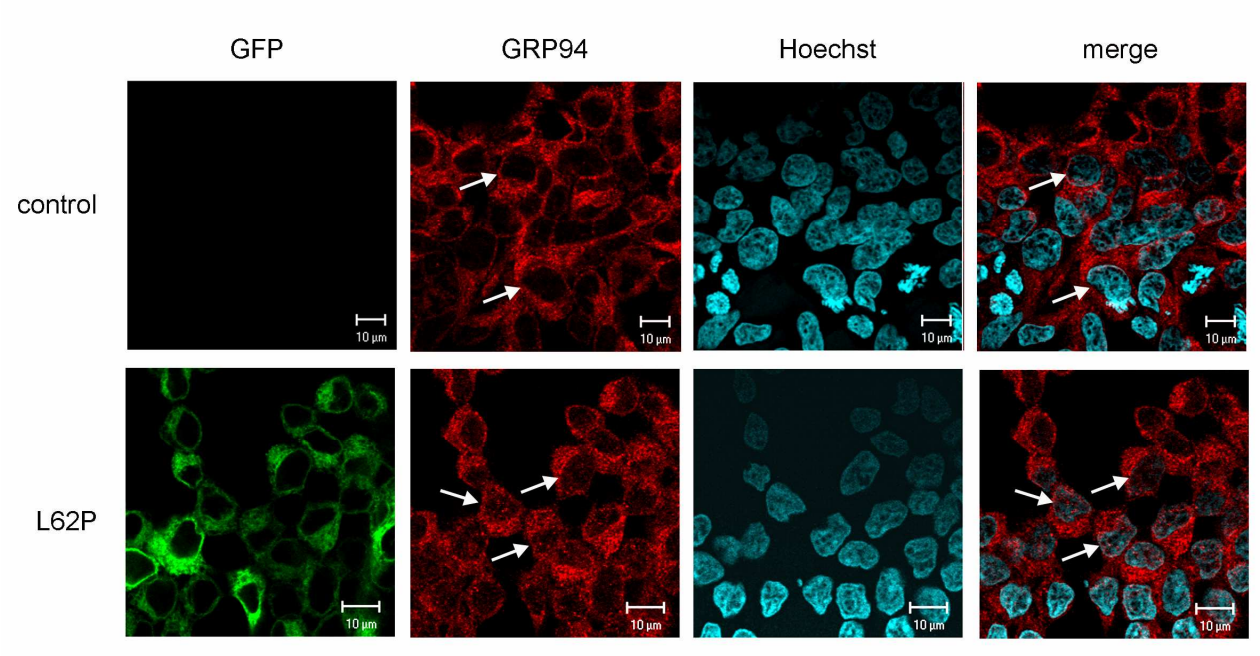

B

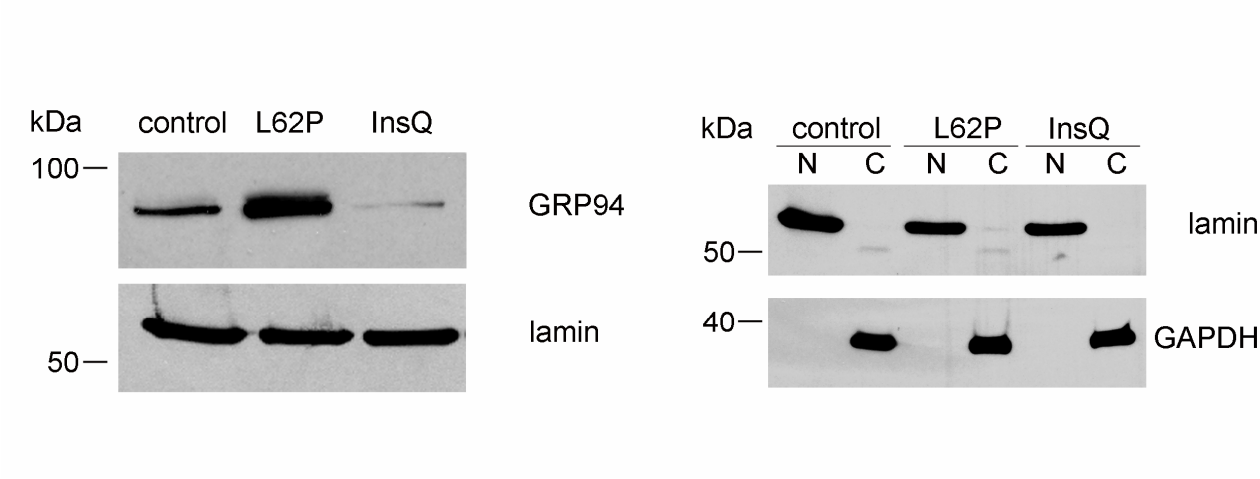

C

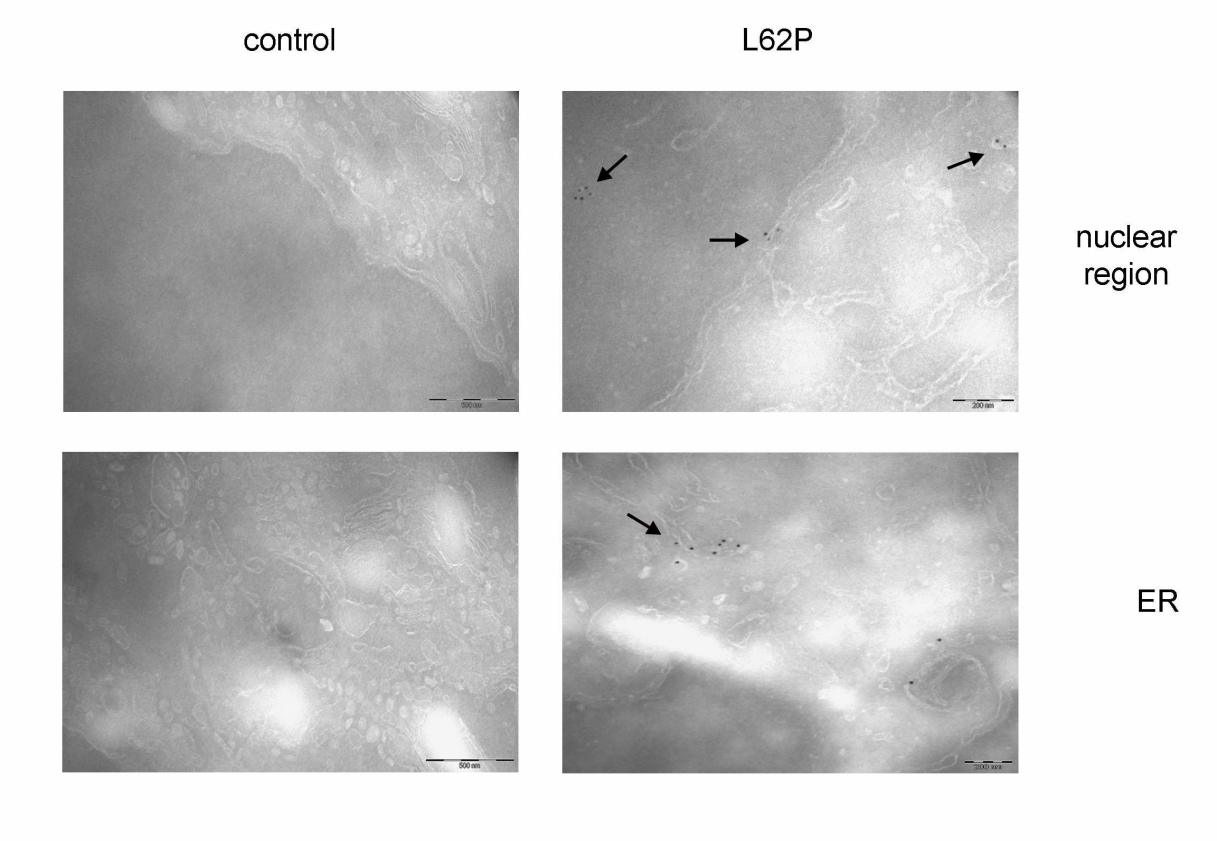

Fig. 4.20: Translocation of GRP94 into the nucleus. A Immunofluorescence analysis of HEK293 cells (control) and cells stably expressing L62P. After permeabilization cells were incubated with an anti-GRP94 antibody (rat) and a secondary goat anti-rat antibody conjugated with cy3. Localization of GRP94 was examined by confocal laser-scanning microscopy with horizontal (*xy*) scans. Receptor GFP fluorescence signals are shown in green (left), GRP94 staining of the same cells is shown in red

and staining of the nucleus by Hoechst 33342 in blue. GFP, GRP94 and nuclear fluorescence signals were computer-overlaid (right). The scans show representative cells. Similar data were obtained in three independent experiments. Scale bar, 10 µm. **B** Immunoblot analysis of HEK293 cells stably expressing mutant receptors L62P and InsQ292 detecting GRP94 with an anti-GRP94 antibody. The mutant InsQ292 is labeled as InsQ. Lamin and GAPDH served as controls of purity of the nuclear (N) and cytosolic (C) fractions. **C** Immunoelectron microscopy. Ultrathin cryosections (80 nm) were obtained using an cryoultramicrotome The sections were immunolabeled with a rat monoclonal anti-GRP94 antibody overnight and subsequently with a gold (15 nm) labeled goat anti-rat IgG for 2 h. Cryosections were contrasted using a mixture of 3% tungstosilicic acid hydrate and 2.5 % PVA. The sections were viewed in a 80kV ZEISS 902 A electron microscope.

Taken together, these findings point to a possible location of chaperone GRP94 in the nucleus, verified by three different approaches. However, the function of GRP94 in the nucleus remains to be elucidated.

4.6 Possible regulation of transcription factor ATF6 by chaperones

The exact mechanism how the activation of the signal transducers PERK, IRE-1 and ATF6 is regulated is controversially discussed. The direct recognition model proposes that unfolded proteins bind directly to the luminal domains of the transducers, whereas the indirect model hypothesizes that binding of abundant ER chaperone BiP keeps PERK, IRE-1 and ATF6 inactive (Ron and Walter 2007). Immunoprecipitation analyses were performed in order to analyze if interactions with other chaperones, like GRP94 as example for an ER resident chaperone and Hsp70 as a cytosolic chaperone, could be found indicating another possible form of regulation.

HEK293 cells stably expressing wild-type and mutant V2Rs were lysed and endogenous ATF6 was precipitated with a rabbit anti-ATF6 antibody. Expression of GRP94 and Hsp70 was detected using appropriate antibodies (Fig. 4.21 A). The strongest expression of GRP94 could be observed in samples of cells expressing mutant InsQ292 and in the positive control, tunicamycin-treated HEK293 cells, while the detection of Hsp70 revealed no major differences in all cells. The detection of precipitated endogenous ATF6 revealed differences in ATF6 expression in the analyzed mutants (∗) even though equal amounts of total proteins were subjected to

the assay. However, despite the fact that the p90 form of ATF6 was precipitated in InsQ292 to minor amounts, the strongest interaction with GRP94 could be found there.

A

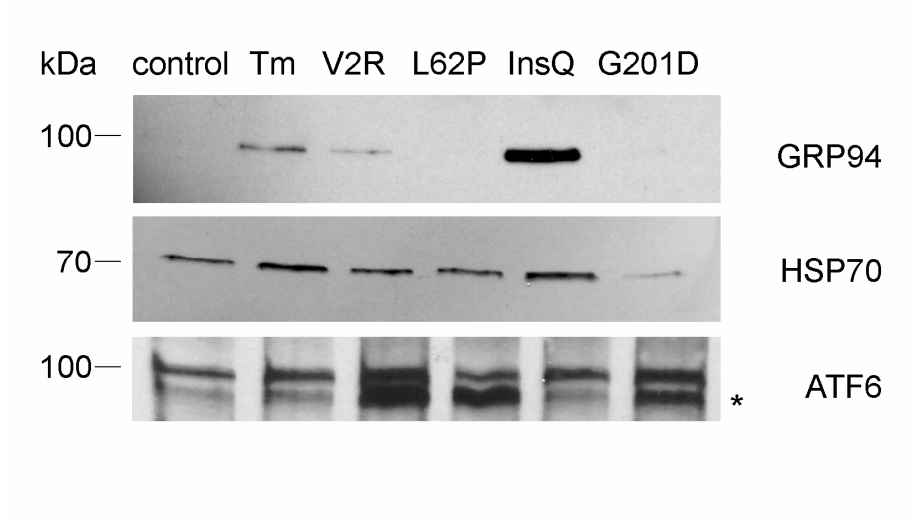

B

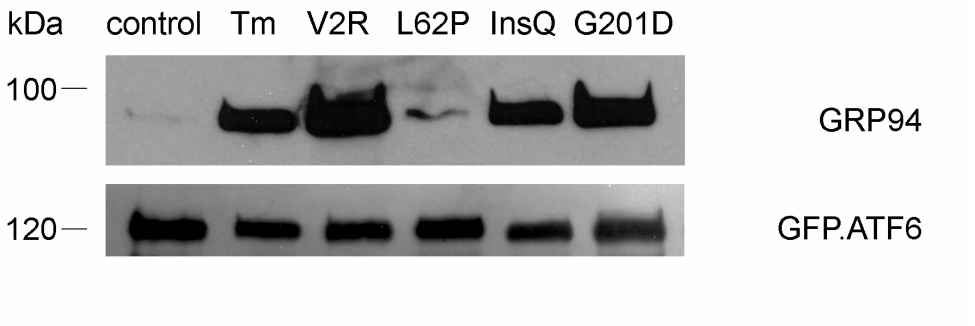

C

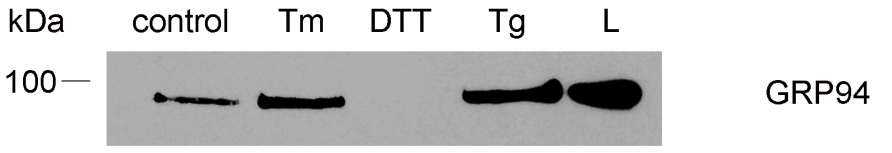

Fig. 4.21: Interaction of ATF6 with GRP94. A Immunoprecipitation of GFP-tagged V2R receptor constructs. HEK293 cells stably expressing wild-type and mutant V2Rs were lysed and endogenous ATF6 was immunoprecipitated with a rabbit anti-ATF6 antibody. Expression of GRP94 was detected with a monoclonal rat anti-GRP94 antibody, and Hsp70 expression with an anti Hsp70 antibody. Amounts of precipitated ATF6 were determined with an anti-ATF6 antibody. The mutant InsQ292 is

labeled as InsQ. The asterisk (*) indicates the p90 form. As a negative control untransfected HEK293 cells and as a positive control HEK293 cells treated with 2.5 µg/ml tunicamycin (Tm) were used. Data are representative of three independent experiments. **B** HEK293 cells stably expressing wild-type and mutant V2Rs were lysed 48 h after transient transfection of the GFP.ATF6 plasmid, ATF6 was precipitated with a rabbit anti-ATF6 antibody. Expression of GRP94 was detected with a monoclonal rat anti-GRP94 antibody. The amount of precipitated GFP.ATF6 was determined with an anti-ATF6 antibody. As a negative control, untransfected HEK293 cells (control) and as a positive control HEK293 cells treated with 2.5 µg/ml tunicamycin (Tm) were used. Data are representative of three independent experiments. **C** Immunoprecipitation of ATF6 in untransfected HEK293 cells. Cells were lysed and endogenous ATF6 was immunoprecipitated with a rabbit anti-ATF6 antibody. Expression of GRP94 was detected with a monoclonal rat anti-GRP94 antibody. As positive controls HEK293 cells treated with 2.5 µg/ml tunicamycin for 16 h (Tm), HEK293 cells treated with 2 mM DTT for 1 h (DTT) and HEK293 cells treated with 2 µM thapsigargin for 2 h (Tg) were used. L indicates the lysate of HEK293 cells.

To increase the amounts of co-precipitated GRP94, HEK293 cells were transiently transfected with GFP.ATF6 to increase the quantity of ATF6 in the lysates. The results are shown in Fig. 4.21 B. HEK293 cells stably expressing wild-type and mutant V2Rs were lysed 48 h after transient transfection of the GFP.ATF6 plasmid. The overall signal intensity of detected GRP94 was now much stronger than before (Fig. 4.21 A). Interaction of ATF6 with the chaperone GRP94 could now be detected in the positive control, in cells expressing the wild-type receptor and in mutants InsQ292 and G201D expressing cells, whereas mutant L62P was comparable to the control. To determine whether the unveiled interaction of ATF6 with GRP94 was connected with induction of UPR, the effects of different chemical inducers of UPR on this interaction were analyzed (Fig. 4.21 C). Treatment with thapsigargin and tunicamycin led to an enhanced interaction whereas DTT-treated cells showed no interaction at all. The whole cell lysate (L) was used as a control for detection of GRP94.

In summary, these results allude to a possible interaction of transcription factor ATF6 and chaperone GRP94. However, not all studied cell lines showed this interaction. The interaction could be traced back to ER stress because of the enhanced interaction after chemical induction of UPR. The outcome and function of this association remains to be elucidated.

4.7 Adaptation to chronic ER stress

Stably expressing HEK293 cell lines have to endure chronic ER stress conditions for a long time. However, these cells do not become apoptotic. They appear to develop an adaptation towards these stress conditions, resulting in the survival of the cell. One specific survival pathway is described to proceed via proteasomal degradation of pro-apoptotic protein ASK1 by binding of thioredoxin resulting in the inhibition of p38/JNK.

By immunoblot analysis of HEK293 cells stably expressing wild-type and mutant V2Rs with anti-ASK1 and anti-thioredoxin antibodies the expression of pro-apoptotic protein ASK1 and thioredoxin was examined to determine whether this pathway is used to prevent cell death. Cells expressing mutant L62P showed a reduced expression of ASK1 (Fig. 4.22 A). To find out whether this reduced expression is due to proteasomal degradation, HEK293 cells were incubated with the proteasome inhibitor MG132. An enhanced expression of ASK1 was detectable in all studied cell lines including L62P (Fig. 4.22 B). Furthermore, the expression of thioredoxin was checked after treatment with MG132. Expression of thioredoxin without inhibition of the proteasome shown in Fig. 4.24 indicated an increased expression of thioredoxin in HEK293 cells stably expressing L62P and InsQ292. After treatment with MG132, thioredoxin was strongly upregulated in this particular mutant, indicating a possible connection of these two proteins.

A

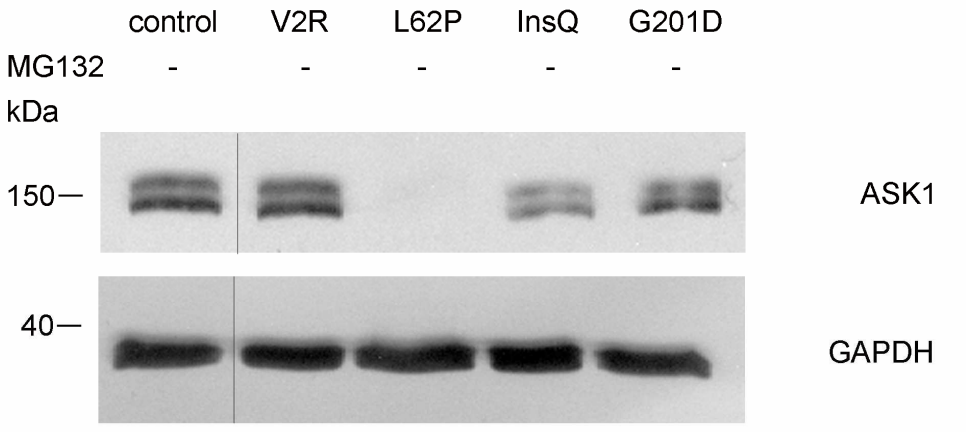

B

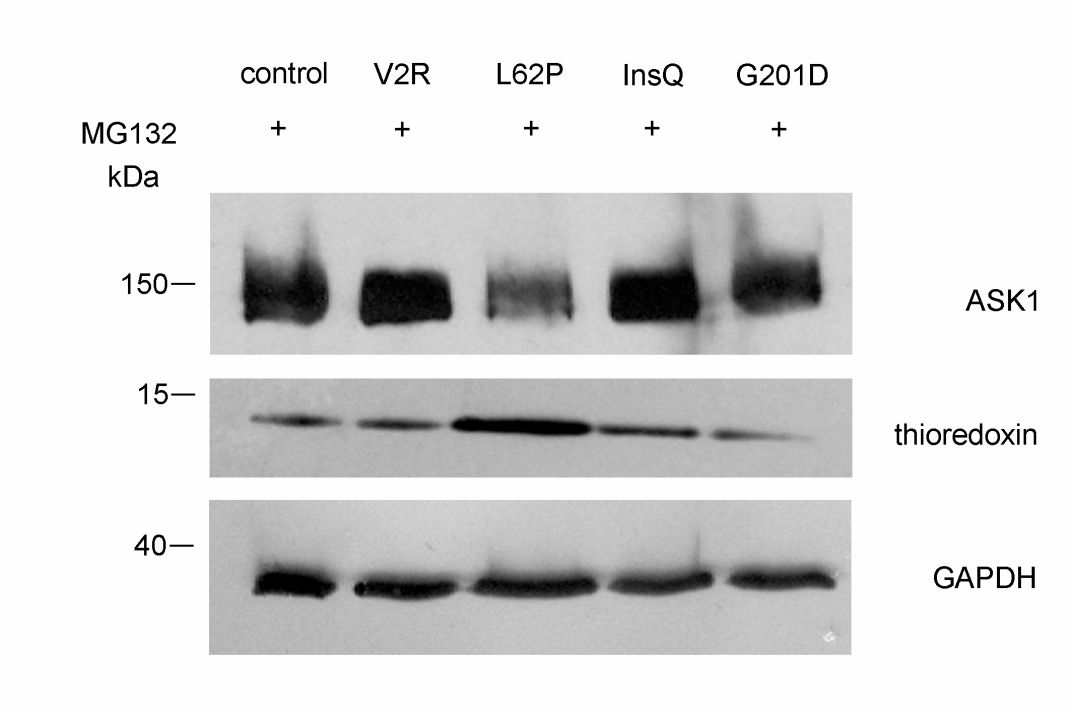

Fig. 4.22: Degradation of ASK1. A Immunoblot analysis of HEK293 cells stably expressing the wild-type and mutant V2Rs detecting ASK1 with an anti-ASK1 antibody. As a negative control non-transfected HEK293 cells were used (control). The mutant InsQ292 is labeled as InsQ. Vertical lines indicate positional markings where lanes were extracted. GAPDH served as a loading control. **B** Immunoblot analysis of HEK293 cells stably expressing the wild-type and mutant V2Rs detecting ASK1 and thioredoxin with anti-ASK1 and anti-thioredoxin antibodies, respectively. Cells were treated with 20 µM MG132 for 16 h. As a negative control non-transfected HEK293 cells were used (control). GAPDH served as a loading control.

Taken together, these findings demonstrate a complete downregulation of the pro-apoptotic protein ASK1 in cells expressing mutant L62P due to proteasomal degradation, while thioredoxin was upregulated simultaneously in this particular mutant.

As a next approach the possible interaction of ASK1 with thioredoxin and its ubiquitination status were analyzed (Fig. 4.23). Therefore, HEK293 cells stably expressing wild-type and mutant V2Rs were treated with 20 µM MG132 for 16 h. Immunoprecipitation of the control (untransfected HEK293 cells) and cells expressing the wild-type V2R and mutant receptors was carried out in order to analyze a possible interaction of ASK1 and thioredoxin as described in the literature, resulting in an inhibition of the pro-apoptotic pathway via p38/JNK (Saitoh et al. 1998). The

amount of precipitated ASK1 was nearly the same in all studied cell lines, only cells expressing wild-type V2R showed a slightly stronger content. In contrast, the highest detection of thioredoxin appeared to be in mutant L62P expressing cells indicating the strongest interaction (*). Concerning the ubiquitination status of ASK1 in mutant L62P expressing cells after inhibition of the proteasome it could be found that ASK1 is ubiquitinated (*). An increased level of polyubiquitinated proteins (short smear running over 150 kDa) appeared at the upper part of the blot, most probably reflecting the ubiquitinated forms of ASK1.

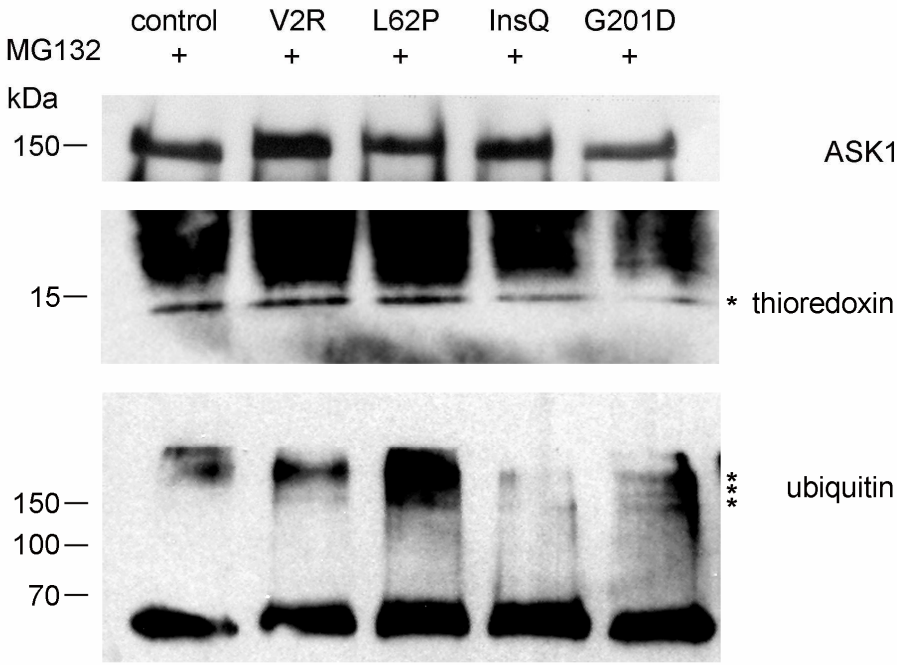

Fig. 4.23: Interaction of ASK1 with thioredoxin and ubiquitin. HEK293 cells stably expressing wild-type and mutant V2Rs were treated with 20 µM MG132 for 16 h. Immunoprecipitation of control (untransfected HEK293 cells), the wild-type V2R and mutant receptors was carried out. The amount of precipitated ASK1 was detected by immunoblotting using an anti-ASK1 antibody. The interaction of ASK1 with thioredoxin and its ubiquitination status was analyzed by immunoblotting using anti-thioredoxin and anti-ubiquitin antibodies. The mutant InsQ292 is labeled as InsQ.

Taken together, these results show a link between enhanced expression of thioredoxin and the proteasomal degradation of pro-apoptotic protein ASK1 in cells expressing mutant L62P. This is indicated by the appearance of ASK1 only after inhibition of the proteasome in this particular mutant. Furthermore, an enhanced expression of and interaction with thioredoxin was detectable under these conditions. Analysis of the ubiquitination status of ASK1 revealed a higher amount of ubiquitinylated ASK1, which is in good agreement with the enhanced proteasomal degradation of this pro-apoptotic protein in cells expressing mutant L62P. Inhibition of of the pro-apoptotic pathway via p38/JNK due to proteasomal degradation of ASK1 seems to be one possible adaptation process in cells expressing mutant L62P, which assures a survival despite of persistent and severe ER stress.

4.8 Measurement of redox activity upon chronic ER stress

The inhibition of programmed cell death in cells expressing mutant L62P by enhanced interaction of ASK1 and thioredoxin is just one possible adaptation mechanism.

In addition to the analysis of molecular chaperones originally involved in the UPR, the expression of chaperones implied in redox-regulation was examined including the foldase PDI, the oxidoreductases thioredoxin and ERp57 and Ero1α, a so-called oxidoreductin involved in ER redox control (Fig. 4.24). Whole cell lysates of HEK293 cells stably expressing the wild-type V2R or mutant receptors L62P, InsQ292 or G201D were subjected to immunoblot analysis. All chaperones showed an enhanced expression in tunicamycin-treated cells. In contrast, HEK293 cells expressing the wild-type V2R demonstrated only a slight effect for ERp57 as compared to untransfected HEK293 cells. Thioredoxin, Ero1α and ERp57 showed an increased expression in samples from mutants L62P and InsQ292. PDI was slightly upregulated only in samples from mutant InsQ292. GAPDH was used as a loading control to verify equal amounts of protein.

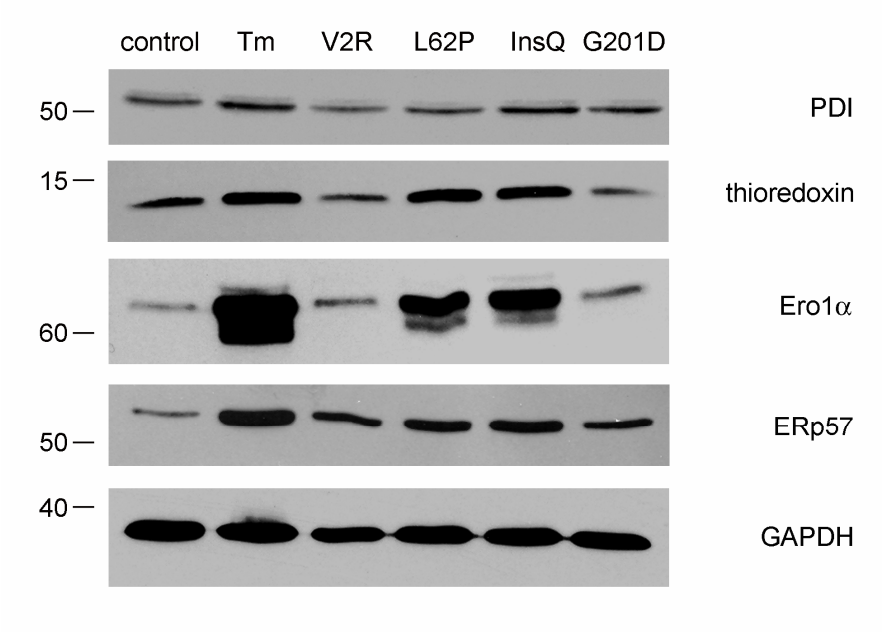

Fig. 4.24: Expression analysis of chaperones involved in redox regulation. Whole cell lysates of HEK293 cells stably expressing the V2R constructs as indicated, were subjected to immunoblot analysis detecting PDI, thioredoxin, Ero1α and ERp57 with appropriate antibodies (top). Non-transfected HEK293 cells served as a negative control (control) and tunicamycin-treated cells (Tm; 2.5 µg/ml, 16 h) as a positive control. The mutant InsQ292 is labeled as InsQ. GAPDH was detected as a loading control. Similar data were obtained in three independent experiments.

Due to the increased expression of chaperones involved in redox regulation (thioredoxin, ERo1α, PDI and ERp57) in cells expressing mutants L62P and InsQ292, the redox activity of these cell clones was determined by analyzing the antioxidative power and capacity of both mutants and the wild-type receptor and untransfected HEK293 cells as controls.

Cell line	**AP ($N_{(FR)/cell*min}$)**	**AP (AU)**	**T_r (min)**
HEK293	1.185×10^{11}	0.005	0.59
V2R	1.23×10^{11}	0.005	0.64
L62P	4.9×10^{12}	0.2	0.22
InsQ292	4.8×10^{12}	0.2	0.22

Tab. 4.2: Determination of the antioxidative status of living cells was carried out using the Antioxidative Power (AP) test method. Three different concentrations of each cell line were

added to 0.2 mM DPPH (test radical) and the signal intensity decay was measured over 40 min by ESR.

Measurement of antioxidative power is based on electron spin resonance (ESR). The antioxidative power informs about the capacity of an antioxidant to neutralize free radicals, but also about the reactivity of the substance. In Tab. 4.2 the antioxidative status of HEK293 cells stably expressing the V2R constructs as indicated was determined. Cell lines expressing L62P and InsQ292 showed significant changes in comparison to untransfected HEK293 cells and wild-type receptor. The redox activity of the first two cell lines (AP 0.2 AU/cell) was forty times higher than the activity measured in control cells and V2R (AP 0.005 AU/cell). One could argue that the smaller the reaction time (T_r), the faster are the cells in neutralizing the added free radicals.

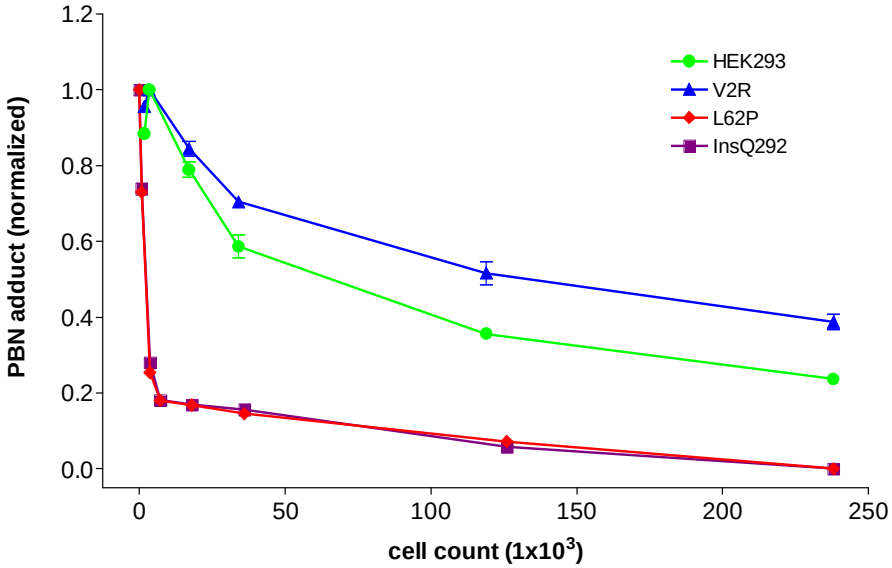

Fig. 4.25: Determination of the Antiradical Potential (ARP). Test radical PBN (20 mM) was added to different dilutions of each cell line and immediately exposed to UV radiation (2 min) to generate hydroxyl free radicals. The radical scavenging activity of the cells measured by Electron Spin Resonance Spectroscopy (ESR) is inverse proportional to the signal intensity of the PBN adduct. Data represent mean values of two independent experiments each performed in triplicate.

Another possibility to study the redox activity in whole cells is the determination of the antiradical potential (ARP). The detection of the redox capacity was carried out by adding PBN, a semi stable test radical used to produce free hydroxyl radicals, to different concentrations of the studied cell lines. In the present study the reduction of

radical concentration was measured. The cell lines showed differences in their ability to trap free radicals. The amount of free radicals (PBN) was reduced much faster in cells expressing mutants L62P and InsQ292, even in smaller cell numbers. The capacity to neutralize free hydroxyl radicals (•OH) can be described as followed:

V2R < HEK293 < L62P ~ InsQ292

These results indicate a connection between the enhanced redox activity in the studied mutants and the inhibition of ER stress-mediated apoptosis. Therefore, a second possibility of adaptation to chronic ER stress could be detected resulting in the survival of cell lines stably expressing misfolded proteins.

In summary, this work shows for the first time that UPR but not EOR are activated after stable and/or transient expression of misfolded V2Rs. Induction of the UPR was measured by an upregulation of different chaperones by immunoblot analysis and luciferase assay and verified by the complete activation study of the three known UPR-specific pathways. Simultaniously, analyses of activation of NF-κB revealed no induction of this pathway involved in EOR in cells expressing NDI-causing mutants. Furthermore, it could be shown that different mutants of a single receptor protein activate different UPR branches. ER-retained mutant L62P and ER/ERGIC-localized mutant InsQ292 induce the PERK and ATF6 pathways while mutant G201D, which reaches the Golgi network, exclusively activates the IRE-1 pathway. In addition, the rescue of the intracellularly retained murine V2R at the plasma membrane by different pharmaco- and chemical chaperones resulted in a reduction of UPR detected by a decreased expression of chaperones GRP78 and GRP94 and a reduced activation of eIF2α. Micro array analysis of cells expressing ER-retained mutant L62P revealed new and yet unknown target genes of UPR. Some of them were involved in negative regulation of apoptosis and redox regulation and therefore elucidated novel and as yet undescribed possibilities to inhibit cell death after persistent ER stress. Further analysis of the three known UPR transducers revealed chaperone GRP94 as a novel interaction partner of the transcription factor ATF6, possibly connected with ER stress. Until this work, activation of UPR and induction of ATF6 was assumed to be exclusively regulated by binding and dissociation of GRP78/BiP. Furthermore, for the first time the usually ER-resident molecular chaperone GRP94 could be found in the nucleus in cells expressing ER-retained

mutant L62P, verified by different methodical approaches and pointing to a possible adaptive function resulting in survival of the cell upon persistent ER stress.

5 Discussion

Conformational diseases are a class of disorders associated with aberrant protein accumulation in tissues and cellular compartments. To date, more and more evidence indicates that these disorders are accompanied by ER stress and that they are linked to the induction of the unfolded protein response (UPR) and/or the ER overload response (EOR). One of these diseases may be the X-linked nephrogenic diabetes insipidus (NDI), which is characterized by the inability of the kidney to absorb water in response to the hormone arginin vasopressin (AVP) (Oksche and Rosenthal 1998). This rare hereditary disorder is due to different mutations within the coding sequence of the *AVPR2* gene resulting in binding- or transport-defective vasopressin V2 receptors. These receptors are recognized by the cellular quality control system and are retained intracellularly. Besides a disturbed water absorption little is known about cellular effects induced by these retained receptor proteins. The connection between transport-deficient V2 receptors retained in intracellular compartments, especially in the ER, and the molecular mechanisms underlying the induction of UPR and EOR remains to be elucidated.

In the present study the activation of different signaling pathways involved in ER stress were analyzed and characterized using cells expressing mutant V2Rs. Since no cell line is known to express the human V2R endogenously, HEK293 cells stably expressing the wild-type receptor and different NDI-causing V2Rs were generated in order to obtain a useful tool to study chronic ER stress conditions. Furthermore, acute ER stress was analyzed in HEK293 cells transiently transfected with the wild-type V2R and different NDI-causing mutants. The correct localization and minimal variability in expression within each cell line of the GFP-tagged receptors was confirmed by laser scanning microscopy allowing direct analyses and comparison between the cell lines. The investigated effects were not attributable to an overexpression of the mutant V2Rs; since comparable expression intensities in HEK293 cells expressing the wild-type V2R, no cell stress was most likely induced.

5.1 Activation of the UPR

Chaperones play a major role in the folding of proteins and their enhanced expression served as a first proof of induction of ER stress. It is currently accepted that an intracellular accumulation of misfolded proteins results in elevated expression levels of molecular chaperones to cope with the higher folding load in the ER (Malhotra and Kaufman 2007). Cells adapt to this increased demand by an upregulation of chaperones of the quality control system in order to assure that no misfolded proteins abandon the ER and enter the secretory pathway. The ER-resident molecular chaperones bind their unfolded substrates to facilitate the correct three-dimensional protein structure. One of these chaperones involved in protein folding is the lectin calnexin as part of the calnexin/calreticulin cycle (Molinari and Helenius 1999). It specifically recognizes monoglycosylated core N-linked glycans and subsequently binds to the glycoprotein. In the present work immunofluorescence studies and immunoblot analyses of cell lysates of HEK293 cells stably expressing the ER-retained mutant L62P revealed an upregulation of calnexin. The enhanced expression pointed to a grown requirement of folding proteins in cells expressing this specific mutant. Further analysis of chaperones involved in ER stress (GRP78, GRP94) revealed an increased expression in cells stably expressing mutants L62P, InsQ292 and G201D. Chaperone GRP78 also showed a slightly increased expression level in cells expressing the wild-type V2R. This observation could be explained by the fact that up to 30% even of the wild-type V2R are retained in the ER in HEK293 cells representing transport intermediates on their way to the cell surface (Oksche et al. 2002). The high amount of newly synthesized receptor proteins due to the transfection subsequently also results in a higher demand of chaperone GRP78. A more precise response to the retention of misfolded V2R mutants was observed in the expression analysis of chaperone GRP94. GRP94 is a constitutively expressed ER lumenal protein, which is upregulated upon cellular stress such as heat shock, oxidative stress or ER stress. Furthermore, it is thought to play a role in protein translocation to the ER, in their subsequent folding and assembly, and in regulating protein secretion (Ruddon and Bedows 1997). Only in cells expressing disease-causing V2R mutants a clear upregulation was detectable suggesting an induction of cell stress.

Another cellular stress pathway, which might possibly be induced by misfolded proteins, is the heat shock response (HSR). In contrast to the UPR, which serves the secretory pathway, the heat shock response is predominantly activated in answer to stress conditions in the cytosol (Mager and Ferreira 1993). In analogy to the UPR, the HSR causes transcriptional activation of molecular chaperones and elements of the ubiquitin–proteasome system (Parsell and Lindquist 1993). Although formerly discovered as a response to thermal stress (heat shock), the HSR is triggered by a variety of stress conditions that interfere with folding and result in accumulation of misfolded or aggregated proteins (Liu and Chang 2008).
It could be shown that the HSR is activated upon ER stress in vivo, although to a lower level than after heat shock conditions (Liu and Chang 2008). Chang et al. proposed that the HSR can relieve stress in UPR-deficient cells by affecting multiple ER activities. Thus, this stress response appears to be an alternative stress pathway and compensates the absence of the UPR. A characteristic marker for the presence of HSR is the enhanced expression of cytosolic heat shock proteins (Hsps). Immunoblot analysis of Hsp70, Hsc70 and Hsp90 chaperones revealed no induction at all indicating that HSR is most likely not activated in HEK293 cells expressing wild-type V2R and retained mutants.

Since increased chaperone expression could be connected with cell stress in general the different UPR specific pathways were analyzed to verify a possible involvement. It is described that upon induction of the UPR all three pathways (PERK, ATF6 and IRE-1) are activated. In order to characterize the activation of the UPR induced by intracellular retention of misfolded V2R mutants all three transducers of the UPR were examined regarding their status of activation (Kaufman 1999). In the present work it could be shown that not all three transducers were activated in cells expressing each of the studied mutants. ER-retained mutant L62P and ER/ERGIC-localized mutant InsQ292 induced the PERK and ATF6 pathways while mutant G201D, which reaches the Golgi network, activated the IRE-1 pathway. Until now, it was shown that the chemical induction of the UPR by tunicamycin or thapsigargin led to the activation of all three UPR pathways resulting in attenuation of translation, increased expression of chaperones and foldases to alleviate ER stress (Kaufman 1999). However, the present findings indicate that misfolded proteins, which are retained in different compartments of the secretory pathway, seem to activate

different UPR pathways depending on their intracellular localization. Thus, it can be suggested, that no single specific UPR response is existent. The cell seems to distinguish between the grade of ER stress, which relies on the site of retention of the misfolded proteins and activates one, two or all three UPR pathways.
In addition to the UPR pathways mentioned the ER-associated degradation (ERAD) pathway is also activated during ER stress via transcriptional upregulation to reduce the amount of unfolded proteins in the ER. Misfolded and defective proteins can be released into the cytoplasm where they are degraded by the proteasome, a multi-catalytic 26S proteolytic protein complex that is enriched at the ER membrane (Rivett and Knecht 1993). The selection, retro-translocation to the cytoplasm and proteasome-targeting of proteins has been termed ERAD (Brodsky and McCracken 1999). In effect, the ERAD pathway clears the secretory pathway of potentially dangerous proteins. Accordingly, this pathway becomes essential if the concentration of misfolded proteins accumulates to very high levels and/or if UPR induction is simultaneously compromised (Hampton 2002). Recently, Schwieger et al. demonstrated the existence of a Derlin-1-mediated ERAD pathway degrading the wild-type receptor and disease-causing V2R mutants. The authors observed that V2R mutants retained in different cellular compartments (ER, ER/ERGIC, Golgi apparatus) were able to coprecipitate the ERAD components p97/valosin-containing protein, Derlin-1 and the 26S proteasome regulatory subunit 7 (Schwieger et al. 2008). These findings confirm the existence of the UPR in V2R mutants analyzed in the present work.

Recently, it has been proposed that the UPR is a key feature in the mechanism of pathogenicity of different conformational diseases. Studies in models of cystic fibrosis revealed that GRP78 as a UPR-marker and the ATF6 branch are activated upon ER-retention of the misfolded cystic fibrosis transmembrane conductance regulator (CFTR) mutant F508del (Kerbiriou et al. 2007). In addition, analysis of UPR in a Drosophila model for retinal degeneration (retinitis pigmentosa) uncovered an activation of the IRE-1 pathway (XBP-1) upon transcription of misfolded rhodopsin (Ryoo et al. 2007). To date, no complete examination of the whole UPR signal transduction is described, including different temporal steps of ER stress induced by a misfolded protein. Furthermore, only one single ER-retained mutant served as misfolded protein in these studies (Schroder and Kaufman 2005a). In contrast, the

present work includes the analysis of different phases of ER stress and additionally the analysis of three differently retained disease-causing mutants of the V2R in comparison to the wild-type receptor.

The results of this work reveal differences in the expression patterns of chaperones under chronic and acute UPR conditions. This could be due to the fact that only the PERK pathway is activated upon acute UPR indicated by an enhanced phosphorylation of eIF2α whereas an induction of the other two pathways was absent. A possible explanation could be that after 6 h of transient transfection the amount of retained misfolded receptor mutants was not sufficient to activate all three pathways. Although the three UPR pathways are simultaneously activated upon severe ER stress, it was shown before that the immediate response occurs through the PERK pathway (DuRose et al. 2006). After 6 h of acute and mild ER stress only this pathway is activated due to the small amount of expressed misfolded and retained receptor proteins. This induction results in a slighty increased expression of GRP78 and GRP94 in cells expressing the ERGIC-retained mutant InsQ292. In HEK293 cells transiently expressing mutant L62P, which is exclusively retained in the ER, no upregulation of these chaperones could be measured whereas induction of apoptosis via release of cytochrome c was detectable. These findings emphasize the observation that the different activation patterns of the UPR are dependent on the retention sites of the misfolded proteins both upon acute and chronic UPR conditions. So far, the UPR pathway was only examined by analyzing one ER-retained mutant of a single protein. In this study it could be demonstrated that activation of all three UPR pathways depends on the compartment of retention of the misfolded protein within the secretory pathway.

Another evidence of an existing UPR in HEK293 cells expressing retained V2Rs could be provided by the analysis of the reduction of UPR after rescuing retained murine V2R (mV2R) to the plasma membrane. It was shown before that the effects of pharmacological chaperones facilitated the rescue of intracellularly retained receptor mutants (Wuller et al. 2004). In the present study the mV2R was indicative of a misfolded protein retained in several compartments of the secretory pathway, namely ER, ERGIC and Golgi apparatus. In HEK293 cells stably expressing mV2R.GFP an increased expression of chaperones GRP78 and GRP94 as markers for the UPR was detectable. It could be demonstrated that treatment of the cells with different

pharmacochaperones that are known to stabilize the receptor confirmation (SR121463B, SR49059, OPC-31260) led to a rescue of these receptors to the plasma membrane. The reduced amount of retained proteins in the secretory pathway resulted in a reduction of the UPR in these cells indicated by a decreased expression level of the molecular chaperones GRP78 and GRP94 and a diminished activation of the PERK pathway. The results of the first clinical studies revealed that the application of pharmacochaperones may be a therapeutical approach for conformational diseases like NDI (Bernier et al. 2006), cystic fibrosis (Vij et al. 2006) and phenylketonurie (Nascimento et al. 2008). In addition to these studies, the present work points out the effects of these pharmacochaprones on the UPR pathway on a molecular level for the first time. Moreover, the effects of chemical chaperones were studied. As an example for chemical chaperones DMSO was used. It is assumed that the effect of DMSO as a chemical chaperone is based on an increased solvent density, masking of exposed hydrophobic residues or direct/indirect influence on components of the quality control system of the cell (Brown et al. 1996). Consistent with the data obtained after treatment with pharmacochaperones the results in this work demonstrate that treatment of cells with DMSO results in a rescue of the retained mV2R to the plasma membrane and a reduced expression of the UPR-specific chaperones GRP78 and GRP94. Furthermore, these findings are in good agreement with Hotamisligil et al., who could reduce ER stress and restore glucose homeostasis in a mouse model of type II diabetes by the help of chemical chaperones (Ozcan et al. 2006), Additionally, the obtained rescue effects seem to be dose- (DMSO) and time-dependent (SR121463B). One may argue that this approach may not represent a common therapeutic application, but it appears to be an option for certain patients with specific mutations in the V2R, not only to restore receptor function but also to reduce the additional negative effects of ER stress.

Until now, micro array analyses regarding UPR target genes in different organisms were performed in several studies (Kamauchi et al. 2005; MacKenzie et al. 2005; Matsumoto et al. 2005). These studies include different models of UPR induced by several chemical triggers (MacKenzie et al. 2005; Hamamura et al. 2008), knock-out models (Iida et al. 2007), cell lines secreting high protein amounts (Martinez et al. 2008) and viral infections (Ruby et al. 2006). Just a few studies are known to

investigate the effects of the intracellular retention of misfolded proteins (Turner et al. 2005) and diseases (Zabner et al. 2005). However, the results of a study of cystic fibrosis indicated that CFTR dysfunction has little impact on airway epithelial gene expression in samples of primary cultures of human CF airway epithelia as compared to non-CF cells (Zabner et al. 2005). The objective of the current study was to conduct a complete analysis of the UPR in HEK293 cells stably expressing misfolded V2R mutants including a further characterization of affected target genes in order to discover and elucidate novel and yet unknown involved pathways of adaptation. For this purpose HEK293 cells stably expressing mutant flag.L62P under chronic UPR conditions were subjected to micro array analysis of 47,000 genes and compared to flag.V2R expressing cells. As expected, the obtained data indicated an important role of genes involved in folding and unfolding processes in chronic ER stress. In addition, the micro array analysis revealed a great amount of novel UPR target genes and involved pathways yet unknown to be linked to ER stress and UPR. Negative regulators of apoptosis, like the suppressor of cytokine signaling or BAX inhibitor 1 were upregulated, while inducers of apoptosis (apoptosis-inducing factor 3, apoptotic protease-activating factor 1) were downregulated. Several genes implicated in redox regulation, like thioredoxin or glutaredoxin were also upregulated. Therefore, both regulation of apoptosis and redox regulation revealed a connection with outliving ER stress. These findings implicate new and promising targets for therapeutic modulation in order to reduce the negative effects of prolonged UPR and prevent induction of apoptosis, which is an important step in several conformational diseases. Although the induction of UPR does not appear to be the fatal point in NDI, an adaptation to the effects of ER stress conditions and the involved pathways seems to be an improvement for the renal collecting duct cells.

5.2 Adaptation to ER stress by inhibition of apoptosis

One possibility to cope with chronic stress is the selective activation or inhibition of signals through one or two UPR pathways. The final decision for adaptation and against apoptosis requires that the signaling cascades enhancing ER and cellular function are maintained, whereas those leading to apoptosis are suppressed. If adaptation requires suppression of one or two UPR pathways one possibility is the PERK pathway, resulting in the inhibition of the pro-apoptotic transcription factor CHOP. ATF6 might also be a promising candidate for a pathway that could remain

activated during persistent ER stress, resulting in a continuous expression of pro-survival genes. From this point of view, the findings of this study regarding the different activation pattern of the specific UPR pathways support this theory. The pro-survival pathway mediated by ATF6 is activated in two of the three cell lines expressing the studied mutants (L62P and InsQ292). Although cells expressing the third mutant (G201D) showed no activation of ATF6 and the pro-apoptotic pathway via PERK also remains inactive. In this context, a small-molecule inhibitor of the eIF2α phosphorylation salubrinal was identified (Wiseman and Balch 2005). Salubrinal specifically inhibits the PP1-GADD34 phosphatase activity resulting in continuous eIF2α phosphorylation and therefore in a sustained activated PERK pathway. The discovery of this specific inhibitor may have several implications for pharmacologically regulated UPR pathways. Salubrinal could be used to maintain convenient levels of insulin synthesis in the ER when treating type II diabetes. Maintaining eIF2α in an inactive state may help the ER to balance insulin production and reduce the amount of premature B-cell death due to ER stress-mediated apoptosis (Harding and Ron 2002). Besides PERK, a further regulation step of ATF6 may also be a promising target for pharmacological modulation.

5.2.1 Survival of the cells by an enhanced redox potential in mutants

As described before, activation of UPR also increases expression of antioxidant genes (Tu and Weissman 2004) implying that generation of reactive oxygen species (ROS) contributes to cellular damage during ER stress. ROS can be produced either in mitochondria (oxidative phosphorylation) or in the ER due to an imbalanced oxidative folding capacity. Thus, it is possible that a major component of the adaptive response during UPR is the protection against ROS. The formation of disulphide bonds by oxidation of two cysteine residues within and between polypeptide chains enables the stability of the mature protein. In the present study the increased expression of ER chaperones and folding enzymes involved in redox regulation (PDI, thioredoxin, Ero1α and ERp57) was pointing to a possible association of protection against ROS and pro-survival adaptation in cells expressing misfolded L62P and InsQ292. Furthermore, the antioxidative status of HEK293 cells expressing these V2R constructs was determined by electron spin resonance. Measurement of the redox activity in these cells manifested a higher capacity to neutralize free radicals

and a shorter reaction time as compared to untransfected HEK293 cells and cells expressing the wild-type receptor. A connection between inhibition of apoptosis due to oxidative stress and enhanced redox activity was shown and discussed by various groups before (Nordberg and Arner 2001; Seiler et al. 2008). However, here it could be demonstrated for the first time that the intracellular retention of misfolded proteins not only induces an upregulation of molecular chaperones to reduce the folding load, but also causes an enhanced redox activity, which could be beneficial for an adaptation and survival of these cells despite chronic ER stress conditions.

5.2.2 Inhibition of apoptosis by degradation of ASK1

Apoptosis signal-regulating kinase 1 (ASK1) is a member of the mitogen-activated protein (MAP) kinase kinase kinase (MAPKKK) family and plays an important role in cellular stress responses induced by reactive oxygen species (ROS), especially in oxidative (Matsuzawa et al. 2002) and ER stress (Nishitoh et al. 2002). It was shown before that thioredoxin inhibits ASK1 activity by directly binding to its N-terminus (Saitoh et al. 1998) suggesting a possible mechanism for redox regulation of the apoptosis signal transduction pathway. The ASK1-thioredoxin system is thought to be a redox sensor which functions as a signal transducer of intracellular redox changes. In this work, an inhibition of apoptosis via induction of this pro-survival pathway could be detected and was further characterized in HEK293 cell lines stably expressing ER-retained mutant L62P. From previous publications (Liu and Min 2002), it is known that an enhanced expression of the redox-regulating protein thioredoxin promotes ubiquitination and proteasomal degradation of ASK1. These findings could be confirmed in this work. In addition, the possibility to use ASK1 as therapeutic target to prevent apoptosis caused by ER stress in conformational diseases like type II diabetes or Alzheimer's disease was discussed and studied before (Akterin et al. 2006; Imoto et al. 2006; Nishikawa and Araki 2007). Recently, evidence was provided that ASK1 is significantly activated in diet-induced diabetic mice and contributes to cardiovascular diseases (Yamamoto et al. 2008). Moreover, it could be shown that the inhibition of ASK1 activation by olmesartan (angiotensin II receptor antagonist) seems to mediate beneficial effects on dietary diabetic mice.

In this work, the association of ASK1 in the initiation of apoptosis upon ER stress could be demonstrated in HEK293 cells stably expressing NDI-causing mutant L62P. Moreover, the adaptive response could be shown resulting in the survival of the cells

despite persistent and severe ER stress. This observation supports the relevance of ASK1 as a therapeutic target in conformational diseases, such as Alzheimer's disease, type II diabetes but also NDI.

5.2.3 Interaction of ATF6 and GRP94

Under resting conditions, the transcription factor ATF6 resides in the ER membrane. Trafficking of ATF6 appears to be inhibited by the binding of GRP78 to the luminal domain of ATF6. ER stress disrupts GRP78 binding and ATF6 is delivered to the Golgi apparatus (Chen et al. 2002). Little is known about the sensing of ER stress and the regulation of activation upon these conditions. For the UPR transducers PERK and IRE-1, different models are proposed and discussed (Ron and Walter 2007). The direct recognition model suggests that unfolded proteins bind directly to the luminal domains of the transducers, whereas the indirect (chaperone-mediated) model hypothesizes that binding of the abundant ER chaperone GRP78 keeps both transducers inactive. A combination of both models could fit; proposing both GRP78 dissociation and binding of unfolded proteins result in an activation of ATF6 or in an additional regulation step in or beyond the ER. In the case of ATF6, the only regulation appears to be the binding of GRP78 under resting conditions. A post-translational modification of ATF6, like phosphorylation by p38 MAPK, seems to enhance the ability of the nuclear form of ATF6 to transactivate the *grp78* promoter (Luo and Lee 2002). These results provide evidence that in addition to its activation by proteolytic cleavage, ATF6 undergoes specific ER stress-induced phosphorylation. Furthermore, an underglycosylated form of ATF6 is proposed as a sensing mechanism to monitor ER homeostasis (Hong et al. 2004) and the protein nucleobindin 1 is discussed to be a repressor of the S1P-mediated ATF6 cleavage (Tsukumo et al. 2007). It was demonstrated that overexpression of nucleobindin 1 inhibits S1P-mediated ATF6 cleavage without affecting ER-to-Golgi transport of ATF6, whereas knock-down of NUCB1 by siRNA accelerates ATF6 cleavage during ER stress. Until now, in addition to GRP78 no other chaperone was detected to be associated with ATF6 upon ER stress or normal cellular conditions. In the present study, an interaction between ATF6 and GRP94 could be demonstrated for the first time. Immunoprecipitation analyses confirmed that in HEK293 cells expressing different NDI-causing V2R mutants as well as in cells treated with several chemical inducers of ER stress (tunicamycin, DTT, thapsigargin), the UPR transducer ATF6

interrelates with GRP94. However, analyses of a possible association of ATF6 with the cytosolic chaperone Hsp70 showed no specific interaction at all, Hsp70 was detectable in each of the studied cell lines. The rise of detectable GRP94 upon ER stress conditions points to a possible association to stress conditions. Consistent with these data, a regulation of a transcription factor by binding of a chaperone was shown before (Shi et al. 1998). Recently, Morimoto et al. showed that the repression of heat shock gene transcription is due to the association of Hsp70 with the HSF1 transactivation domain, thus providing a plausible explanation for the role of molecular chaperones in at least one key step in the autoregulation of the heat shock response (Shi et al. 1998). This result would be a possible explanation for the obtained data, since GRP94 may regulate its own expression like Hsp70 by binding the transcription factor ATF6. The present interaction of ATF6 with its target gene GRP94 demonstrates a novel form of regulation of this transducer independent from its binding to GRP78 in the ER membrane. Upon ER stress, a reduced binding of GRP78 to ATF6 was detectable, whereas its interaction with GRP94 is enhanced. This feedback regulation of chaperones could represent a second regulation step for ATF6, possibly independent from the regulation by GRP78 in the ER. Autoregulation of this transcription factor in response to ER stress might represent a novel feedback mechanism that sustains the ER stress response UPR.

Taken together, the data presented here provide a novel regulation mechanism of ATF6, besides its binding to GRP78. In line with these findings is a hypothesis of Lee et al., who assumed a further ER-retention mechanism for ATF6 besides its association with GRP78 (Parker et al. 2001). But no further studies were performed to elucidate other chaperones involved. Interestingly, although GRP78 and GRP94 are described to have equal functions (protein chaperone, Ca^{2+}-binding protein, cytoprotection), these ER chaperones act differently upon ER stress. GRP78 is known to dissociate from ATF6 while interaction with GRP94 seems to increase under these conditions. These findings suggest a further regulation step of ATF6, comparable with the autoregulative function of Hsp70 with HSF-1 (Shi et al. 1998).

5.2.4 Nuclear expression of GRP94

Chaperones are known to be involved in the protection of nuclear proteins upon stress conditions. As a novel version of this role, Hsp70 was demonstrated to transport damaged nuclear proteins to the nucleolus, clearing other nuclear components of misfolded proteins and therefore decreasing the danger of their widespread aggregation (Nollen et al. 2001). Molecular chaperones regulate both the activation and the disassembly of numerous transcriptional complexes (Morimoto 2002). Thus, chaperones emerge as regulators of the transcriptional network (Lee et al. 2002). The stress-induced nuclear translocation of chaperones may preserve the nuclear remodeling capacity during enviromental damage and protect the integrity of DNA (Soti et al. 2005).

GRP94 is an ER resident member of the HSP90 family of molecular chaperones. The abundant chaperone is ubiquitously expressed in multicellular eukaryotes. While it is constitutively expressed in all tissues, GRP94 levels are increased by a number of conditions that disrupt protein folding in the ER (Kozutsumi et al. 1988; Maki et al. 1990; Little et al. 1994). Low glucose levels, oxygen deprivation, low extracellular pH, expression of mutant proteins and viral infections are examples of physiological forms of stress which upregulate GRP94. In cell culture such stress conditions also include treatment with reducing agents, ionophores or tunicamycin or overexpression of transfected proteins. It was shown before that overexpression of GRP78 or GRP94 obtains a cytoprotective function and that these chaperones protect cells against cell death (Reddy et al. 2003; Nozaki et al. 2004). Although the exact mechanisms for the anti-apoptotic effects of these GRPs are not completely understood it is assumed that one mechanism involves the prevention of the formation of a functional apoptosome (Lee 2001).In addition, several studies suggest that GRP78 may also protect the host cell against cell death by suppressing oxyradical accumulation and stabilizing mitochondrial function (Liu et al. 1998; Yu et al. 1999).

In the present work the nuclear localization of GRP94 could be demonstrated by immunofluorescence analysis, immunoblot assay and electron microscopy revealing a possible function of GRP94 to undertake the task of dealing with chronic ER stress. Consistent with these findings, several reports have determined the redistribution of GRP78 to the cytosol, nucleus and cell surface (Delpino and Castelli 2002; Rao et al. 2004; Qian et al. 2005). These effects suggest that, under stress conditions, GRP78 may also exist as an ER transmembrane protein but it is not clear how transient this

effect is. The potential explanations for the presence of GRP78 outside the ER may be saturation effects of the KDEL receptors in the ER, resulting in targeting overflow; interactions with other proteins or lipids that consequently hinder binding to the KDEL receptor, allowing GRP78 to leave the ER; or an active release from intact cells during cellular stress (Wiest et al. 1997; Delpino and Castelli 2002). This phenomenon was also observed for the lectin calreticulin that redistributes from the ER and appears in the cytosol during heat shock conditions (Panaretakis et al. 2008). Similarly, a subpopulation of GRP94 associates with the ER membrane during an apoptotic insult and becomes a target of calpain activity (Reddy et al. 1999). Recent studies also suggested that either a cytosolic pool of GRP78 or a subpopulation of GRP78 exist as an ER transmembrane protein may form a complex with caspase-7 and -12 at the ER surface and prevent their activation and release (Rao et al. 2004). These studies highlight the importance of GRP78 as an anti-apoptotic protein, and shed new light on the mechanisms underlying the association between ER stress and the cell death program. It remains to be elucidated if GRP94 has equal functions regarding apoptosis and cytoprotection.

5.3 Activation of EOR

It was shown before that ER stress is not only induced by the presence of mis- or unfolded proteins in the organelle. Another possible trigger could be the overloading of the ER with correctly folded proteins. Each stress situation triggers a unique cellular response using various signal transduction pathways to induce specific transcription factors. The first cellular stress response, the UPR was analyzed and characterized in the first part of this study. The second stress pathway, the ER overload response (EOR) comprises activation of the transcription factor NF-κB. Exposure of cells to pathological agents, such as proinflammatory cytokines, UV and γ-irradiation, or upon bacterial and viral infections, EOR and therefore NF-κB activity is also rapidly induced (Pahl and Baeuerle 1997). Activation of NF-κB occurs via phosphorylation of IκB-α on two serine residues, Ser-32 and Ser-36, and subsequent degradation of the inhibitor IκB-α by the 26S proteasome. The degradation of IκB releases the NF-κB dimer, which subsequently translocates to the nucleus, where it activates transcription of its target genes.

It is assumed that the occurrence of ER stress results in an activation of both pathways, the UPR and the EOR (Pahl 1999). In HEK293 cells transiently and stably expressing misfolded and retained NDI-causing mutants of the V2R the induction of UPR could be shown. It was shown that the three UPR pathways were differently activated dependent on the retention sites of the misfolded proteins both upon acute and chronic UPR conditions. In the same manner, an induction of the EOR pathway via activation of NF-κB was hypothesized.

NF-κB induction was examined by luciferase assay and immunoblot analysis, but HEK293 cells transiently and stably expressing V2R mutants revealed no induction of NF-κB though ER stress. The observation that the retention of misfolded proteins results in activation of UPR but not EOR suggests that the transient and stable transfection of HEK293 cells with GFP-tagged V2R constructs does not lead to effects of overexpression and reveals a novel one-sided cellular response to ER stress.

The results of the present work regarding the missing induction of NF-κB/EOR could be clarified by the fact that activation of NF-κB is inhibited by a variety of antioxidants (Schreck et al. 1992; Schreck and Baeuerle 1994). This finding, together with the observation that exogenously applied H_2O_2 can activate NF-κB in some cell lines (Baeuerle 1991; Pahl and Baeuerle 1996) suggests that ROS can act as second messengers for NF-κB activation by ER overload. Pretreatment of cells with a variety of structurally unrelated antioxidants abolishes the ER-overload response (Pahl 1999). In this context, it is noted that accumulation of wild-type or misfolded proteins in the ER leads to a release of Ca^{2+} resulting in the production of ROS and activation of NF-κB. This activation can be blocked by antioxidants and by Ca^{2+} chelators or activated by drugs that cause the release of Ca^{2+} from the ER (Pahl and Baeuerle 1996). The results obtained in this study regarding the strong increase of the antiradical potential in HEK293 cells expressing mutants L62P and InsQ292 (up to forty times higher) are in good agreement with these observations and may explain the existing absence of NF-κB activation and therefore the missing induction of the EOR.

Furthermore, no pro-inflammatory response mediated by an induction of the EOR and therefore of the transcription factor NF-κB could be demonstrated. These findings are in disagreement with the enhanced expression of urinary prostaglandin E2 detected in patients suffering from congenital nephrogenic diabetes insipidus

(Fichman et al. 1980) and in a rat model of lithium-induced NDI (Kotnik.Nielsen.2005), both indicating a possible pro-inflammatory response and involvement of NF-κB due to accumulated V2R or aquaporine-2 (AQP2). The observed upregulation of pro-inflammatory prostaglandin E2 (PGE2) has to be explained by a present activation of other inflammatory pathways different from NF-κB. In addition to this, the measurement of excreted PGE2 in the urine represents an inaccurate method to determine the abundance of PGE2, since the amount of excreted PGE2 can not be related to the exact amount of synthesized PGE2.

The results obtained in this thesis demonstrate that the ER stress response UPR is not only regulated by the chaperone GRP78 in the ER. Furthermore, the activation of the three different UPR branches mediated by PERK, ATF6 and IRE-1 seems to be dependent on the retention site of the misfolded protein. Moreover, the data of the present work reveal a possible participation of the chaperone GRP94 in the regulation of the transcription factor ATF6, which represents a novel modulatory step in the UPR.

In addition, several pathways could be elucidated, which may prevent or at least reduce ER stress-mediated apoptosis upon persistent ER stress and therefore represent interesting and new targets for pharmacological modulation.

6 Literature

Accili, D., A. Cama, F. Barbetti, H. Kadowaki, T. Kadowaki and S. I. Taylor (1992). "Insulin resistance due to mutations of the insulin receptor gene: an overview." *J Endocrinol Invest* **15**(11): 857-64.

Adachi, Y., K. Yamamoto, T. Okada, H. Yoshida, A. Harada and K. Mori (2008). "ATF6 is a transcription factor specializing in the regulation of quality control proteins in the endoplasmic reticulum." *Cell Struct Funct* **33**(1): 75-89.

Akterin, S., R. F. Cowburn, A. Miranda-Vizuete, A. Jimenez, N. Bogdanovic, B. Winblad and A. Cedazo-Minguez (2006). "Involvement of glutaredoxin-1 and thioredoxin-1 in beta-amyloid toxicity and Alzheimer's disease." *Cell Death Differ* **13**(9): 1454-65.

Baeuerle, P. A. (1991). "The inducible transcription activator NF-kappa B: regulation by distinct protein subunits." *Biochim Biophys Acta* **1072**(1): 63-80.

Baeuerle, P. A. and D. Baltimore (1988). "I kappa B: a specific inhibitor of the NF-kappa B transcription factor." *Science* **242**(4878): 540-6.

Baeuerle, P. A. and T. Henkel (1994). "Function and activation of NF-kappa B in the immune system." *Annu Rev Immunol* **12**: 141-79.

Bankir, L., S. Fernandes, P. Bardoux, N. Bouby and D. G. Bichet (2005). "Vasopressin-V2 receptor stimulation reduces sodium excretion in healthy humans." *J Am Soc Nephrol* **16**(7): 1920-8.

Bannykh, S., M. Aridor, H. Plutner, T. Rowe and W. E. Balch (1995). "Regulated export of cargo from the endoplasmic reticulum of mammalian cells." *Cold Spring Harb Symp Quant Biol* **60**: 127-37.

Bareil, C., V. Delague, B. Arnaud, J. Demaille, C. Hamel and M. Claustres (2000). "W179R: a novel missense mutation in the peripherin/RDS gene in a family with autosomal dominant retinitis pigmentosa." *Hum Mutat* **15**(6): 583-4.

Bartoszewski, R., A. Rab, A. Jurkuvenaite, M. Mazur, J. Wakefield, J. F. Collawn and Z. Bebok (2008). "Activation of the unfolded protein response by DeltaF508 CFTR." *Am J Respir Cell Mol Biol* **39**(4): 448-57.

Bernales, S., K. L. McDonald and P. Walter (2006). "Autophagy counterbalances endoplasmic reticulum expansion during the unfolded protein response." *PLoS Biol* **4**(12): e423.

Bernier, V., M. Lagace, M. Lonergan, M. F. Arthus, D. G. Bichet and M. Bouvier (2004). "Functional rescue of the constitutively internalized V2 vasopressin receptor mutant R137H by the pharmacological chaperone action of SR49059." *Mol Endocrinol* **18**(8): 2074-84.

Bernier, V., J. P. Morello, A. Zarruk, N. Debrand, A. Salahpour, M. Lonergan, M. F. Arthus, A. Laperriere, R. Brouard, M. Bouvier and D. G. Bichet (2006). "Pharmacologic chaperones as a potential treatment for X-linked nephrogenic diabetes insipidus." *J Am Soc Nephrol* **17**(1): 232-43.

Bertolotti, A., Y. Zhang, L. M. Hendershot, H. P. Harding and D. Ron (2000). "Dynamic interaction of BiP and ER stress transducers in the unfolded-protein response." *Nat Cell Biol* **2**(6): 326-32.

Bichet, D. G., A. Oksche and W. Rosenthal (1997). "Congenital nephrogenic diabetes insipidus." *J Am Soc Nephrol* **8**(12): 1951-8.

Birnbaumer, M., A. Seibold, S. Gilbert, M. Ishido, C. Barberis, A. Antaramian, P. Brabet and W. Rosenthal (1992). "Molecular cloning of the receptor for human antidiuretic hormone." *Nature* **357**(6376): 333-5.

Brodsky, J. L. and A. A. McCracken (1999). "ER protein quality control and proteasome-mediated protein degradation." *Semin Cell Dev Biol* **10**(5): 507-13.

Brown, C. R., L. Q. Hong-Brown, J. Biwersi, A. S. Verkman and W. J. Welch (1996). "Chemical chaperones correct the mutant phenotype of the delta F508 cystic fibrosis transmembrane conductance regulator protein." *Cell Stress Chaperones* **1**(2): 117-25.

Burdakov, D., O. H. Petersen and A. Verkhratsky (2005). "Intraluminal calcium as a primary regulator of endoplasmic reticulum function." *Cell Calcium* **38**(3-4): 303-10.

Burdon, R. H., V. M. Gill and C. Rice-Evans (1987). "Oxidative stress and heat shock protein induction in human cells." *Free Radic Res Commun* **3**(1-5): 129-39.

Chaudiere, J. and R. Ferrari-Iliou (1999). "Intracellular antioxidants: from chemical to biochemical mechanisms." *Food Chem Toxicol* **37**(9-10): 949-62.

Chen, X., J. Shen and R. Prywes (2002). "The luminal domain of ATF6 senses endoplasmic reticulum (ER) stress and causes translocation of ATF6 from the ER to the Golgi." *J Biol Chem* **277**(15): 13045-52.

Cox, J. S., C. E. Shamu and P. Walter (1993). "Transcriptional induction of genes encoding endoplasmic reticulum resident proteins requires a transmembrane protein kinase." *Cell* **73**(6): 1197-206.

Credle, J. J., J. S. Finer-Moore, F. R. Papa, R. M. Stroud and P. Walter (2005). "On the mechanism of sensing unfolded protein in the endoplasmic reticulum." *Proc Natl Acad Sci U S A* **102**(52): 18773-84.

Delpino, A. and M. Castelli (2002). "The 78 kDa glucose-regulated protein (GRP78/BIP) is expressed on the cell membrane, is released into cell culture medium and is also present in human peripheral circulation." *Biosci Rep* **22**(3-4): 407-20.

DenBoer, L. M., P. W. Hardy-Smith, M. R. Hogan, G. P. Cockram, T. E. Audas and R. Lu (2005). "Luman is capable of binding and activating transcription from the unfolded protein response element." *Biochem Biophys Res Commun* **331**(1): 113-9.

Deng, J., P. D. Lu, Y. Zhang, D. Scheuner, R. J. Kaufman, N. Sonenberg, H. P. Harding and D. Ron (2004). "Translational repression mediates activation of nuclear factor kappa B by phosphorylated translation initiation factor 2." *Mol Cell Biol* **24**(23): 10161-8.

Dobson, C. M. (2004). "Principles of protein folding, misfolding and aggregation." *Semin Cell Dev Biol* **15**(1): 3-16.

DuRose, J. B., A. B. Tam and M. Niwa (2006). "Intrinsic capacities of molecular sensors of the unfolded protein response to sense alternate forms of endoplasmic reticulum stress." *Mol Biol Cell* **17**(7): 3095-107.

Elbi, C., D. A. Walker, G. Romero, W. P. Sullivan, D. O. Toft, G. L. Hager and D. B. DeFranco (2004). "Molecular chaperones function as steroid receptor nuclear mobility factors." *Proc Natl Acad Sci U S A* **101**(9): 2876-81.

Ellgaard, L. and A. Helenius (2001). "ER quality control: towards an understanding at the molecular level." *Curr Opin Cell Biol* **13**(4): 431-7.

Ellgaard, L., M. Molinari and A. Helenius (1999). "Setting the standards: quality control in the secretory pathway." *Science* **286**(5446): 1882-8.

Ellis, R. J. and S. M. Hemmingsen (1989). "Molecular chaperones: proteins essential for the biogenesis of some macromolecular structures." *Trends Biochem Sci* **14**(8): 339-42.

Fels, D. R. and C. Koumenis (2006). "The PERK/eIF2alpha/ATF4 module of the UPR in hypoxia resistance and tumor growth." *Cancer Biol Ther* **5**(7): 723-8.

Fenton, R. A., C. P. Smith and M. A. Knepper (2006). "Role of collecting duct urea transporters in the kidney--insights from mouse models." *J Membr Biol* **212**(2): 119-31.

Ferguson, S. S. (2001). "Evolving concepts in G protein-coupled receptor endocytosis: the role in receptor desensitization and signaling." *Pharmacol Rev* **53**(1): 1-24.

Fichman, M., P. Zia and R. Zipser (1980). "Contribution of urine volume to the elevated urinary prostaglandin E in Bartter's syndrome and central and nephrogenic diabetes insipidus." *Adv Prostaglandin Thromboxane Res* **7**: 1193-7.

Fujiwara, T. M. and D. G. Bichet (2005). "Molecular biology of hereditary diabetes insipidus." *J Am Soc Nephrol* **16**(10): 2836-46.

Gething, M. J. and J. Sambrook (1992). "Protein folding in the cell." *Nature* **355**(6355): 33-45.

Hamamura, K., Y. Liu and H. Yokota (2008). "Microarray analysis of thapsigargin-induced stress to the endoplasmic reticulum of mouse osteoblasts." *J Bone Miner Metab* **26**(3): 231-40.

Hammond, C., I. Braakman and A. Helenius (1994). "Role of N-linked oligosaccharide recognition, glucose trimming, and calnexin in glycoprotein folding and quality control." *Proc Natl Acad Sci U S A* **91**(3): 913-7.

Hampton, R. Y. (2002). "ER-associated degradation in protein quality control and cellular regulation." *Curr Opin Cell Biol* **14**(4): 476-82.

Harding, H. P., I. Novoa, Y. Zhang, H. Zeng, R. Wek, M. Schapira and D. Ron (2000a). "Regulated translation initiation controls stress-induced gene expression in mammalian cells." *Mol Cell* **6**(5): 1099-108.

Harding, H. P. and D. Ron (2002). "Endoplasmic reticulum stress and the development of diabetes: a review." *Diabetes* **51 Suppl 3**: S455-61.

Harding, H. P., Y. Zhang, A. Bertolotti, H. Zeng and D. Ron (2000b). "Perk is essential for translational regulation and cell survival during the unfolded protein response." *Mol Cell* **5**(5): 897-904.

Harding, H. P., Y. Zhang and D. Ron (1999). "Protein translation and folding are coupled by an endoplasmic-reticulum-resident kinase." *Nature* **397**(6716): 271-4.

Harding, H. P., Y. Zhang, H. Zeng, I. Novoa, P. D. Lu, M. Calfon, N. Sadri, C. Yun, B. Popko, R. Paules, D. F. Stojdl, J. C. Bell, T. Hettmann, J. M. Leiden and D. Ron (2003). "An integrated stress response regulates amino acid metabolism and resistance to oxidative stress." *Mol Cell* **11**(3): 619-33.

Henkel, T., T. Machleidt, I. Alkalay, M. Kronke, Y. Ben-Neriah and P. A. Baeuerle (1993). "Rapid proteolysis of I kappa B-alpha is necessary for activation of transcription factor NF-kappa B." *Nature* **365**(6442): 182-5.

Hermosilla, R., M. Oueslati, U. Donalies, E. Schonenberger, E. Krause, A. Oksche, W. Rosenthal and R. Schulein (2004). "Disease-causing V(2) vasopressin receptors are retained in different compartments of the early secretory pathway." *Traffic* **5**(12): 993-1005.

Hinnebusch, A. G. (1997). "Translational regulation of yeast GCN4. A window on factors that control initiator-trna binding to the ribosome." *J Biol Chem* **272**(35): 21661-4.

Hinnebusch, A. G. and K. Natarajan (2002). "Gcn4p, a master regulator of gene expression, is controlled at multiple levels by diverse signals of starvation and stress." *Eukaryot Cell* **1**(1): 22-32.

Hong, M., S. Luo, P. Baumeister, J. M. Huang, R. K. Gogia, M. Li and A. S. Lee (2004). "Underglycosylation of ATF6 as a novel sensing mechanism for activation of the unfolded protein response." *J Biol Chem* **279**(12): 11354-63.

Hurtley, S. M. and A. Helenius (1989). "Protein oligomerization in the endoplasmic reticulum." *Annu Rev Cell Biol* **5**: 277-307.

Iida, K., Y. Li, B. C. McGrath, A. Frank and D. R. Cavener (2007). "PERK eIF2 alpha kinase is required to regulate the viability of the exocrine pancreas in mice." *BMC Cell Biol* **8**: 38.

Imoto, K., D. Kukidome, T. Nishikawa, T. Matsuhisa, K. Sonoda, K. Fujisawa, M. Yano, H. Motoshima, T. Taguchi, K. Tsuruzoe, T. Matsumura, H. Ichijo and E. Araki (2006). "Impact of mitochondrial reactive oxygen species and apoptosis signal-regulating kinase 1 on insulin signaling." *Diabetes* **55**(5): 1197-204.

Jiang, H. Y., S. A. Wek, B. C. McGrath, D. Lu, T. Hai, H. P. Harding, X. Wang, D. Ron, D. R. Cavener and R. C. Wek (2004). "Activating transcription factor 3 is integral to the eukaryotic initiation factor 2 kinase stress response." *Mol Cell Biol* **24**(3): 1365-77.

Jiang, H. Y., S. A. Wek, B. C. McGrath, D. Scheuner, R. J. Kaufman, D. R. Cavener and R. C. Wek (2003). "Phosphorylation of the alpha subunit of eukaryotic initiation factor 2 is required for activation of NF-kappaB in response to diverse cellular stresses." *Mol Cell Biol* **23**(16): 5651-63.

Jiang, X. and X. Wang (2004). "Cytochrome C-mediated apoptosis." *Annu Rev Biochem* **73**: 87-106.

Jung, K., J. Richter, K. Kabrodt, I. M. Lucke, I. Schellenberg and T. Herrling (2006). "The antioxidative power AP--A new quantitative time dependent (2D) parameter for the determination of the antioxidant capacity and reactivity of different plants." *Spectrochim Acta A Mol Biomol Spectrosc* **63**(4): 846-50.

Kalies, K. U., D. Gorlich and T. A. Rapoport (1994). "Binding of ribosomes to the rough endoplasmic reticulum mediated by the Sec61p-complex." *J Cell Biol* **126**(4): 925-34.

Kamauchi, S., H. Nakatani, C. Nakano and R. Urade (2005). "Gene expression in response to endoplasmic reticulum stress in Arabidopsis thaliana." *Febs J* **272**(13): 3461-76.

Kargel, E., R. Menzel, H. Honeck, F. Vogel, A. Bohmer and W. H. Schunck (1996). "Candida maltosa NADPH-cytochrome P450 reductase: cloning of a full-length cDNA, heterologous expression in Saccharomyces cerevisiae and function of the N-terminal region for membrane anchoring and proliferation of the endoplasmic reticulum." *Yeast* **12**(4): 333-48.

Kaufman, R. J. (1999). "Stress signaling from the lumen of the endoplasmic reticulum: coordination of gene transcriptional and translational controls." *Genes Dev* **13**(10): 1211-33.

Kerbiriou, M., M. A. Le Drevo, C. Ferec and P. Trouve (2007). "Coupling cystic fibrosis to endoplasmic reticulum stress: Differential role of Grp78 and ATF6." *Biochim Biophys Acta* **1772**(11-12): 1236-49.

Kerem, B., J. M. Rommens, J. A. Buchanan, D. Markiewicz, T. K. Cox, A. Chakravarti, M. Buchwald and L. C. Tsui (1989). "Identification of the cystic fibrosis gene: genetic analysis." *Science* **245**(4922): 1073-80.

Kimata, Y., Y. Ishiwata-Kimata, T. Ito, A. Hirata, T. Suzuki, D. Oikawa, M. Takeuchi and K. Kohno (2007). "Two regulatory steps of ER-stress sensor Ire1 involving its cluster formation and interaction with unfolded proteins." *J Cell Biol* **179**(1): 75-86.

Klussmann, E., K. Maric and W. Rosenthal (2000). "The mechanisms of aquaporin control in the renal collecting duct." *Rev Physiol Biochem Pharmacol* **141**: 33-95.

Klussmann, E., G. Tamma, D. Lorenz, B. Wiesner, K. Maric, F. Hofmann, K. Aktories, G. Valenti and W. Rosenthal (2001). "An inhibitory role of Rho in the vasopressin-mediated translocation of aquaporin-2 into cell membranes of renal principal cells." *J Biol Chem* **276**(23): 20451-7.

Knorre, A., M. Wagner, H. E. Schaefer, W. H. Colledge and H. L. Pahl (2002). "DeltaF508-CFTR causes constitutive NF-kappaB activation through an ER-overload response in cystic fibrosis lungs." *Biol Chem* **383**(2): 271-82.

Kokame, K., H. Kato and T. Miyata (2001). "Identification of ERSE-II, a new cis-acting element responsible for the ATF6-dependent mammalian unfolded protein response." *J Biol Chem* **276**(12): 9199-205.

Kozutsumi, Y., M. Segal, K. Normington, M. J. Gething and J. Sambrook (1988). "The presence of malfolded proteins in the endoplasmic reticulum signals the induction of glucose-regulated proteins." *Nature* **332**(6163): 462-4.

Lanneau, D., M. Brunet, E. Frisan, E. Solary, M. Fontenay and C. Garrido (2008). "Heat shock proteins: essential proteins for apoptosis regulation." *J Cell Mol Med* **12**(3): 743-61.

Lee, A. H., N. N. Iwakoshi and L. H. Glimcher (2003). "XBP-1 regulates a subset of endoplasmic reticulum resident chaperone genes in the unfolded protein response." *Mol Cell Biol* **23**(21): 7448-59.

Lee, A. S. (2001). "The glucose-regulated proteins: stress induction and clinical applications." *Trends Biochem Sci* **26**(8): 504-10.

Lee, T. I., N. J. Rinaldi, F. Robert, D. T. Odom, Z. Bar-Joseph, G. K. Gerber, N. M. Hannett, C. T. Harbison, C. M. Thompson, I. Simon, J. Zeitlinger, E. G. Jennings, H. L. Murray, D. B. Gordon, B. Ren, J. J. Wyrick, J. B. Tagne, T. L. Volkert, E. Fraenkel, D. K. Gifford and R. A. Young (2002). "Transcriptional regulatory networks in Saccharomyces cerevisiae." *Science* **298**(5594): 799-804.

Little, E., M. Ramakrishnan, B. Roy, G. Gazit and A. S. Lee (1994). "The glucose-regulated proteins (GRP78 and GRP94): functions, gene regulation, and applications." *Crit Rev Eukaryot Gene Expr* **4**(1): 1-18.

Liu, H., E. Miller, B. van de Water and J. L. Stevens (1998). "Endoplasmic reticulum stress proteins block oxidant-induced Ca2+ increases and cell death." *J Biol Chem* **273**(21): 12858-62.

Liu, L., S. C. Done, J. Khoshnoodi, A. Bertorello, J. Wartiovaara, P. O. Berggren and K. Tryggvason (2001). "Defective nephrin trafficking caused by missense mutations in the NPHS1 gene: insight into the mechanisms of congenital nephrotic syndrome." *Hum Mol Genet* **10**(23): 2637-44.

Liu, Y. and A. Chang (2008). "Heat shock response relieves ER stress." *Embo J* **27**(7): 1049-59.

Liu, Y. and W. Min (2002). "Thioredoxin promotes ASK1 ubiquitination and degradation to inhibit ASK1-mediated apoptosis in a redox activity-independent manner." *Circ Res* **90**(12): 1259-66.

Luo, S. and A. S. Lee (2002). "Requirement of the p38 mitogen-activated protein kinase signalling pathway for the induction of the 78 kDa glucose-regulated protein/immunoglobulin heavy-chain binding protein by azetidine stress: activating transcription factor 6 as a target for stress-induced phosphorylation." *Biochem J* **366**(Pt 3): 787-95.

Ma, Y. and L. M. Hendershot (2003). "Delineation of a negative feedback regulatory loop that controls protein translation during endoplasmic reticulum stress." *J Biol Chem* **278**(37): 34864-73.

MacKenzie, D. A., T. Guillemette, H. Al-Sheikh, A. J. Watson, D. J. Jeenes, P. Wongwathanarat, N. S. Dunn-Coleman, N. van Peij and D. B. Archer (2005). "UPR-independent dithiothreitol stress-induced genes in Aspergillus niger." *Mol Genet Genomics* **274**(4): 410-8.

Mager, W. H. and P. M. Ferreira (1993). "Stress response of yeast." *Biochem J* **290 (Pt 1)**: 1-13.

Maki, R. G., L. J. Old and P. K. Srivastava (1990). "Human homologue of murine tumor rejection antigen gp96: 5'-regulatory and coding regions and relationship to stress-induced proteins." *Proc Natl Acad Sci U S A* **87**(15): 5658-62.

Malhotra, J. D. and R. J. Kaufman (2007). "The endoplasmic reticulum and the unfolded protein response." *Semin Cell Dev Biol* **18**(6): 716-31.

Marchetti, P., M. Bugliani, R. Lupi, L. Marselli, M. Masini, U. Boggi, F. Filipponi, G. C. Weir, D. L. Eizirik and M. Cnop (2007). "The endoplasmic reticulum in pancreatic beta cells of type 2 diabetes patients." *Diabetologia* **50**(12): 2486-94.

Martinez, V. G., K. J. Williams, I. J. Stratford, M. Clynes and R. O'Connor (2008). "Overexpression of cytochrome P450 NADPH reductase sensitises MDA 231 breast carcinoma cells to 5-fluorouracil: possible mechanisms involved." *Toxicol In Vitro* **22**(3): 582-8.

Matsumoto, R., K. Akama, R. Rakwal and H. Iwahashi (2005). "The stress response against denatured proteins in the deletion of cytosolic chaperones SSA1/2 is different from heat-shock response in Saccharomyces cerevisiae." *BMC Genomics* **6**: 141.

Matsuzawa, A., H. Nishitoh, K. Tobiume, K. Takeda and H. Ichijo (2002). "Physiological roles of ASK1-mediated signal transduction in oxidative stress- and endoplasmic reticulum stress-induced apoptosis: advanced findings from ASK1 knockout mice." *Antioxid Redox Signal* **4**(3): 415-25.

McCracken, A. A. and J. L. Brodsky (2003). "Evolving questions and paradigm shifts in endoplasmic-reticulum-associated degradation (ERAD)." *Bioessays* **25**(9): 868-77.

Michalak, M., J. M. Robert Parker and M. Opas (2002). "Ca2+ signaling and calcium binding chaperones of the endoplasmic reticulum." *Cell Calcium* **32**(5-6): 269-78.

Molinari, M., V. Calanca, C. Galli, P. Lucca and P. Paganetti (2003). "Role of EDEM in the release of misfolded glycoproteins from the calnexin cycle." *Science* **299**(5611): 1397-400.

Molinari, M. and A. Helenius (1999). "Glycoproteins form mixed disulphides with oxidoreductases during folding in living cells." *Nature* **402**(6757): 90-3.

Montie, H. L., F. Kayali, A. J. Haezebrouck, N. F. Rossi and D. J. Degracia (2005). "Renal ischemia and reperfusion activates the eIF 2 alpha kinase PERK." *Biochim Biophys Acta* **1741**(3): 314-24.

Mori, K. (1999). "[Cellular response to endoplasmic reticulum stress mediated by unfolded protein response pathway]." *Tanpakushitsu Kakusan Koso* **44**(15 Suppl): 2442-8.

Mori, K., W. Ma, M. J. Gething and J. Sambrook (1993). "A transmembrane protein with a cdc2+/CDC28-related kinase activity is required for signaling from the ER to the nucleus." *Cell* **74**(4): 743-56.

Morimoto, R. I. (2002). "Dynamic remodeling of transcription complexes by molecular chaperones." *Cell* **110**(3): 281-4.

Murakami, T., S. Kondo, M. Ogata, S. Kanemoto, A. Saito, A. Wanaka and K. Imaizumi (2006). "Cleavage of the membrane-bound transcription factor OASIS in response to endoplasmic reticulum stress." *J Neurochem* **96**(4): 1090-100.

Nascimento, C., J. Leandro, I. Tavares de Almeida and P. Leandro (2008). "Modulation of the activity of newly synthesized human phenylalanine hydroxylase mutant proteins by low-molecular-weight compounds." *Protein J* **27**(6): 392-400.

Nikawa, J. and S. Yamashita (1992). "IRE1 encodes a putative protein kinase containing a membrane-spanning domain and is required for inositol phototrophy in Saccharomyces cerevisiae." *Mol Microbiol* **6**(11): 1441-6.

Nishikawa, T. and E. Araki (2007). "Impact of mitochondrial ROS production in the pathogenesis of diabetes mellitus and its complications." *Antioxid Redox Signal* **9**(3): 343-53.

Nishitoh, H., A. Matsuzawa, K. Tobiume, K. Saegusa, K. Takeda, K. Inoue, S. Hori, A. Kakizuka and H. Ichijo (2002). "ASK1 is essential for endoplasmic reticulum stress-induced neuronal cell death triggered by expanded polyglutamine repeats." *Genes Dev* **16**(11): 1345-55.

Nollen, E. A., F. A. Salomons, J. F. Brunsting, J. J. Want, O. C. Sibon and H. H. Kampinga (2001). "Dynamic changes in the localization of thermally unfolded nuclear proteins associated with chaperone-dependent protection." *Proc Natl Acad Sci U S A* **98**(21): 12038-43.

Nordberg, J. and E. S. Arner (2001). "Reactive oxygen species, antioxidants, and the mammalian thioredoxin system." *Free Radic Biol Med* **31**(11): 1287-312.

Novoa, I., Y. Zhang, H. Zeng, R. Jungreis, H. P. Harding and D. Ron (2003). "Stress-induced gene expression requires programmed recovery from translational repression." *Embo J* **22**(5): 1180-7.

Nozaki, J., H. Kubota, H. Yoshida, M. Naitoh, J. Goji, T. Yoshinaga, K. Mori, A. Koizumi and K. Nagata (2004). "The endoplasmic reticulum stress response is stimulated through the continuous activation of transcription factors ATF6 and XBP1 in Ins2+/Akita pancreatic beta cells." *Genes Cells* **9**(3): 261-70.

Oda, Y., N. Hosokawa, I. Wada and K. Nagata (2003). "EDEM as an acceptor of terminally misfolded glycoproteins released from calnexin." *Science* **299**(5611): 1394-7.

Oda, Y., T. Okada, H. Yoshida, R. J. Kaufman, K. Nagata and K. Mori (2006). "Derlin-2 and Derlin-3 are regulated by the mammalian unfolded protein response and are required for ER-associated degradation." *J Cell Biol* **172**(3): 383-93.

Oksche, A., G. Leder, S. Valet, M. Platzer, K. Hasse, S. Geist, G. Krause, A. Rosenthal and W. Rosenthal (2002). "Variant amino acids in the extracellular loops of murine and human vasopressin V2 receptors account for differences in cell surface expression and ligand affinity." *Mol Endocrinol* **16**(4): 799-813.

Oksche, A. and W. Rosenthal (1998). "The molecular basis of nephrogenic diabetes insipidus." *J Mol Med* **76**(5): 326-37.

Ozcan, U., E. Yilmaz, L. Ozcan, M. Furuhashi, E. Vaillancourt, R. O. Smith, C. Z. Gorgun and G. S. Hotamisligil (2006). "Chemical chaperones reduce ER stress and restore glucose homeostasis in a mouse model of type 2 diabetes." *Science* **313**(5790): 1137-40.

Pahl, H. L. (1999). "Signal transduction from the endoplasmic reticulum to the cell nucleus." *Physiol Rev* **79**(3): 683-701.

Pahl, H. L. and P. A. Baeuerle (1996). "Activation of NF-kappa B by ER stress requires both Ca2+ and reactive oxygen intermediates as messengers." *FEBS Lett* **392**(2): 129-36.

Pahl, H. L. and P. A. Baeuerle (1997). "The ER-overload response: activation of NF-kappa B." *Trends Biochem Sci* **22**(2): 63-7.

Panaretakis, T., N. Joza, N. Modjtahedi, A. Tesniere, I. Vitale, M. Durchschlag, G. M. Fimia, O. Kepp, M. Piacentini, K. U. Froehlich, P. van Endert, L. Zitvogel, F. Madeo and G. Kroemer (2008). "The co-translocation of ERp57 and calreticulin determines the immunogenicity of cell death." *Cell Death Differ* **15**(9): 1499-509.

Parker, R., T. Phan, P. Baumeister, B. Roy, V. Cheriyath, A. L. Roy and A. S. Lee (2001). "Identification of TFII-I as the endoplasmic reticulum stress response element binding factor ERSF: its autoregulation by stress and interaction with ATF6." *Mol Cell Biol* **21**(9): 3220-33.

Parsell, D. A. and S. Lindquist (1993). "The function of heat-shock proteins in stress tolerance: degradation and reactivation of damaged proteins." *Annu Rev Genet* **27**: 437-96.

Qian, Y., Y. Zheng, K. S. Ramos and E. Tiffany-Castiglioni (2005). "GRP78 compartmentalized redistribution in Pb-treated glia: role of GRP78 in lead-induced oxidative stress." *Neurotoxicology* **26**(2): 267-75.

Rao, R. V., H. M. Ellerby and D. E. Bredesen (2004). "Coupling endoplasmic reticulum stress to the cell death program." *Cell Death Differ* **11**(4): 372-80.

Reddy, P. S. and R. B. Corley (1998). "Assembly, sorting, and exit of oligomeric proteins from the endoplasmic reticulum." *Bioessays* **20**(7): 546-54.

Reddy, R. K., J. Lu and A. S. Lee (1999). "The endoplasmic reticulum chaperone glycoprotein GRP94 with Ca(2+)-binding and antiapoptotic properties is a novel proteolytic target of calpain during etoposide-induced apoptosis." *J Biol Chem* **274**(40): 28476-83.

Reddy, R. K., C. Mao, P. Baumeister, R. C. Austin, R. J. Kaufman and A. S. Lee (2003). "Endoplasmic reticulum chaperone protein GRP78 protects cells from

apoptosis induced by topoisomerase inhibitors: role of ATP binding site in suppression of caspase-7 activation." *J Biol Chem* **278**(23): 20915-24.

Rivett, A. J. and E. Knecht (1993). "Protein turnover: proteasome location." *Curr Biol* **3**(2): 127-9.

Ron, D. and P. Walter (2007). "Signal integration in the endoplasmic reticulum unfolded protein response." *Nat Rev Mol Cell Biol* **8**(7): 519-29.

Rosenthal, W., A. Seibold, A. Antaramian, M. Lonergan, M. F. Arthus, G. N. Hendy, M. Birnbaumer and D. G. Bichet (1992). "Molecular identification of the gene responsible for congenital nephrogenic diabetes insipidus." *Nature* **359**(6392): 233-5.

Ruby, T., C. Whittaker, D. R. Withers, M. K. Chelbi-Alix, V. Morin, A. Oudin, J. R. Young and R. Zoorob (2006). "Transcriptional profiling reveals a possible role for the timing of the inflammatory response in determining susceptibility to a viral infection." *J Virol* **80**(18): 9207-16.

Ruddon, R. W. and E. Bedows (1997). "Assisted protein folding." *J Biol Chem* **272**(6): 3125-8.

Ryoo, H. D., P. M. Domingos, M. J. Kang and H. Steller (2007). "Unfolded protein response in a Drosophila model for retinal degeneration." *Embo J* **26**(1): 242-52.

Sadeghi, H. and M. Birnbaumer (1999). "O-Glycosylation of the V2 vasopressin receptor." *Glycobiology* **9**(7): 731-7.

Saitoh, M., H. Nishitoh, M. Fujii, K. Takeda, K. Tobiume, Y. Sawada, M. Kawabata, K. Miyazono and H. Ichijo (1998). "Mammalian thioredoxin is a direct inhibitor of apoptosis signal-regulating kinase (ASK) 1." *Embo J* **17**(9): 2596-606.

Schoneberg, T., A. Schulz, H. Biebermann, T. Hermsdorf, H. Rompler and K. Sangkuhl (2004). "Mutant G-protein-coupled receptors as a cause of human diseases." *Pharmacol Ther* **104**(3): 173-206.

Schreck, R., K. Albermann and P. A. Baeuerle (1992). "Nuclear factor kappa B: an oxidative stress-responsive transcription factor of eukaryotic cells (a review)." *Free Radic Res Commun* **17**(4): 221-37.

Schreck, R. and P. A. Baeuerle (1994). "Assessing oxygen radicals as mediators in activation of inducible eukaryotic transcription factor NF-kappa B." *Methods Enzymol* **234**: 151-63.

Schroder, M. and R. J. Kaufman (2005a). "ER stress and the unfolded protein response." *Mutat Res* **569**(1-2): 29-63.

Schroder, M. and R. J. Kaufman (2005b). "The mammalian unfolded protein response." *Annu Rev Biochem* **74**: 739-89.

Schulein, R., U. Liebenhoff, H. Muller, M. Birnbaumer and W. Rosenthal (1996). "Properties of the human arginine vasopressin V2 receptor after site-directed mutagenesis of its putative palmitoylation site." *Biochem J* **313 (Pt 2)**: 611-6.

Schulein, R., K. Zuhlke, A. Oksche, R. Hermosilla, J. Furkert and W. Rosenthal (2000). "The role of conserved extracellular cysteine residues in vasopressin V2 receptor function and properties of two naturally occurring mutant receptors with additional extracellular cysteine residues." *FEBS Lett* **466**(1): 101-6.

Schulze-Osthoff, K., M. Los and P. A. Baeuerle (1995). "Redox signalling by transcription factors NF-kappa B and AP-1 in lymphocytes." *Biochem Pharmacol* **50**(6): 735-41.

Schwieger, I., K. Lautz, E. Krause, W. Rosenthal, B. Wiesner and R. Hermosilla (2008). "Derlin-1 and p97/valosin-containing protein mediate the endoplasmic reticulum-associated degradation of human V2 vasopressin receptors." *Mol Pharmacol* **73**(3): 697-708.

Seiler, A., M. Schneider, H. Forster, S. Roth, E. K. Wirth, C. Culmsee, N. Plesnila, E. Kremmer, O. Radmark, W. Wurst, G. W. Bornkamm, U. Schweizer and M. Conrad (2008). "Glutathione peroxidase 4 senses and translates oxidative stress into 12/15-lipoxygenase dependent- and AIF-mediated cell death." *Cell Metab* **8**(3): 237-48.

Shamu, C. E. and P. Walter (1996). "Oligomerization and phosphorylation of the Ire1p kinase during intracellular signaling from the endoplasmic reticulum to the nucleus." *Embo J* **15**(12): 3028-39.

Shen, J., X. Chen, L. Hendershot and R. Prywes (2002a). "ER stress regulation of ATF6 localization by dissociation of BiP/GRP78 binding and unmasking of Golgi localization signals." *Dev Cell* **3**(1): 99-111.

Shen, Y., L. Meunier and L. M. Hendershot (2002b). "Identification and characterization of a novel endoplasmic reticulum (ER) DnaJ homologue, which stimulates ATPase activity of BiP in vitro and is induced by ER stress." *J Biol Chem* **277**(18): 15947-56.

Shenoy, S. K. and R. J. Lefkowitz (2005). "Receptor-specific ubiquitination of beta-arrestin directs assembly and targeting of seven-transmembrane receptor signalosomes." *J Biol Chem* **280**(15): 15315-24.

Shi, Y., D. D. Mosser and R. I. Morimoto (1998). "Molecular chaperones as HSF1-specific transcriptional repressors." *Genes Dev* **12**(5): 654-66.

Sitia, R. and S. N. Molteni (2004). "Stress, protein (mis)folding, and signaling: the redox connection." *Sci STKE* **2004**(239): pe27.

Soti, C., C. Pal, B. Papp and P. Csermely (2005). "Molecular chaperones as regulatory elements of cellular networks." *Curr Opin Cell Biol* **17**(2): 210-5.

Sriburi, R., H. Bommiasamy, G. L. Buldak, G. R. Robbins, M. Frank, S. Jackowski and J. W. Brewer (2007). "Coordinate regulation of phospholipid biosynthesis and secretory pathway gene expression in XBP-1(S)-induced endoplasmic reticulum biogenesis." *J Biol Chem* **282**(10): 7024-34.

Sriburi, R., S. Jackowski, K. Mori and J. W. Brewer (2004). "XBP1: a link between the unfolded protein response, lipid biosynthesis, and biogenesis of the endoplasmic reticulum." *J Cell Biol* **167**(1): 35-41.

Stirling, J. and P. O'Hare (2006). "CREB4, a transmembrane bZip transcription factor and potential new substrate for regulation and cleavage by S1P." *Mol Biol Cell* **17**(1): 413-26.

Szanda, G., P. Koncz, A. Rajki and A. Spat (2008). "Participation of p38 MAPK and a novel-type protein kinase C in the control of mitochondrial Ca2+ uptake." *Cell Calcium* **43**(3): 250-9.

Szegezdi, E., S. E. Logue, A. M. Gorman and A. Samali (2006). "Mediators of endoplasmic reticulum stress-induced apoptosis." *EMBO Rep* **7**(9): 880-5.

Tokuyasu, K. (1997). "Immuno-cytochemistry on ultrathin cryosections. ." *In Spector DL, Goodman RD, Leinwand LA, eds. Cells, a Laboratory Manual. Vol 3. Subcellular Localization of Genes and Their Products. Cold Spring Harbor, NY, Cold Spring Harbor Laboratory Press*: 131.1–131.27.

Tournier, C., P. Hess, D. D. Yang, J. Xu, T. K. Turner, A. Nimnual, D. Bar-Sagi, S. N. Jones, R. A. Flavell and R. J. Davis (2000). "Requirement of JNK for stress-induced activation of the cytochrome c-mediated death pathway." *Science* **288**(5467): 870-4.

Trombetta, E. S. and A. J. Parodi (2003). "Quality control and protein folding in the secretory pathway." *Annu Rev Cell Dev Biol* **19**: 649-76.

Tsukumo, Y., A. Tomida, O. Kitahara, Y. Nakamura, S. Asada, K. Mori and T. Tsuruo (2007). "Nucleobindin 1 controls the unfolded protein response by inhibiting ATF6 activation." *J Biol Chem* **282**(40): 29264-72.

Tu, B. P. and J. S. Weissman (2004). "Oxidative protein folding in eukaryotes: mechanisms and consequences." *J Cell Biol* **164**(3): 341-6.

Turner, M. J., D. P. Sowders, M. L. DeLay, R. Mohapatra, S. Bai, J. A. Smith, J. R. Brandewie, J. D. Taurog and R. A. Colbert (2005). "HLA-B27 misfolding in transgenic rats is associated with activation of the unfolded protein response." *J Immunol* **175**(4): 2438-48.

Urano, F., X. Wang, A. Bertolotti, Y. Zhang, P. Chung, H. P. Harding and D. Ron (2000). "Coupling of stress in the ER to activation of JNK protein kinases by transmembrane protein kinase IRE1." *Science* **287**(5453): 664-6.

van Anken, E. and I. Braakman (2005). "Endoplasmic reticulum stress and the making of a professional secretory cell." *Crit Rev Biochem Mol Biol* **40**(5): 269-83.

Van Laethem, A., K. Nys, S. Van Kelst, S. Claerhout, H. Ichijo, J. R. Vandenheede, M. Garmyn and P. Agostinis (2006). "Apoptosis signal regulating kinase-1 connects reactive oxygen species to p38 MAPK-induced mitochondrial apoptosis in UVB-irradiated human keratinocytes." *Free Radic Biol Med* **41**(9): 1361-71.

Vij, N., S. Fang and P. L. Zeitlin (2006). "Selective inhibition of endoplasmic reticulum-associated degradation rescues DeltaF508-cystic fibrosis transmembrane regulator and suppresses interleukin-8 levels: therapeutic implications." *J Biol Chem* **281**(25): 17369-78.

Vincent, M. and R. M. Tanguay (1982). "Different intracellular distributions of heat-shock and arsenite-induced proteins in Drosophila Kc cells. Possible relation with the phosphorylation and translocation of a major cytoskeletal protein." *J Mol Biol* **162**(2): 365-78.

Wang, X. Z. and D. Ron (1996). "Stress-induced phosphorylation and activation of the transcription factor CHOP (GADD153) by p38 MAP Kinase." *Science* **272**(5266): 1347-9.

Wang, Y., J. Shen, N. Arenzana, W. Tirasophon, R. J. Kaufman and R. Prywes (2000). "Activation of ATF6 and an ATF6 DNA binding site by the endoplasmic reticulum stress response." *J Biol Chem* **275**(35): 27013-20.

Wek, R. C. and D. R. Cavener (2007). "Translational control and the unfolded protein response." *Antioxid Redox Signal* **9**(12): 2357-71.

Werner, E. D., J. L. Brodsky and A. A. McCracken (1996). "Proteasome-dependent endoplasmic reticulum-associated protein degradation: an unconventional route to a familiar fate." *Proc Natl Acad Sci U S A* **93**(24): 13797-801.

Wetmore, D. R. and K. D. Hardman (1996). "Roles of the propeptide and metal ions in the folding and stability of the catalytic domain of stromelysin (matrix metalloproteinase 3)." *Biochemistry* **35**(21): 6549-58.

Wickman, K. and D. E. Clapham (1995). "Ion channel regulation by G proteins." *Physiol Rev* **75**(4): 865-85.

Wiest, D. L., A. Bhandoola, J. Punt, G. Kreibich, D. McKean and A. Singer (1997). "Incomplete endoplasmic reticulum (ER) retention in immature thymocytes as revealed by surface expression of "ER-resident" molecular chaperones." *Proc Natl Acad Sci U S A* **94**(5): 1884-9.

Wiseman, R. L. and W. E. Balch (2005). "A new pharmacology--drugging stressed folding pathways." *Trends Mol Med* **11**(8): 347-50.

Wuller, S., B. Wiesner, A. Loffler, J. Furkert, G. Krause, R. Hermosilla, M. Schaefer, R. Schulein, W. Rosenthal and A. Oksche (2004). "Pharmacochaperones post-translationally enhance cell surface expression by increasing conformational stability of wild-type and mutant vasopressin V2 receptors." *J Biol Chem* **279**(45): 47254-63.

Yamamoto, E., Y. F. Dong, K. Kataoka, T. Yamashita, Y. Tokutomi, S. Matsuba, H. Ichijo, H. Ogawa and S. Kim-Mitsuyama (2008). "Olmesartan prevents cardiovascular injury and hepatic steatosis in obesity and diabetes, accompanied by apoptosis signal regulating kinase-1 inhibition." *Hypertension* **52**(3): 573-80.

Yan, W., C. L. Frank, M. J. Korth, B. L. Sopher, I. Novoa, D. Ron and M. G. Katze (2002). "Control of PERK eIF2alpha kinase activity by the endoplasmic reticulum stress-induced molecular chaperone P58IPK." *Proc Natl Acad Sci U S A* **99**(25): 15920-5.

Yoshida, H., K. Haze, H. Yanagi, T. Yura and K. Mori (1998). "Identification of the cis-acting endoplasmic reticulum stress response element responsible for transcriptional induction of mammalian glucose-regulated proteins. Involvement of basic leucine zipper transcription factors." *J Biol Chem* **273**(50): 33741-9.

Yoshida, H., T. Matsui, A. Yamamoto, T. Okada and K. Mori (2001). "XBP1 mRNA is induced by ATF6 and spliced by IRE1 in response to ER stress to produce a highly active transcription factor." *Cell* **107**(7): 881-91.

Yoshida, H., T. Okada, K. Haze, H. Yanagi, T. Yura, M. Negishi and K. Mori (2000). "ATF6 activated by proteolysis binds in the presence of NF-Y (CBF) directly to the cis-acting element responsible for the mammalian unfolded protein response." *Mol Cell Biol* **20**(18): 6755-67.

Yoshida, H., M. Oku, M. Suzuki and K. Mori (2006). "pXBP1(U) encoded in XBP1 pre-mRNA negatively regulates unfolded protein response activator pXBP1(S) in mammalian ER stress response." *J Cell Biol* **172**(4): 565-75.

Young, J. C., N. J. Hoogenraad and F. U. Hartl (2003). "Molecular chaperones Hsp90 and Hsp70 deliver preproteins to the mitochondrial import receptor Tom70." *Cell* **112**(1): 41-50.

Yu, Z., H. Luo, W. Fu and M. P. Mattson (1999). "The endoplasmic reticulum stress-responsive protein GRP78 protects neurons against excitotoxicity and apoptosis: suppression of oxidative stress and stabilization of calcium homeostasis." *Exp Neurol* **155**(2): 302-14.

Zabner, J., T. E. Scheetz, H. G. Almabrazi, T. L. Casavant, J. Huang, S. Keshavjee and P. B. McCray, Jr. (2005). "CFTR DeltaF508 mutation has minimal effect on the gene expression profile of differentiated human airway epithelia." *Am J Physiol Lung Cell Mol Physiol* **289**(4): L545-53.

Zhao, L. and S. L. Ackerman (2006). "Endoplasmic reticulum stress in health and disease." *Curr Opin Cell Biol* **18**(4): 444-52.

Zimmer, T., A. Ogura, A. Ohta and M. Takagi (1999). "Misfolded membrane-bound cytochrome P450 activates KAR2 induction through two distinct mechanisms." *J Biochem* **126**(6): 1080-9.

Zinszner, H., M. Kuroda, X. Wang, N. Batchvarova, R. T. Lightfoot, H. Remotti, J. L. Stevens and D. Ron (1998). "CHOP is implicated in programmed cell death in response to impaired function of the endoplasmic reticulum." *Genes Dev* **12**(7): 982-95.

7 Appendix

functional category	fold induction
endoplasmic reticulum	
grp78/BiP	1.7
grp94	1.6
derlin-1	1.4
selenoprotein m	2.3
calumenin	3.0
endoplasmic reiculum-golgi intermediate compartment (ergic) 1	1.4
coatomer protein complex, subunit alpha	6.1
presenilin 1	3.6
fk506 binding protein 7	2.1
serine palmitoyltransferase, long chain base subunit 2	1.8
chaperones	
dnaj (hsp40) homolog, subfamily c, member 3	1.3
chaperonin containing tcp1, subunit 2 (beta)	1.5
heat shock 70kda protein 9b (mortalin-2)	1.6
calmegin	1.6
dnaj (hsp40) homolog, subfamily c, member 12	1.5
prefoldin subunit 4	1.9
tho complex 4	2.8
Heat shock 22kda protein 8	1.8
heat shock 70kda protein 8	5.0
prefoldin subunit 5	1.4

apoptosis related	
baculoviral IAP repeat-containing 5 (survivin)	1.9
cytochrome c, somatic	1.5
bcl2-antagonist of cell death	1.6
tumor necrosis factor receptor superfamiliy, member 10b	2.4
tumor necrosis factor receptor superfamiliy, member 10d	3.0
calcium binding protein P22 (CHP)	10.0
nuclear factor of kappa light polypeptide gene enhancer in b-cells 2 (p49/p100)	4.0
bcl2-associated x protein	1.3
bcl-like 1	29.0
human myleoid differentiation primary response protein MyD88	3.7

Tab. 7.1: Micro array analysis of cells expressing mutant L62P. Total RNA from two different clones of stably transfected HEK293 cells expressing the wild-type V2R or mutant L62P tagged with FLAG was isolated and subjected to Affymetrix analysis. After verification of correlation, batch analysis was carried out. Upregulated genes were analyzed and listed by the use of the DAVID database (http://niaid.abcc.ncifcrf.gov/).

Curriculum Vitae

For reasons of data protection,
the curriculum vitae is not included in the online version

Publication List

Schwieger I, Lautz K, Krause E, Wiesner B, Rosenthal W and Hermosilla R. Derlin-1 and p97/VCP mediate the ER-associated degradation of human V2 vasopressin receptors. *Mol. Pharm.* 2008 Mar;73(3):697-708. Epub 2007 Nov 29

Schmidt A, Lautz K, Donalis U, Neuschäfer-Rube F, Schwieger I, Oksche A, Püschel G, Schülein R, Wiesner B, Hermosilla R. β-arrestin-dependent constitutive internalization of the human V2 vasopressin receptor. 2008. *Manuscript in preparation.*

Lautz K, Schwieger I, Stephan M, Hübner N, Wiesner B and Hermosilla R. NDI-causing V2 vasopressin receptor mutants induce ER stress signalling. 2008. *Manuscript in preparation*.

Lautz K, Stephan M, Klussmann, E and Hermosilla R. Lithium-induced activation of NF-κB in rat IMCD-cells. 2008. *Manuscript in preparation.*

Congress Abstracts

Oral Presentations

2007

K. Lautz Intrazellulär retinierte V2-Vasopressin Rezeptor Mutanten aktivieren unterschiedliche UPR Signalwege. March 13 – 15 2007, 48th Spring Meeting of the German Association of Experimental and Clinical Pharmacology and Toxicology, Mainz, Germany

K. Lautz Analysis of acute and chronic ER stress in disease-causing V2 vasopressin receptor mutants, XVII. VETPHARM-Symposium. September 27 – 28, 2006. Institut für Pharmakologie und Toxikologie, Fachbereich Veterinärmedizin der Freien Universität Berlin, Berlin, Germany.

2006

K. Lautz The cell stress response triggered by the retention of disease-causing V2 vasopressin receptor mutants. Seminars of the Institute of Pharmacology, May 21st 2006, Berlin, Germany

K. Lautz ER stress caused by retained disease-causing V2 vasopressin receptor mutants in HEK293 cells, German Pharmaceutical Society: DPhG Doktorandentagung, September 6 – 8, 2006, Nürnberg-Heroldsberg, Germany.

K. Lautz ER stress responses induced by retained disease-causing V2 vasopressin receptor mutants in HEK293 cells. XVI. VETPHARM-Symposium. September 28 – 29, 2006. Tierärztliche Hochschule Hannover, Institut für Pharmakologie, Toxikologie und Pharmazie, Hannover, Germany.

2005

K. Lautz The cell stress response triggered by the retention of disease-causing V2 vasopressin receptor mutants. Seminars of the Institute of Pharmacology, May 20th 2005, Berlin, Germany

Posters

2008

K. Lautz,W. Rosenthal, B. Wiesner and R. Hermosilla. Cellular Response to ER stress caused by Disease-Causing V2 Vasopressin Receptor Mutants. 6th Global Conference of the NDI Foundation, September 25th - 27th 2008, Amelia Island Plantation Resort, Amelia Island, Florida, USA

K. Lautz, W. Rosenthal, B. Wiesner and R. Hermosilla. Cellular Response to ER stress caused by Disease-Causing V2 Vasopressin Receptor Mutants CSHL Meeting Molecular Chaperones and Stress Responses, April 30th - May 4th 2008, Cold Spring Harbor Laboratory, Cold Spring Harbor, New York, USA

2006

K. Lautz, I. Schwieger, U. Brandt, A. Oksche, B. Wiesner, R. Hermosilla. A disease-causing V2 Vasopressin receptor mutant induces UPR in HEK293 cells, Keystone Symposia on Molecular and Cellular Biology, Protein Misfolding Diseases: Mechanisms of Misfolding, Pathology and Therapeutic Strategies, February 21 – 26 2006, Breckenridge, Colorado, USA